NOAA ATLAS No. 7

Atlas of the Tropical and Subtropical Circulation Derived from National Meteorological Center Operational Analyses

Silver Spring, Md.
March 1986

U.S. DEPARTMENT OF COMMERCE
National Oceanic and Atmospheric Administration
National Weather Service

NOAA ATLAS No. 7

Atlas of the Tropical and Subtropical Circulation Derived from National Meteorological Center Operational Analyses

Phillip A. Arkin, V.E. Konsky, J.E. Janowiak, and E.A. O'Lenic
Climate Analysis Center
National Meteorological Center
National Weather Service

Silver Spring, Md.
March 1986

U.S. DEPARTMENT OF COMMERCE
Malcolm Baldrige, Secretary
National Oceanic and Atmospheric Administration
Anthony J. Calio, Administrator
National Weather Service
Dr. Richard E. Hallgren, Assistant Administrator

Table of Contents

COPIES CAN BE OBTAINED FROM:

Climate Analysis Center
W/NMC52
5200 Auth Road
Washington, D. C. 20233

Atlas of the Tropical and Subtropical Circulation Derived from National Meterological Center Analyses

ABSTRACT

An atlas of the monthly and seasonal mean tropical and subtropical circulation of the upper troposphere for the period October 1978-September 1983 as represented by National Meteorological Center operational objective analyses is presented. These analyses are prepared twice daily as a part of the Global Data Assimilation System using an optimum interpolation technique. While the analyses are global with a resolution of 2.5° of latitude and longitude, Mercator maps with an equatorial resolution of 5° are given here. The 200 mb level is chosen to maximize the impact of satellite and aircraft wind observations on the analyses. Both the rotational and the divergent components of the wind field are presented.

1. INTRODUCTION

This atlas contains the 5-year mean u component, vector wind, stream function, and velocity potential for each month and season over the period October 1978-September 1983. The means have been derived from twice daily analyses of the global circulation performed at the National Meteorological Center (NMC). Other aspects of the 5-year mean circulation shown are the annual cycle and the vertical structure in the tropics. The mean annual cycle in these data, as well as in the outgoing longwave radiation (Janowiak et al., 1985), is shown as the first harmonic of the 12 monthly 5-year means. The vertical structure for several latitude bands is shown through longitude/pressure cross sections.

The "long-term" mean state of the tropical and subtropical upper tropospheric circulation has been documented in a number of atlases and data sets since about 1970. Oort and Rasmusson (1971) and Newell et al. (1972) presented 5- and 7.5-year means, respectively, of most atmospheric parameters. The results of the former extended to 10°S, while those of the latter were approximately global; all were derived exclusively from radiosonde observations. The determination of the upper tropospheric circulation on any time scale from such spatially restricted data is difficult; in certain areas (e.g., the equatorial eastern Pacific) it is impossible. The availability of wind observations derived from the tracking of clouds in geostationary satellite imagery and from cross-equatorial jet aircraft flights, beginning in the late 1960s, made more complete analyses of the

circulation possible. Sadler (1975) prepared analyses of the monthly mean streamlines of the flow for several levels in the troposphere using radiosonde observations and aircraft reports of wind from the period 1960-1973. Gray et al. (1976) presented 5-year means of the wind components and their stream function derived from National Meteorological Center (NMC) operational objective analyses of the tropical and subtropical circulation. Arkin (1982) presented 11-year means of the 200 mb winds for January and July from the same source, while Arkin (1984) published 11-year mean maps of the tropical and subtropical wind components and several derived quantities for all four seasons.

None of the analyses mentioned above derive from data capable of representing the local horizontal variability of the divergent component of the upper tropospheric wind field. Radiosonde and aircraft data alone are rarely dense enough to define the divergence field over much of the tropics. In addition, early versions of tropical and global operational data assimilation schemes used at NMC imposed significant constraints on the analysis of the divergent component of the wind (Arkin, 1982). By the mid to late 1970s, the availability of satellite-derived, cloud-tracked winds and the relaxation of some of the imposed constraints began to yield operational analyses of the large-scale circulation of the tropics and subtropics which contained some information regarding the divergent part of the flow. The Global Band Analyses of the U. S. Navy Fleet Numerical Oceanographic Center were the first such analyses of which we are aware. Ten-year means of the stream function, vector wind and velocity potential for the Northern Hemisphere winter and the months November-February derived from the Navy analyses were published by Boyle and Chang (1984). The operational analyses of the European Center for Medium Range Weather Forecasting (ECMWF) have used an optimum interpolation (OI) technique from their beginning in 1979. This analysis, like that used at NMC (see following section), does contain large-scale divergent circulations. As yet no multi-year means derived from ECMWF analyses have been published, although statistics derived from several individual years have (White, 1982, 1983; Lau, 1984).

2. DATA - SOURCES AND ANALYSIS

The analyses used to construct the mean fields presented in this study were generated by the Global Data Assimilation System (GDAS) used at NMC since October 1978. The 5-year mean fields cover the period October 1978-September 1983. Some of the figures in section 3 contain data for the 7-year period ending with September 1985. The operational analysis system used at NMC has covered the domain under consideration here since March 1968, and climatologies based on those earlier analyses were mentioned in section 1. The objective of the present study is to document the "long-term" mean circulation of the tropical and subtropical upper troposphere during a period for which analyses containing divergent circulations are available. No other such atlas is currently available.

The data used here are from the 0000 and 1200 GMT GDAS daily analyses performed at NMC. The characteristics of the GDAS have been described by Bergman (1979), Kistler and Parrish (1981), and Dey and Morone (1985). Their utility for climate studies is discussed by Arkin (1982, 1984). The suitability of the analyses for diagnoses of the planetary scale divergent

flows is not yet known, although comparisons with ECMWF analyses (Rosen and Salstein, 1985) suggest that the two centers have comparable skill in this regard. Sardeshmukh and Hoskins (1985) suggest that the ECMWF analyses do have significant skill in representing divergent circulations. The analyses have been subjected to a non-linear normal mode initialization (Ballish, 1980) since May 1980. The effect of this procedure on the large-scale divergent circulations appears to be in the nature of a smoothing, but does not appear to be of major importance (Rosen and Salstein, 1985).

3. DISCUSSION

a. Seasonal and monthly maps

The analyses used here yielded data on a 2.5° latitude by 2.5° longitude grid. For display purposes, the data have been interpolated to a Mercator grid with a longitudinal spacing of 5° and a latitudinal spacing varying from 5° at the equator to about 3.5° at the poleward boundaries (48.1°N and S). The plots are structured with the date line in the center in order to show the largest divergent circulation, that associated with the Indonesian/Southeast Asian convective activity, in a single piece.

We show maps of the 5-year mean u component, vector wind, stream function, and velocity potential for each month and (3-month) season. The vector wind is plotted with isotachs of the wind speed, while the velocity potential is overlayed with vectors representing the divergent wind. The stream function and velocity potential were computed by relaxation of the vorticity and divergence of the time-mean wind components using the iterative technique of Dey and Brown (1976), which requires boundary conditions only at the poles. The reader should be cautious when using the velocity potential fields not to confuse their pattern with that of divergence, which is the Laplacian of the velocity potential and is characterized by substantially smaller spatial scales (see Rasmusson and Arkin, 1985; Sardeshmukh and Hoskins, 1985).

Seasonal variations in the upper tropospheric circulation result from the annual cycle in solar declination, with longitudinal and hemispheric asymmetries associated with differing distributions of continent and ocean. Since the rotational component of the mean wind is in general quite large compared to the divergent component, the plots of vector wind and isotachs and of stream function contain similar information. The former are more useful in defining regions of local maxima (i.e., "jets") and in showing the speed of the wind, while the latter are more effective at defining the direction of the wind and centers of circulation. Plots of the zonal component of the wind are of interest due to its impact on the propagation of eddy energy (Webster and Holton, 1982; Arkin and Webster, 1985). The velocity potential contains information on the direction and magnitude of the divergent component of the wind. In the time-mean tropical and subtropical troposphere, the divergent component is of importance because of its relationship to the sources and sinks of energy for the circulation.

The most outstanding feature of the 200 mb tropical and subtropical circulation is the reversal of sign between the equator and higher latitudes. To first order, all months and all longitudes are characterized by

winds which are more westerly at latitudes poleward of 20° than equatorward. There are of course exceptions, and the circulation also exhibits rather substantial longitudinal variability. Ridges and/or closed anticyclonic circulations are found in all months in the longitudes of Africa, the Americas, and the West Pacific/Southeast Asian region. In most cases these circulations are found in both hemispheres, with westerly jets along their poleward flanks. However, the circulation in the winter hemisphere is invariably stronger. These features appear to be associated with regions in which the outgoing longwave radiation is relatively low (Janowiak et al., 1985) and which are presumably convectively active.

The divergent circulation at 200 mb is dominated by a center of outflow in the West Pacific. Its latitude varies from about 10°S to 20°N from January to July, and the divergent outflow from it is approximately radially symmetric. Other outflow centers are found in the Americas and, somewhat less frequently, in Africa. The divergent wind is seen to be strongest into the winter hemisphere, with the principal inflow regions being northern China during the northern winter and southern Africa during the southern winter. These depictions of velocity potential may be compared to those of Krishnamurti et al. (1973) and Boyle and Chang (1984) for the northern winter and to Krishnamurti (1971) for the southern winter. The latter agrees reasonably well in its large-scale features with the results shown here, although the center of outflow in Southeast Asia appeared to be weighted more strongly toward Indochina. Krishnamurti et al. (1973) also showed the Indonesian outflow center to be further west than in our results, while Boyle and Chang (1984) had a much stronger outflow region over Africa than here. While the differences between our results and those of Krishnamurti (1971) and Krishnamurti et al. (1973) are most likely due to the great increase in data available, this should not cause large differences between the Navy analyses used by Boyle and Chang (1984) and NMC analyses. Two possible causes for the large differences found are their choice of boundary conditions for calculation of the potential function (the velocity potential is set to 0 at 40°S and 60°N) and differences in the data available to the analysis schemes. In particular, the NMC analysis system does not use cloud-tracked winds over land. This might lead to an underestimation of the divergent outflow in, for example, South America and Africa.

It is apparent from the 5-year mean maps of monthly and seasonal velocity potential that the region of strongest divergent outflow is associated with the Indonesian/Southeast Asian convective region. Furthermore, it is not truly radially symmetric, and the asymmetries vary with the season. The mean divergent wind speed over the tropics (25°N-25°S) in the Eastern Hemisphere is nearly 1 m/s greater than that in the Western Hemisphere during the northern summer (Fig. 1) and greater in nearly all other seasons through the 7-year period ending in September 1985. Both hemispheres peak during the solstices. The alternation between flow into the Northern Hemisphere during the northern winter and into the Southern during the southern winter is seen clearly by the change in sign of the v component of the divergent wind over the Eastern Hemisphere from 20°N-20°S (Fig. 2). The strength of the northern summer monsoon is shown by the mean zonal divergent wind over the region from 40°E-90°E and 40°N-20°S (Fig. 3).

b. The first harmonic of the annual cycle

A common method of depicting any periodic phenomenon is to fit a harmonic function with the appropriate period to the data and present its amplitude and phase. Here we have fit a 12-month harmonic to the sequence of 12 monthly mean values at each grid point for a number of different parameters. We show the amplitude and phase by means of a vector whose orientation indicates the phase and whose size indicates the amplitude. Contours of the amplitude are also presented. The vector turns clockwise with advancing time of year, with a vector pointing north representing mid-July, one pointing east representing mid-October, and so on.

We have chosen to represent the 200 mb circulation by the 12-month harmonics of the u and v components (both total and divergent), the stream function and the velocity potential. The u components in the Northern and Southern Hemispheres are approximately out of phase, with maximum values in each found during the winter. A belt of very small amplitude extends around the globe centered between 10°S and the equator. The northward swings of this belt appear to be correlated with regions which are convectively active during the northern winter, such as Indonesia, eastern Africa, and South America. Maxima are associated with the winter jet streams. The 12-month harmonic of the v component in these data is very much smaller.

The amplitude and phase of the stream function and velocity potential are quite simple in appearance, and yet not nearly so simple to explain. The 12-month harmonics of the divergent u and v components are somewhat more clear. The v component shows the change in sign of the divergent flow across the equator, with flow always into the winter hemisphere. The u component shows the annual cycle in the divergent flow to be strongest north of the equator and to be in the sense of divergent flow away from eastern Asia and Central America. Evidently, the 12-month harmonic is not so well defined south of the equator.

The 12-month harmonic of the 850 mb temperature, which reflects the annual cycle in surface temperature presumably associated with differential radiative heating and cooling, has maxima associated with the continents, strongest in the Northern Hemisphere. That of the outgoing longwave radiation (OLR), which reflects the annual cycle in atmospheric heating due to tropical convection, exhibits maxima (corresponding to the time of minimum OLR and therefore to maxima in convection) during the summer season of each hemisphere.

c. Vertical/longitudinal structure

In this section we present the longitudinal and vertical distribution of the zonal component of the total wind and of the velocity potential averaged over three latitude bands, 0°-20°S, 0°-20°N and 5°N-5°S for each season. Plots of the OLR (inverted) averaged over the same latitudes are shown between each of the cross-sections to indicate the degree of convective activity in the latitude band.

The zonal wind and the velocity potential appear to be rather closely related, with the wind blowing from minima towards maxima in the potential

field. The relationship with the OLR, on the other hand, is not so clear. The u component and, in particular, the velocity potential have a wave 1 pattern both in longitude and in height. However, the OLR shows much greater amplitude in higher wave numbers. Some of this difference may be related to the fact that the NMC GDAS does not use winds derived from satellite tracking of clouds over land and may, therefore, underestimate divergence in those regions.

The authors would like to thank Kathy Stevenson for her help in preparing the manuscript and John Kopman for his assistance in preparing the figures.

REFERENCES

Arkin, P.A., 1982: The relationship between interannual variability in the 200 mb tropical wind field and the Southern Oscillation. Mon. Wea. Rev., 110, 1393-1404.

_____, 1984: An examination of the Southern Oscillation in the upper tropospheric tropical and subtropical wind field. Ph.D. Dissertation, University of Maryland, 240 pp.

_____, and P.J. Webster, 1985: Annual and interannual variability of tropical-extratropical interaction: an empirical study. Mon. Wea. Rev., 113, 1510-1523.

Ballish, B., 1980: Initialization, theory and application to the NMC spectral model. Ph.D. Dissertation, University of Maryland, 151 pp.

Bergman, K.H., 1979: Multivariate analysis of temperature and winds using optimum interpolation. Mon. Wea. Rev., 107, 1423-1444.

Boyle, J.S., and C.-P. Chang, 1984: Monthly and Seasonal Winter Climatology over the Global Tropics and Subtropics for the Decade 1973 to 1983 - Volume I. 200 mb Winds. Technical Report NPS-63-84-006, Naval Postgraduate School, Monterey, California 93943, 172 pp.

Dey, C.H., and J.A. Brown, 1976: Decomposition of a Wind Field on the Sphere. NOAA Tech Memo, NWS/NMC59, 13 pp.

Dey, C.H., and L.L. Morone, 1985: Evolution of the National Meteorological Center global data assimilation system: January 1982-December 1983. Mon. Wea. Rev., 113, 304-318.

Gray, T.I., J.R. Irwin, A.F. Krueger and M.S. Varnadore, 1976: Average Circulation in the Troposphere over the Tropics. NOAA/NESS Atlas. [NTIS No. PB 258551/1].

Janowiak, J.E., A.F. Krueger, P.A. Arkin, and A. Gruber, 1985: Atlas of Outgoing Longwave Radiation Derived from NOAA Satellite Data. NOAA Atlas No. 6, U.S. Dept of Commerce, National Oceanic and Atmospheric Administration, National Weather Service, Silver Spring, MD, 44 pp.

Kistler, R.E., and D.F. Parrish, 1982: Evolution of the NMC data assimilation system: September 1978-January 1982. Mon. Wea. Rev., 110, 1335-1346.

Krishnamurti, T.N., 1971: Tropical east-west circulations during the northern summer. J. Atmos. Sci., 28, 1342-1347.

_____, M. Kanamitsu, W.J. Koss, and J.D. Lee, 1973: Tropical east-west circulations during the northern winter. J. Atmos. Sci., 30, 780-787.

Lau, N.-C., 1984: A Comparison of Circulation Statistics Based on FGGE Level III-B Analyses Produced by GFDL and ECMWF for the Special Observing Periods. NOAA Data Report ERL GFDL-6, U.S. Dept of Commerce, National Oceanic and Atmospheric Administration, Environmental Research Laboratories, Princeton, NJ, 237 pp.

Newell, R.E., J.W. Kidson, D.G. Vincent, and G.J. Boer, 1972: The General Circulation of the Tropical Atmosphere and Interactions with Extratropical Latitudes, Vol 1. The MIT Press, 258 pp.

Oort, A. H., 1983: Global Atmospheric Circulation Statistics, 1958-1973. NOAA Prof. Pap. No. 14, U.S. Government Printing Office, Washington, D.C. 20402.

_____, and E.M. Rasmusson, 1971: Atmospheric Circulation Statistics. NOAA Prof. Pap. No. 5, U.S. Government Printing Office, Washington, D.C., 20402. [NTIS COM-72-50295].

Rasmusson, E.M., and P.A. Arkin, 1985: Interannual climate variability associated with the El Niño/Southern Oscillation. Coupled Ocean-Atmosphere Models, J.C.J. Nihoul (Editor), Elsevier Science Publishers B.V., Amsterdam, Chapter 40, 697-725.

Rosen, R.D., and D.A. Salstein, 1985: Effect of initialization on diagnoses of NMC large-scale circulation statistics. Mon. Wea. Rev., 113, 1321-1337.

Sadler, J.C., 1975: The Upper Tropospheric Circulation over the Global Tropics. Rep. UH-MET 75-05, Dept. Meteor., University of Hawaii, 35 pp.

Sardeshmukh, P.D., and B.J. Hoskins, 1985: Vorticity balances in the tropics during the 1982-83 El Niño-Southern Oscillation event. Quart. J. Roy. Meteor. Soc., 111, 261-278.

Webster, P.J., and J.R. Holton, 1982: Cross-equatorial response to middle-latitude forcing in a zonally varying basic state. J. Atmos. Sci., 39, 722-733.

White, G.H., 1982: The Global Circulation of the Atmosphere December 1980-November 1981 Based on ECMWF Analyses. University of Reading Technical Report, 211 pp.

White, G.H., 1983: The Global Circulation of the Atmosphere December 1981-November 1982 Based on ECMWF Analyses. University of Reading Technical Report, 162 pp.

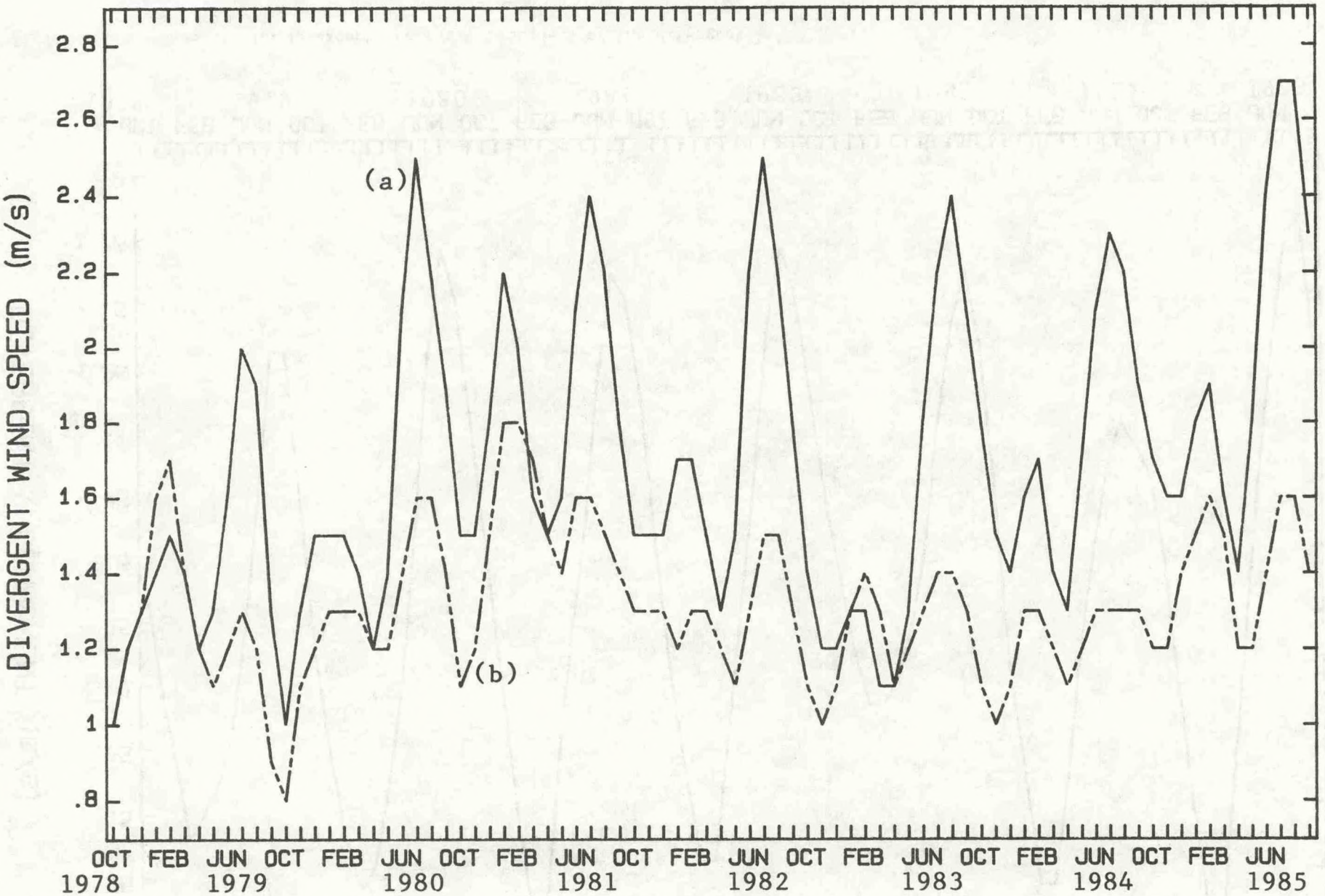

Figure 1. The speed (m/s) of the mean divergent component of the 200 mb wind for each month from October 1978-September 1985 averaged over the latitudes 25°N-25°S for the Eastern (a) and Western (b) Hemispheres.

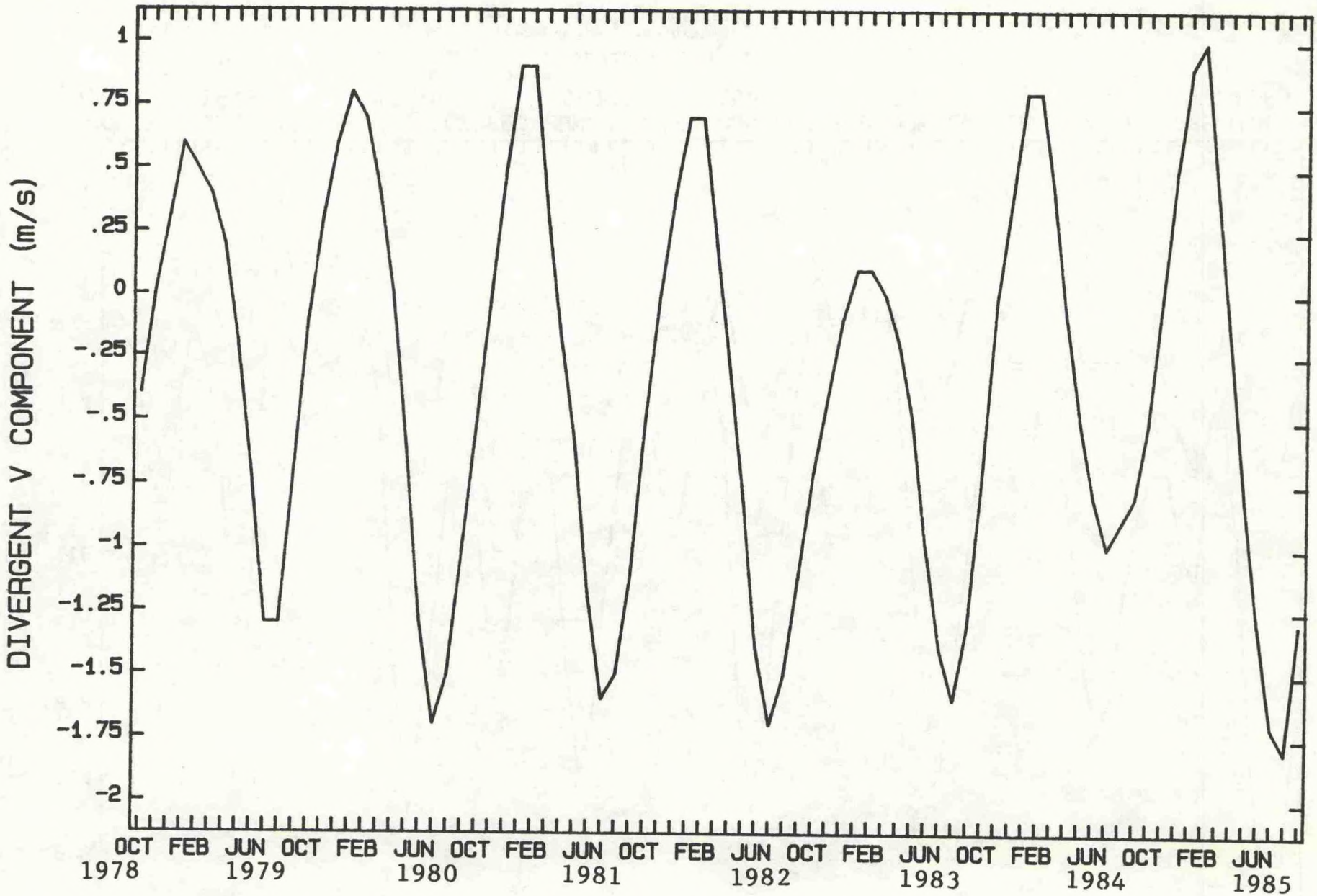

Figure 2. Same as Fig. 1a except for the v component of the divergent 200 mb wind.

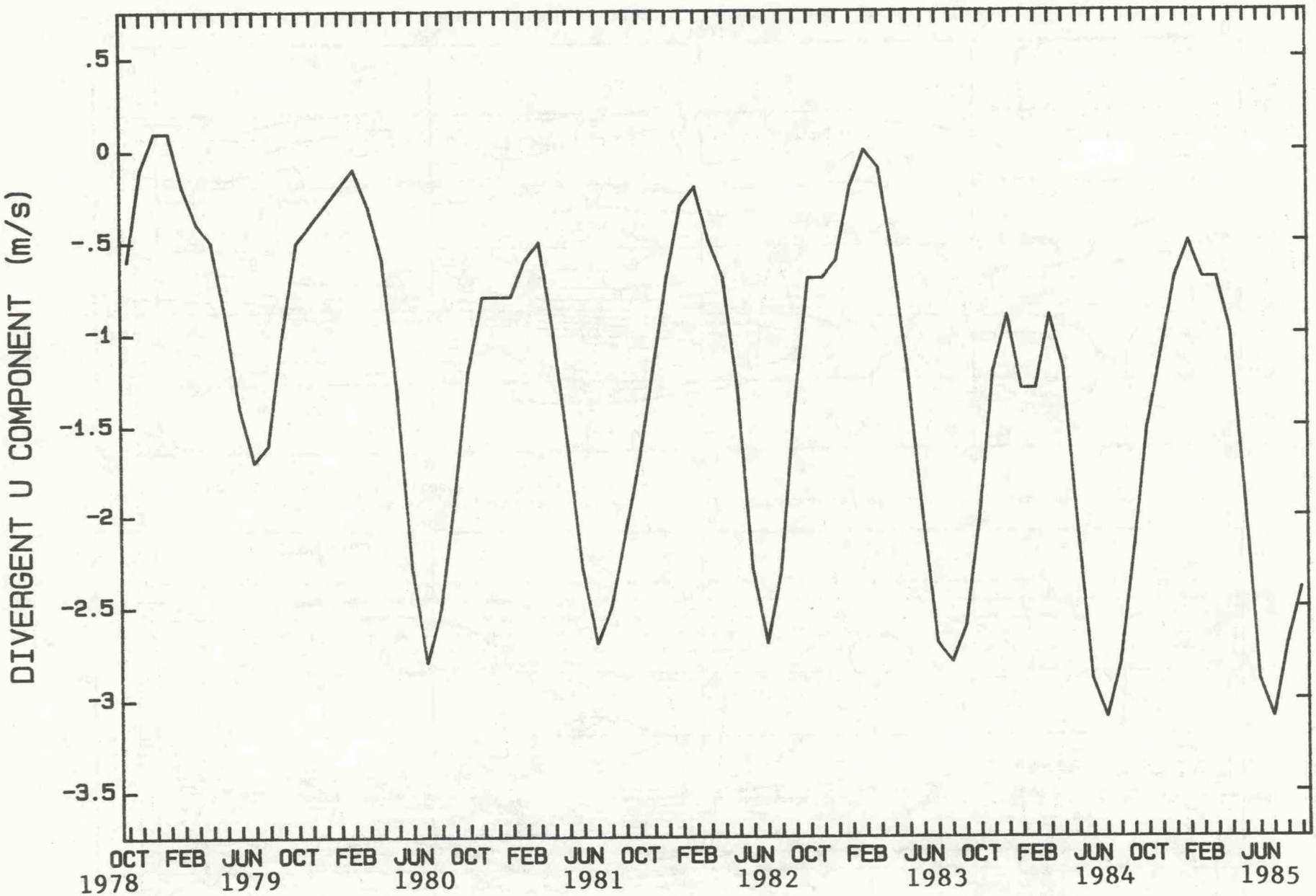

Figure 3. Same as Fig. 2 except for the u component of the divergent 200 mb wind averaged over the area 40^{o}N-20^{o}S and 40^{o}E-90^{o}E.

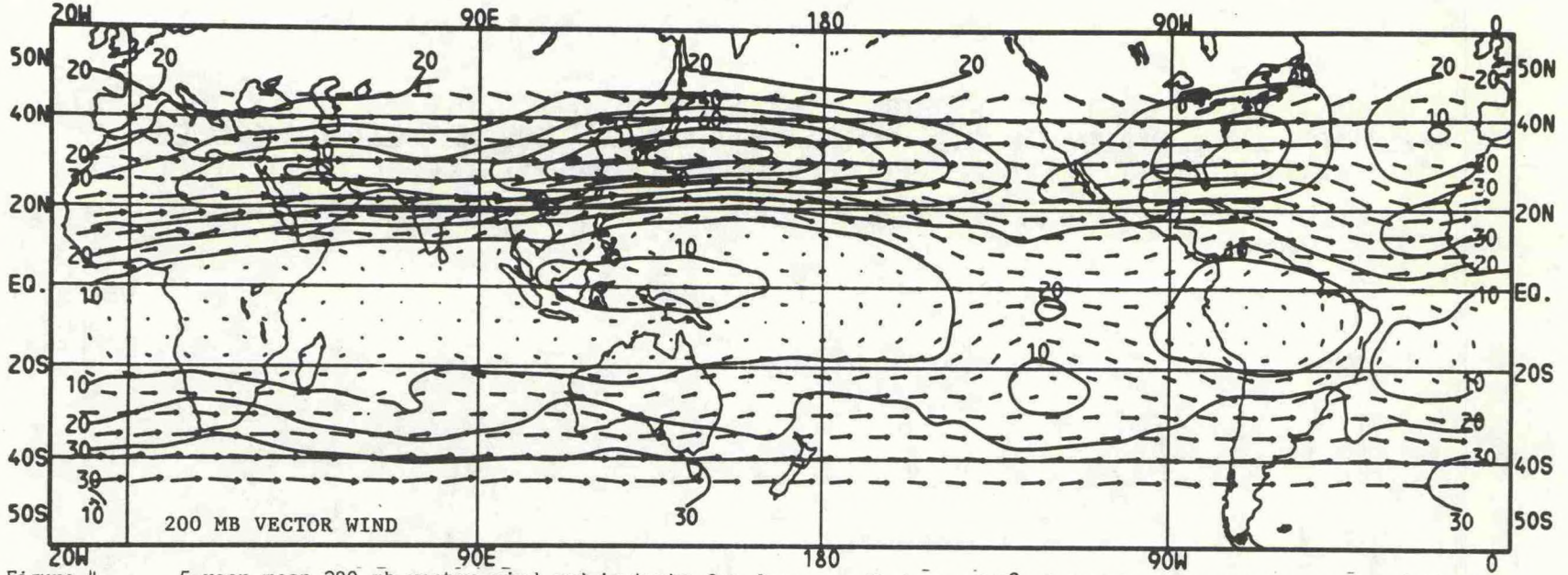

Figure 4. 5-year mean 200 mb vector wind and isotachs for January. Vectors of 5° of longitude represent speeds of 20 m/s. Contour interval for isotachs is 10 m/s.

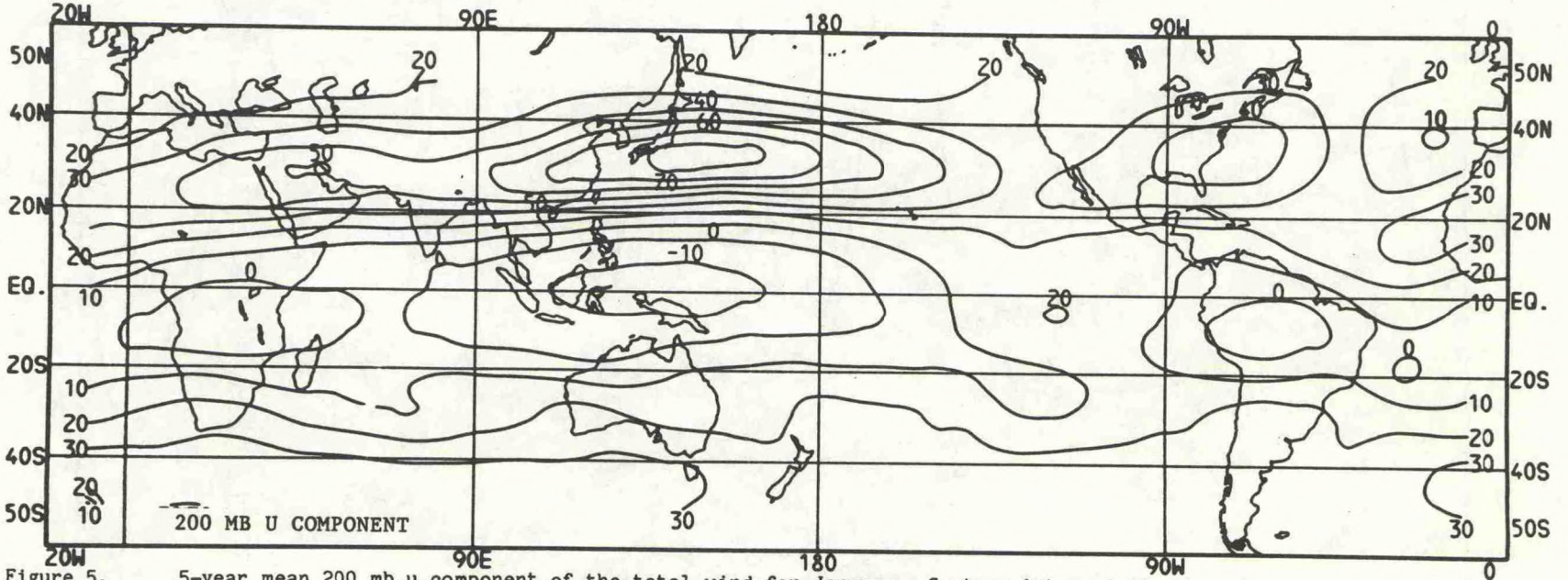

Figure 5. 5-year mean 200 mb u component of the total wind for January. Contour interval 10 m/s.

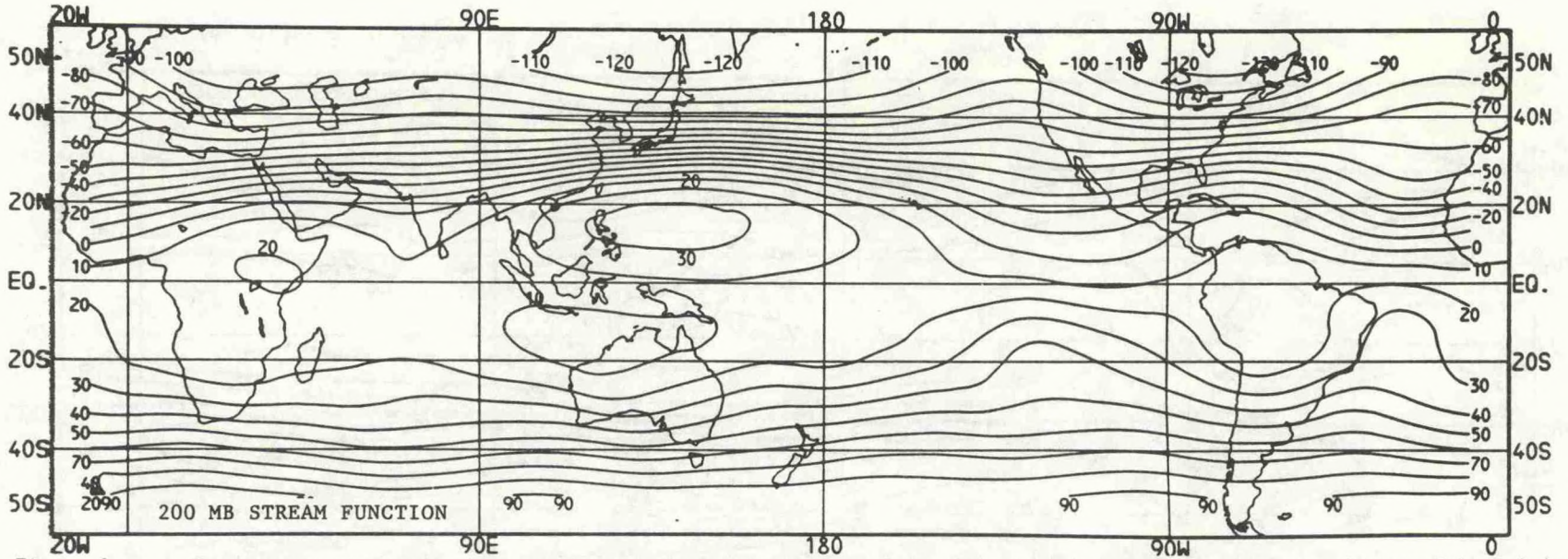

Figure 6. 5-year mean stream function of the non-divergent portion of the 200 mb circulation for January. Contour interval is 10×10^6 m^2/s. Flow is along the contours with speed proportional to the gradient, clockwise about maxima and counterclockwise about minima in both hemispheres.

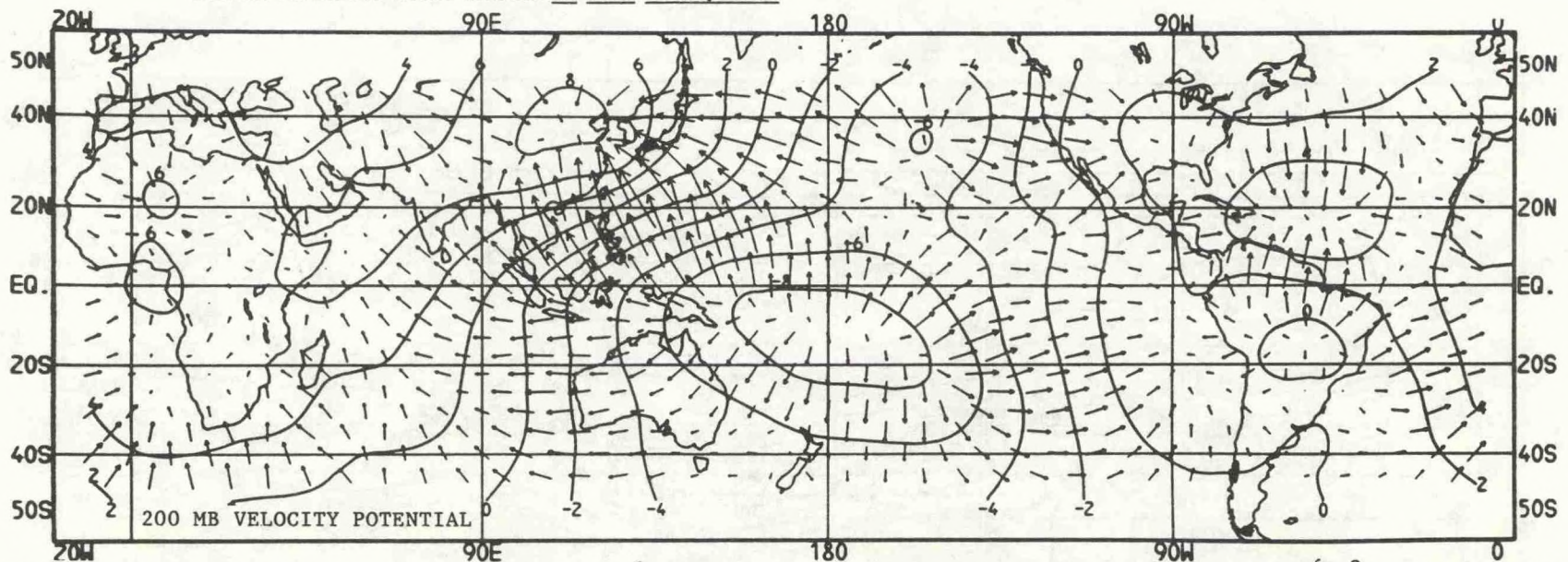

Figure 7. 5-year mean velocity potential of the 200 mb circulation for January. Contour interval is 2×10^6 m^2/s. The divergent portion of the flow is perpindicular to the contours with velocity proportional to their gradient. Vectors represent the divergent wind at alternate grid points. A vector of length 5^o of longitude represents a divergent wind speed of

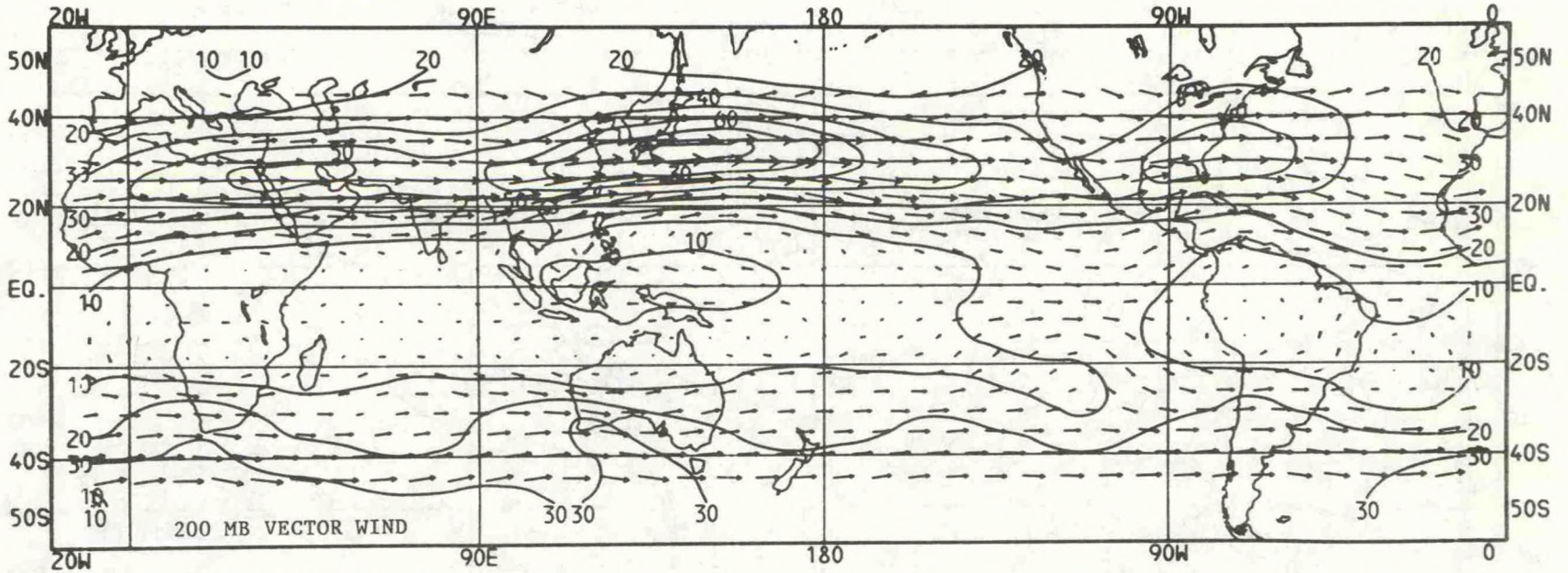

Figure 8. As in Fig. 4 except for February.

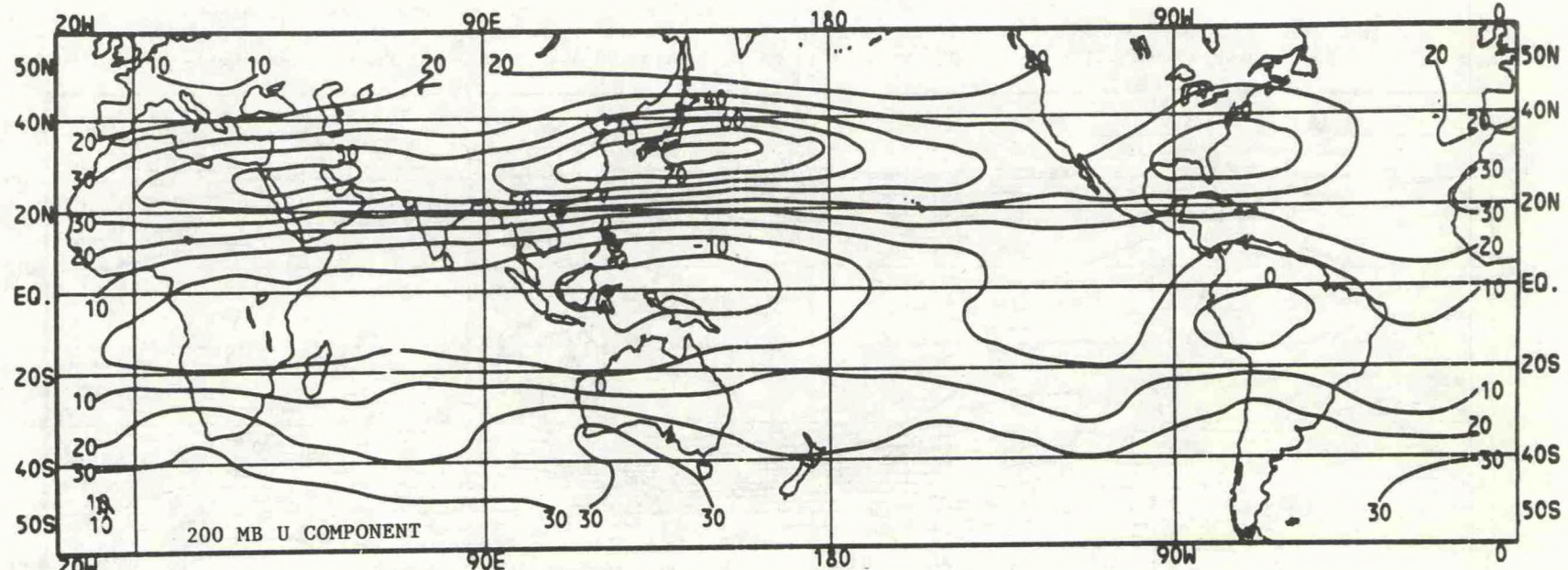

Figure 9. As in Fig. 5 except for February.

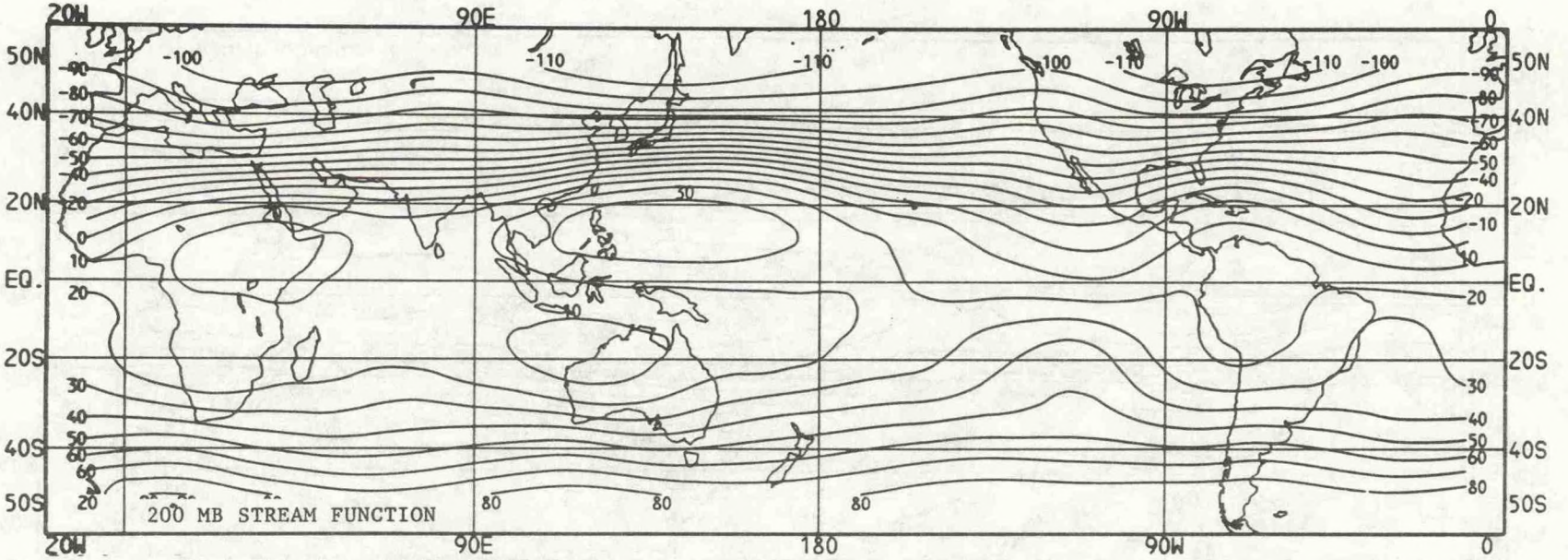

Figure 10. As in Fig. 6 except for February.

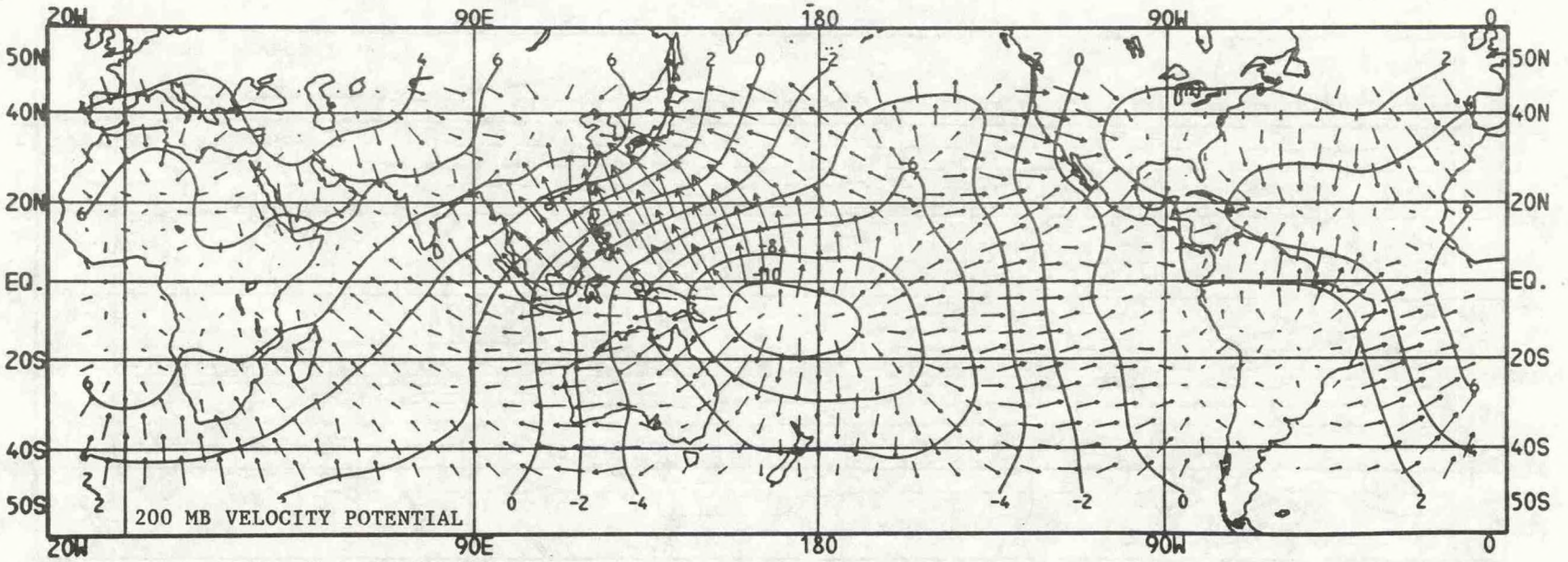

Figure 11. As in Fig. 7 except for February.

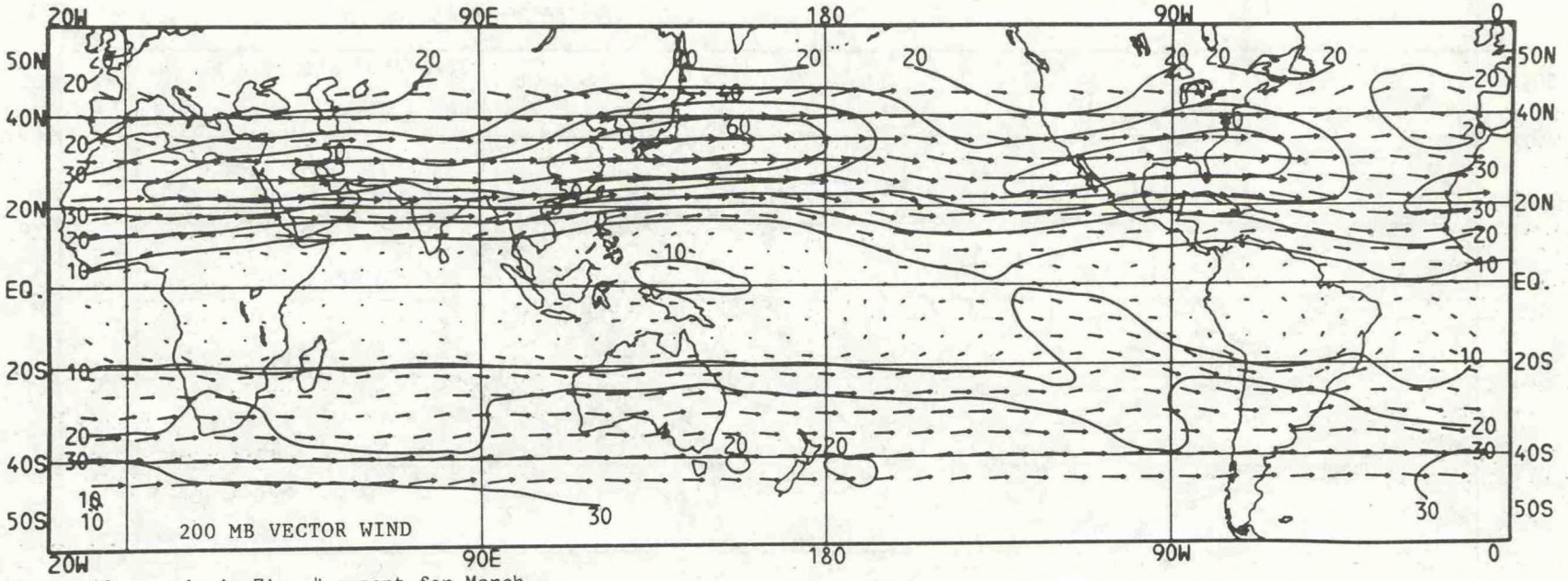

Figure 12. As in Fig. 4 except for March.

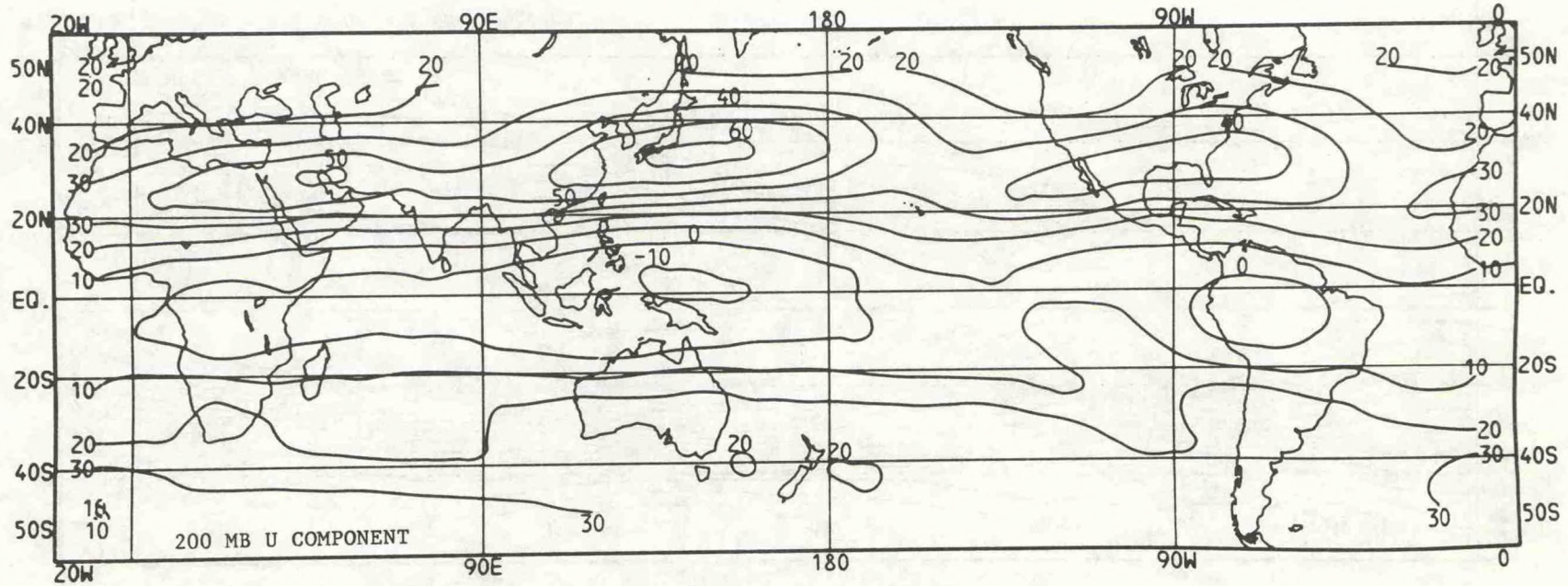

Figure 13. As in Fig. 5 except for March.

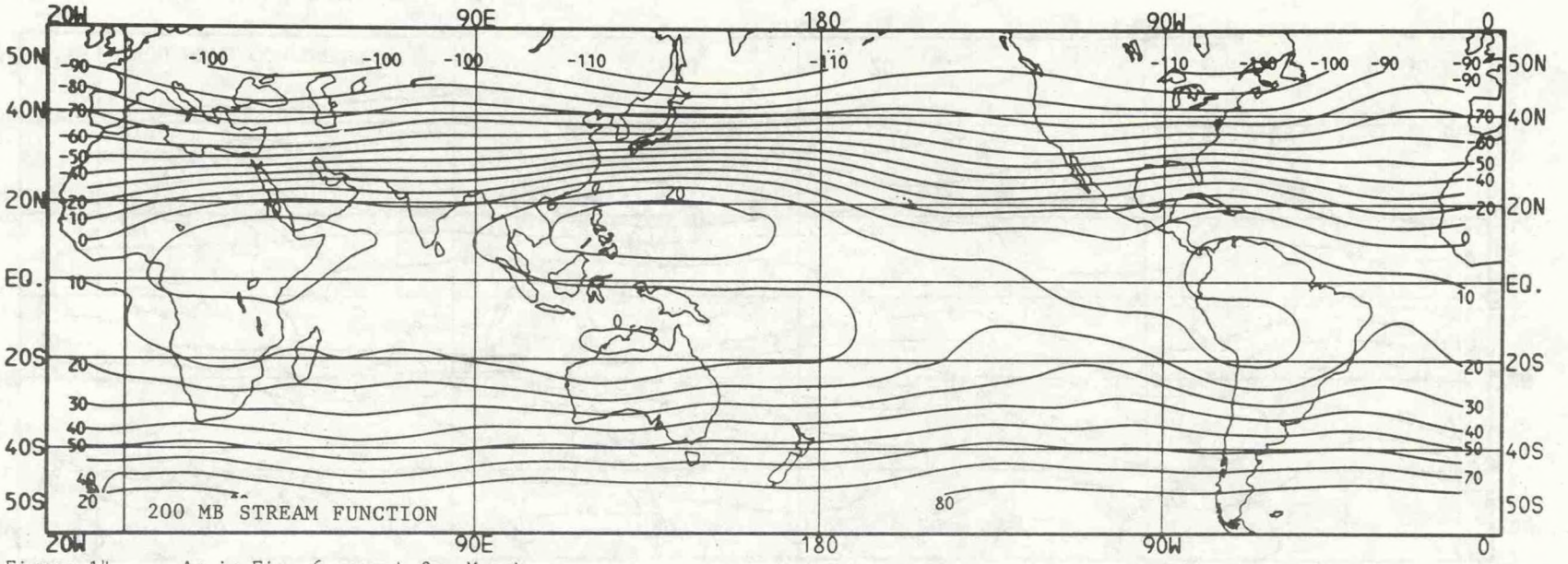

Figure 14. As in Fig. 6 except for March.

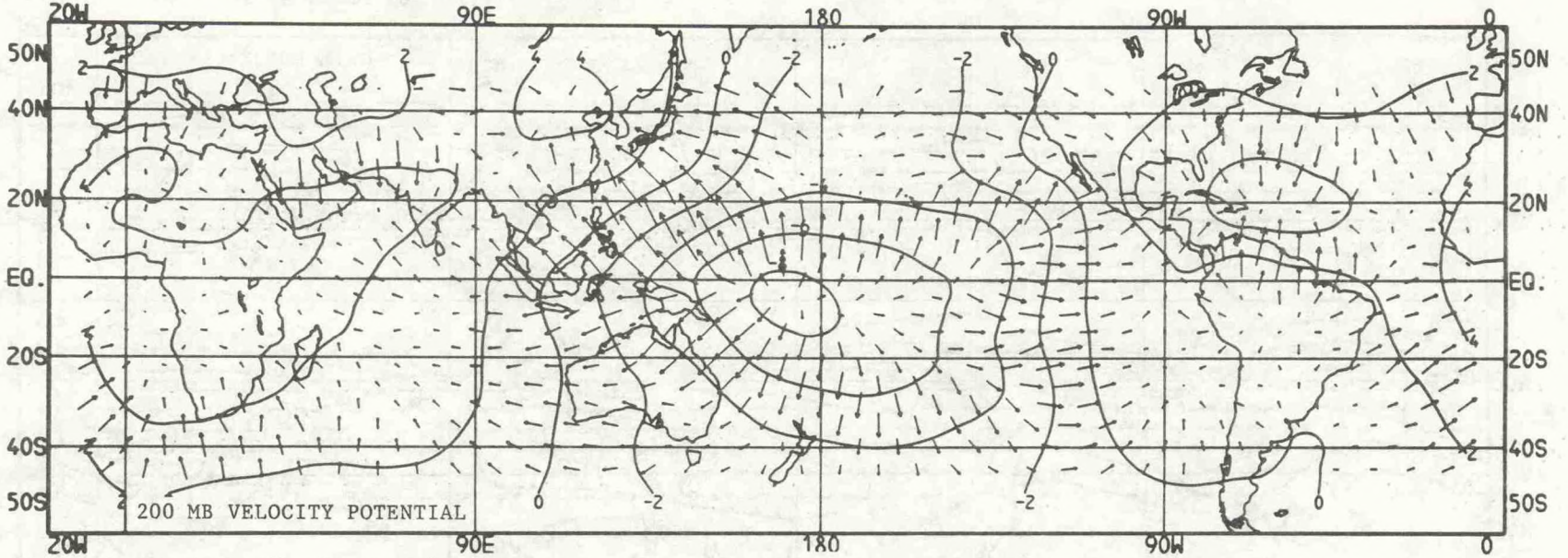

Figure 15. As in Fig. 7 except for March.

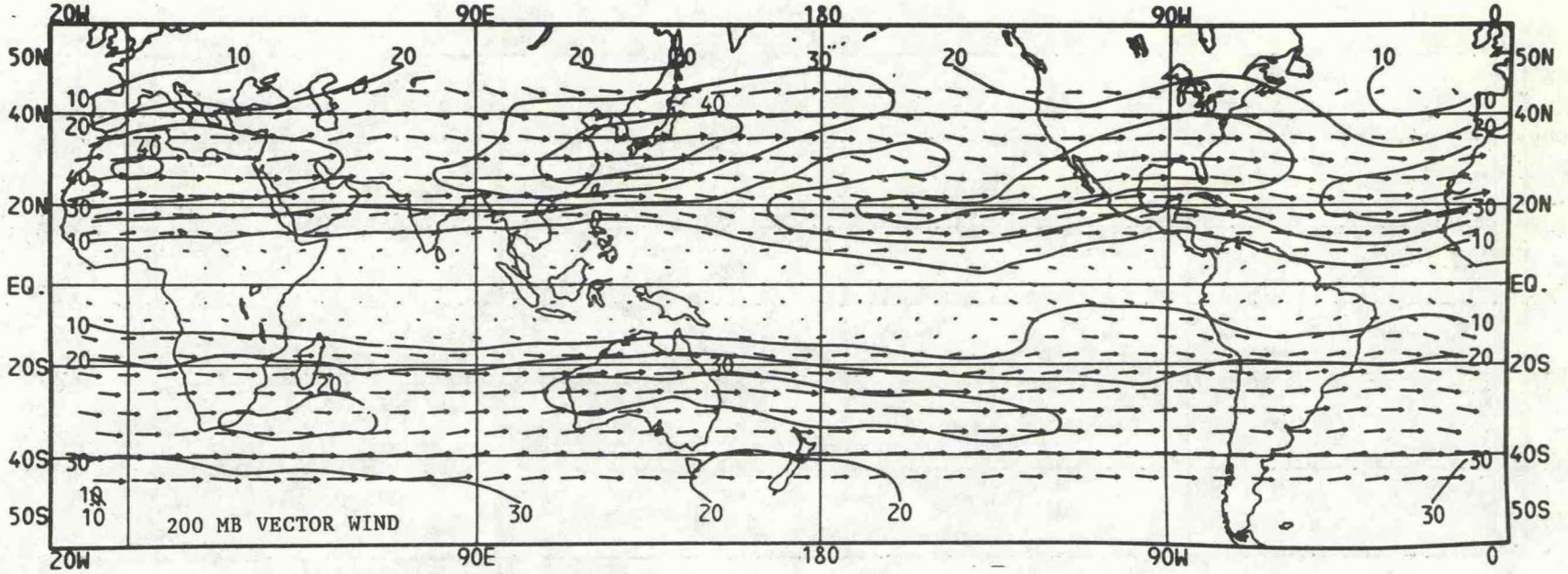

Figure 16. As in Fig. 4 except for April.

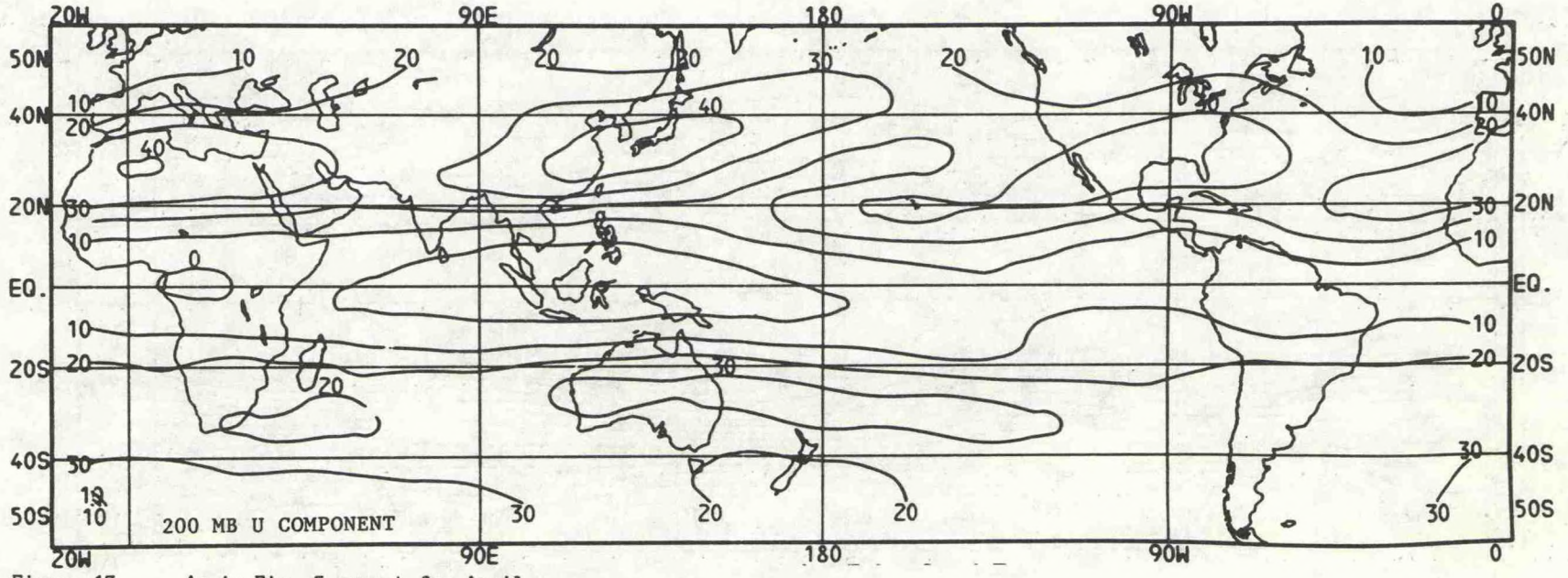

Figure 17. As in Fig. 5 except for April.

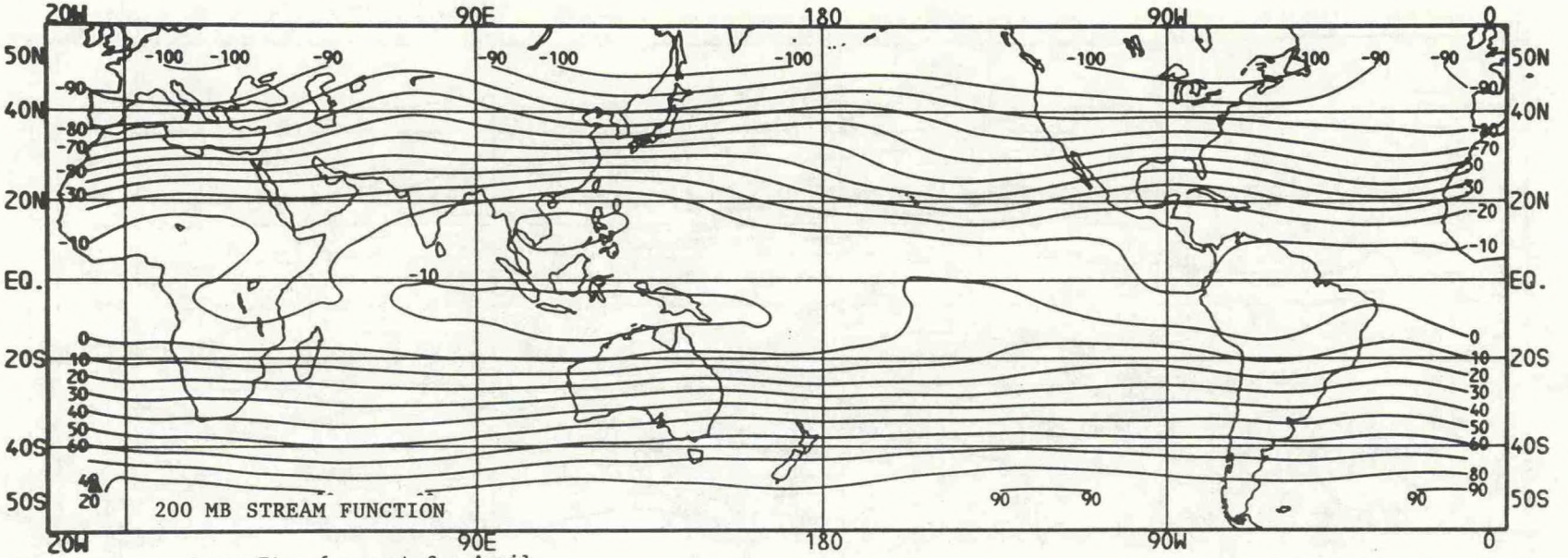

Figure 18. As in Fig. 6 except for April.

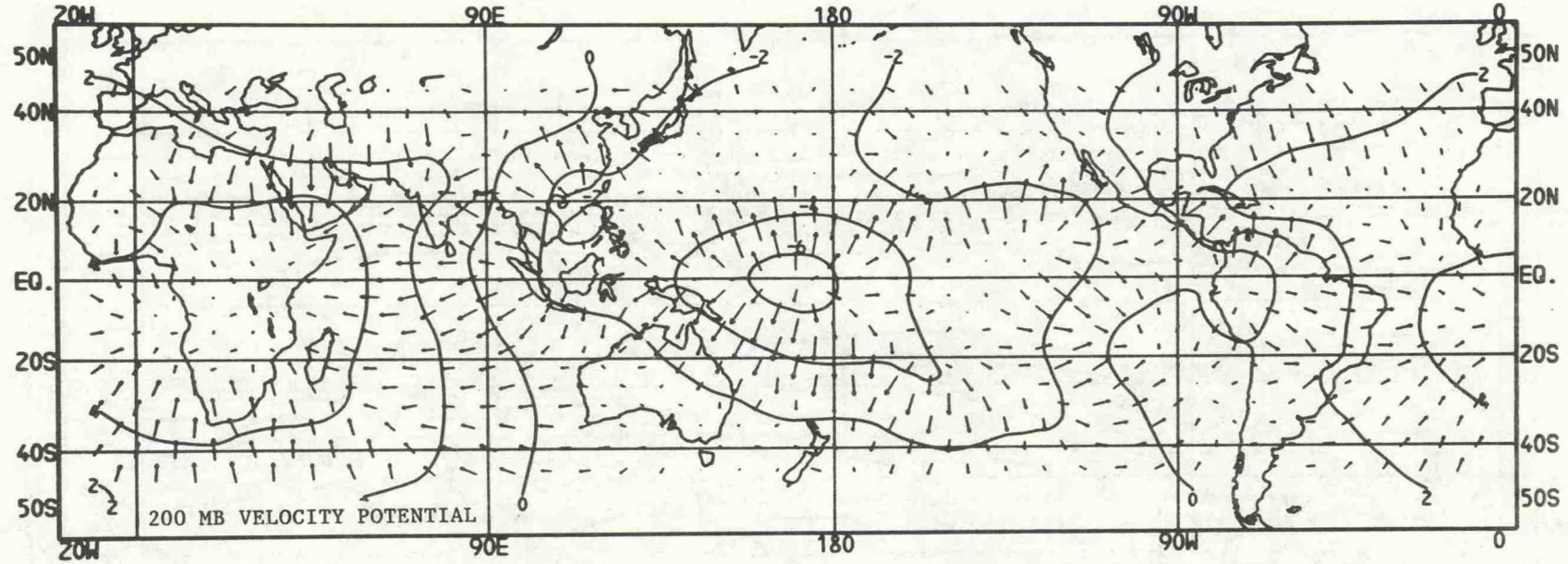

Figure 19. As in Fig. 7 except for April.

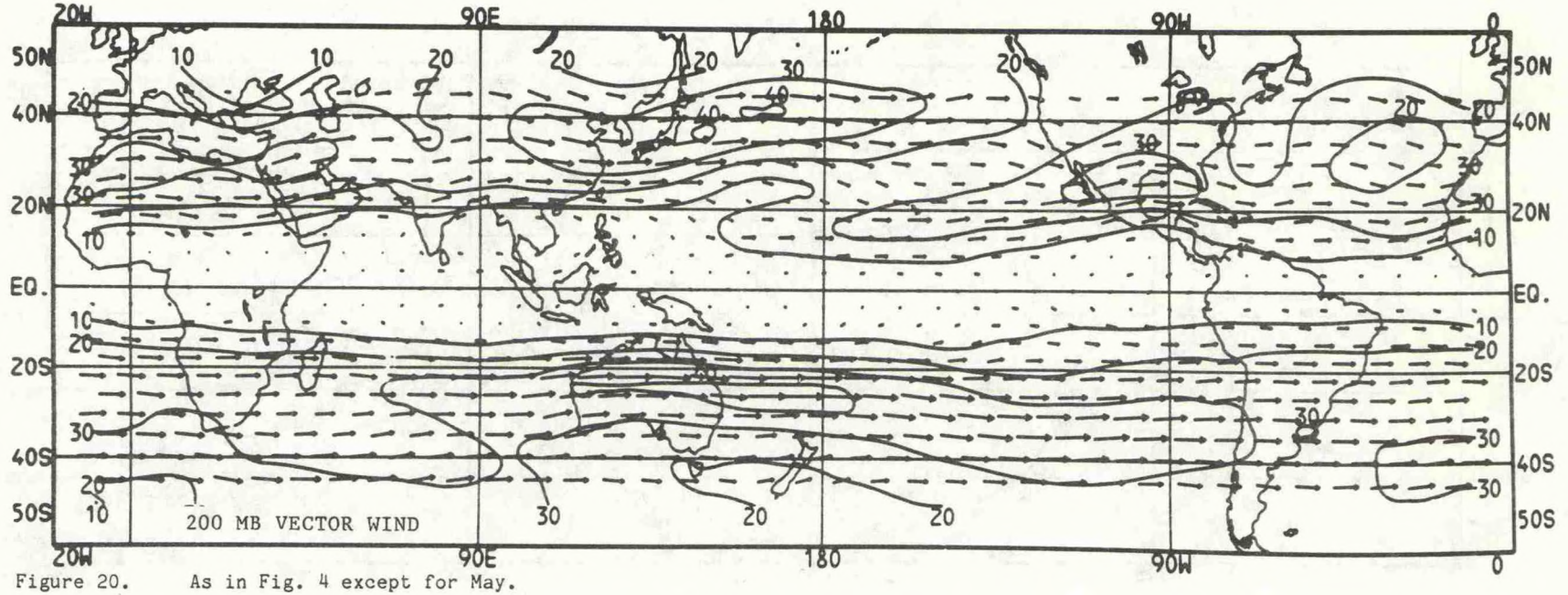

Figure 20. As in Fig. 4 except for May.

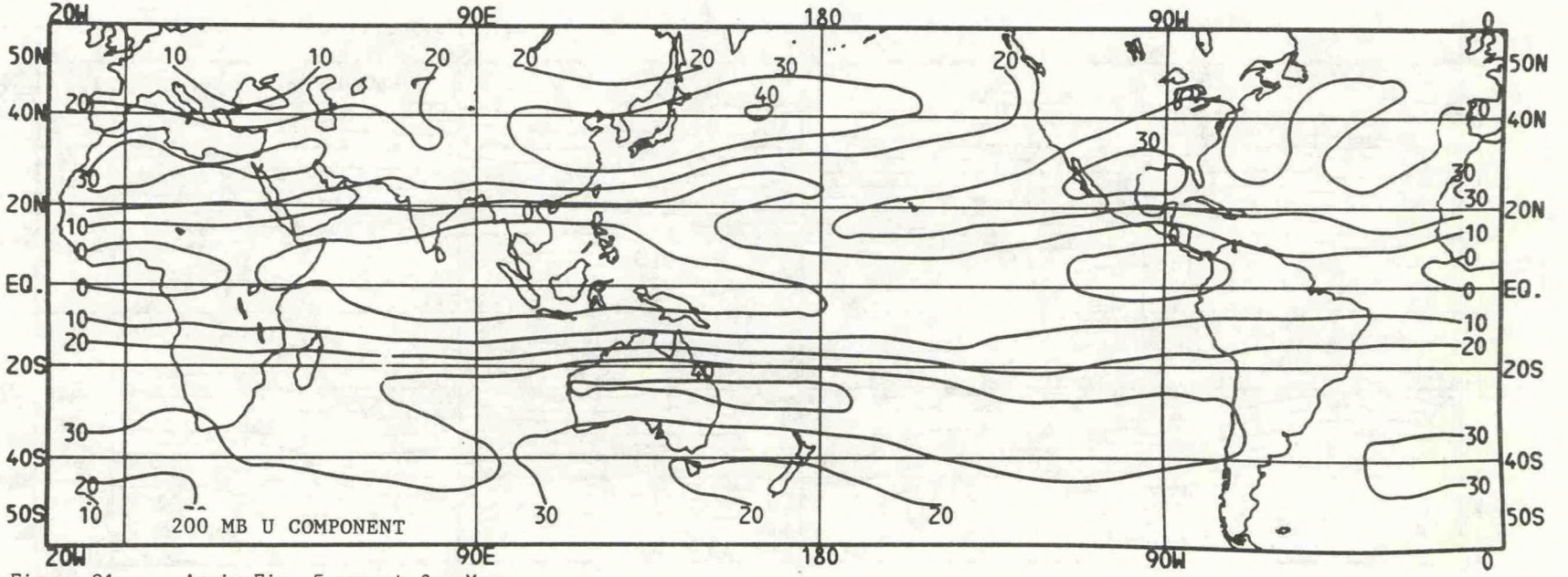

Figure 21. As in Fig. 5 except for May.

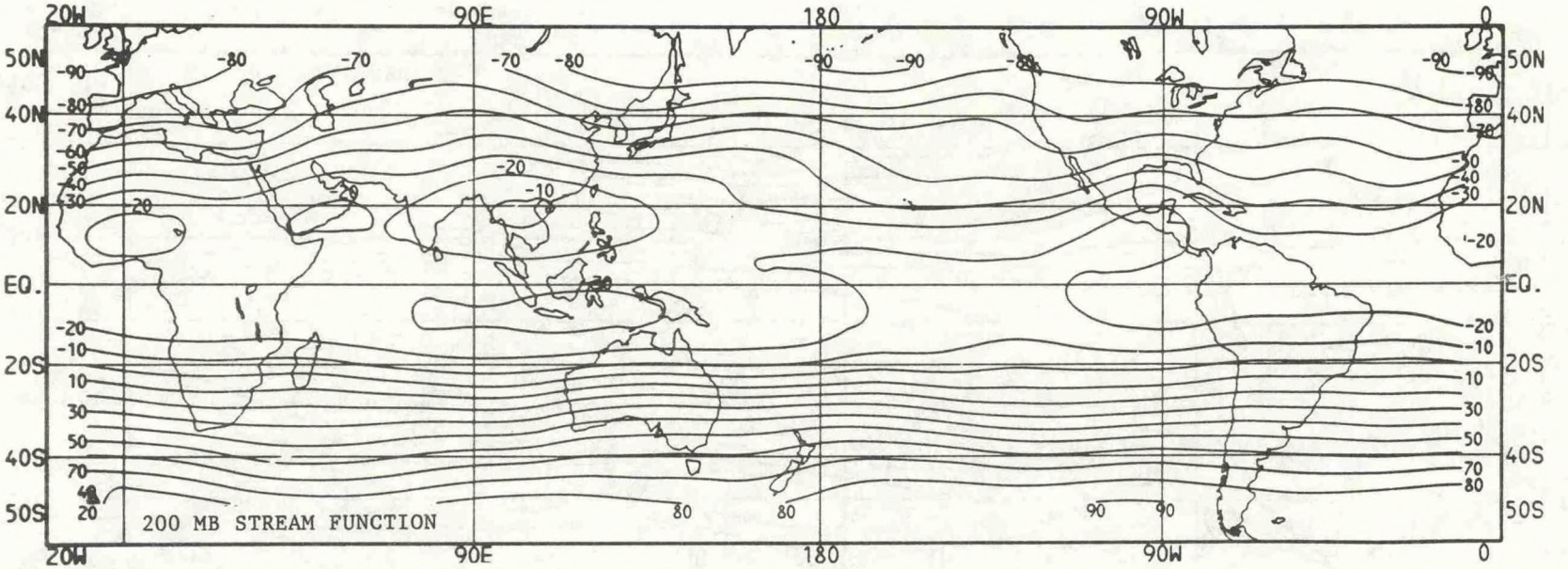

Figure 22. As in Fig. 6 except for May.

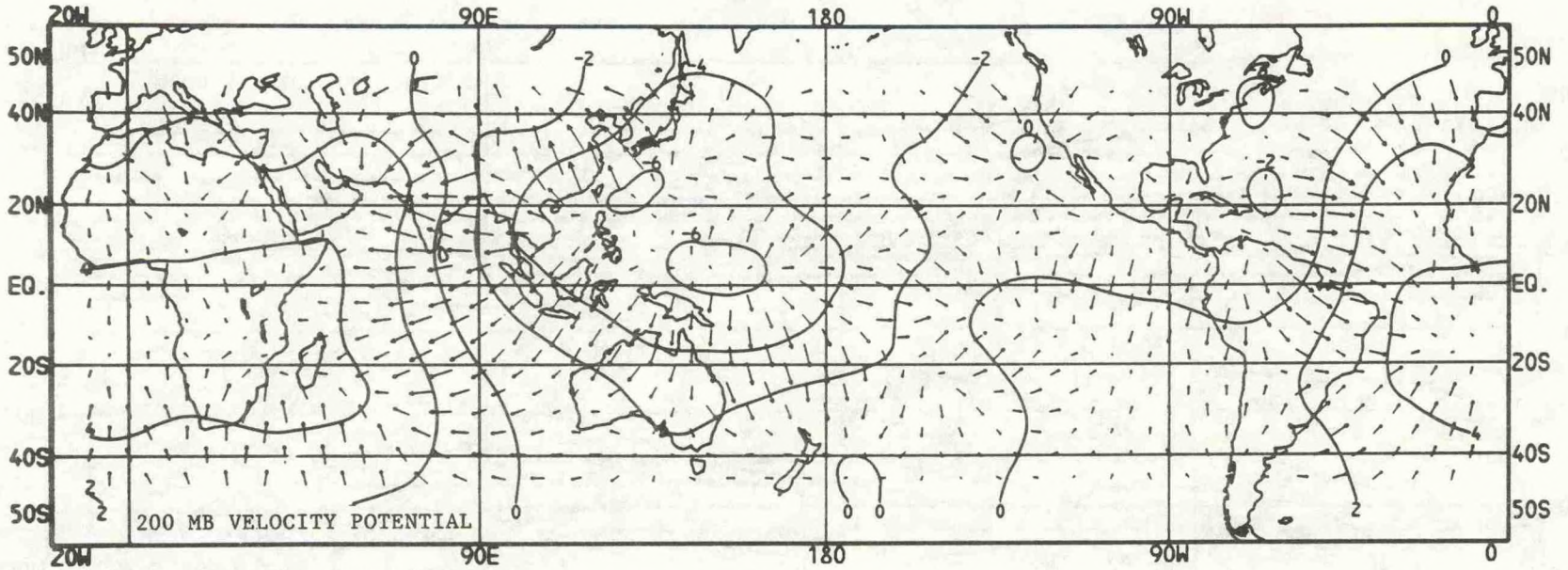

Figure 23. As in Fig. 7 except for May.

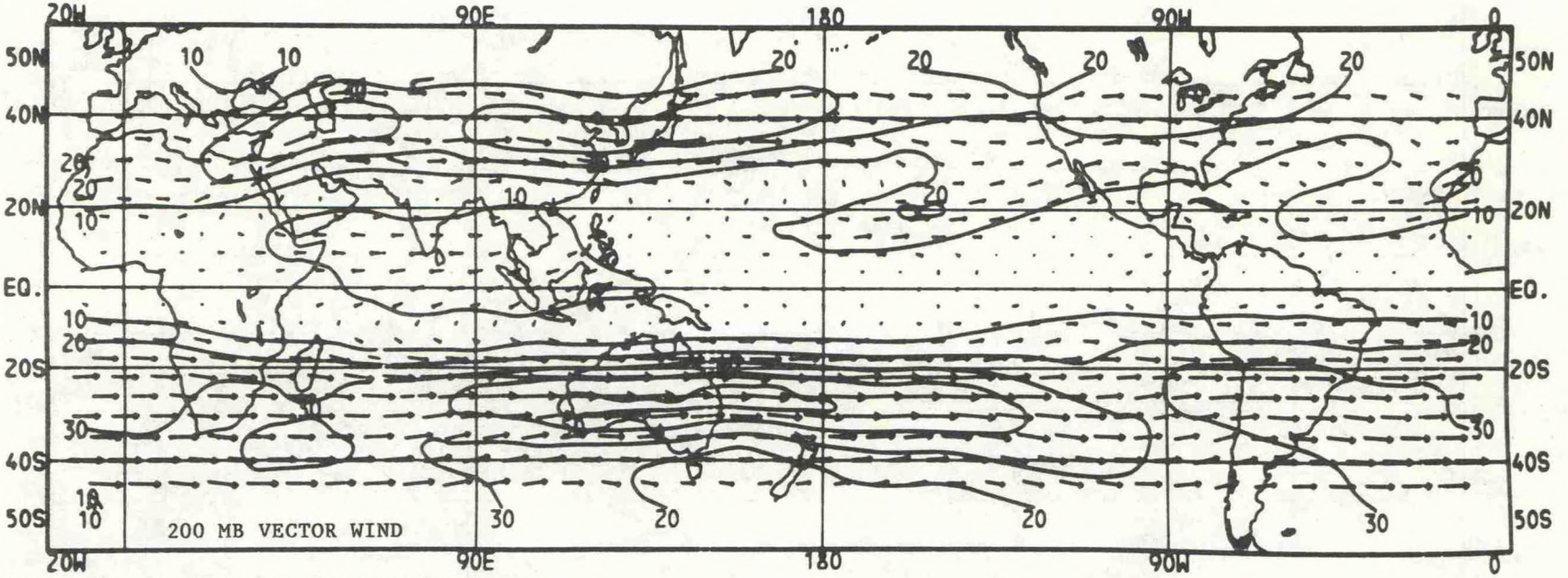

Figure 24. As in Fig. 4 except for June.

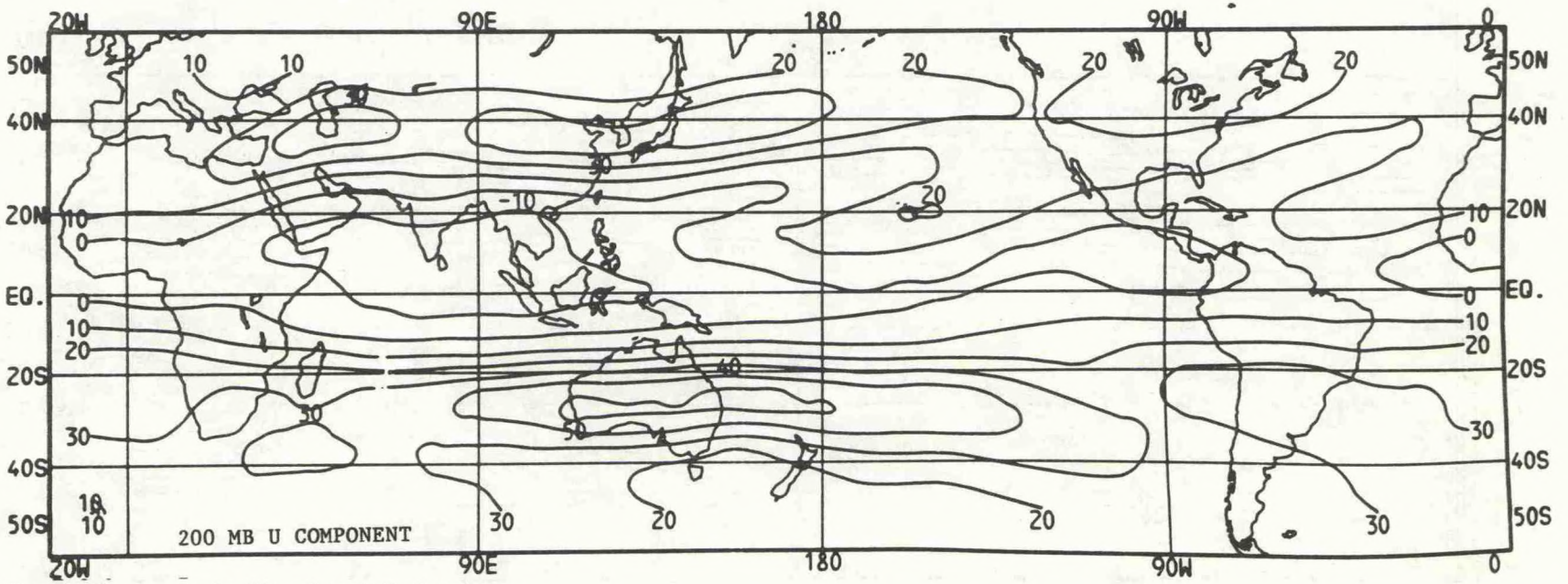

Figure 25. As in Fig. 5 except for June.

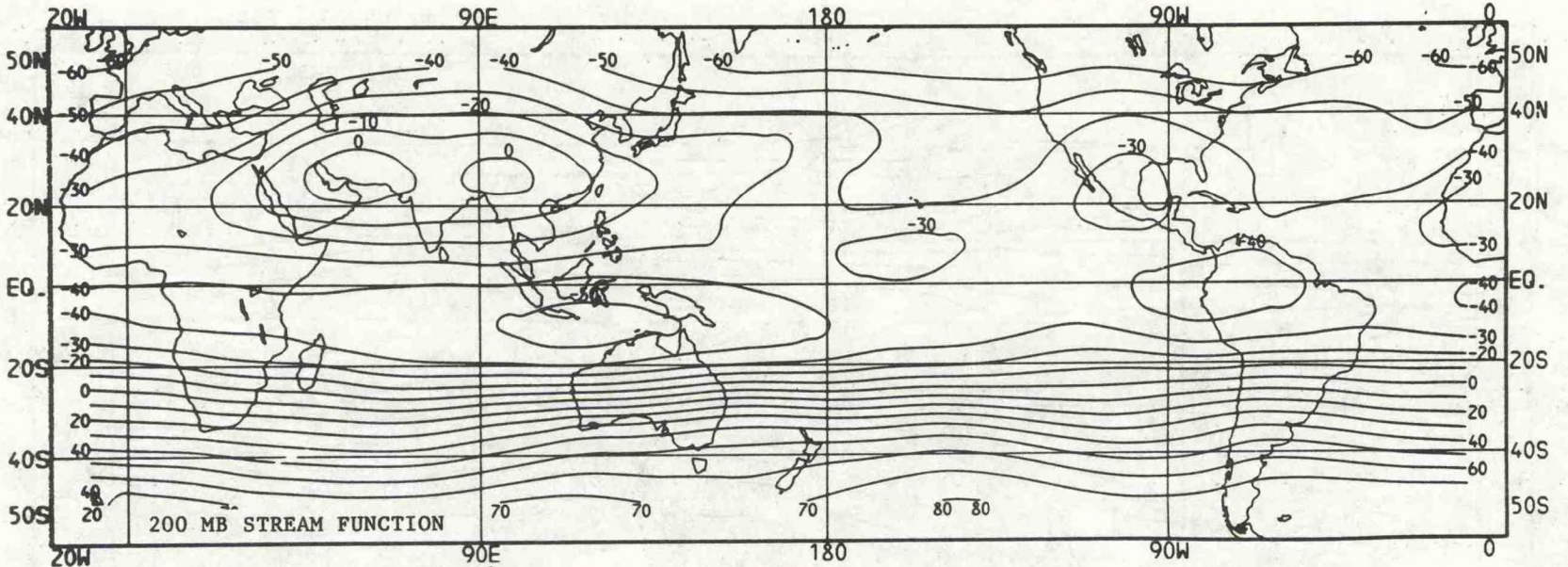

Figure 26. As in Fig. 6 except for June.

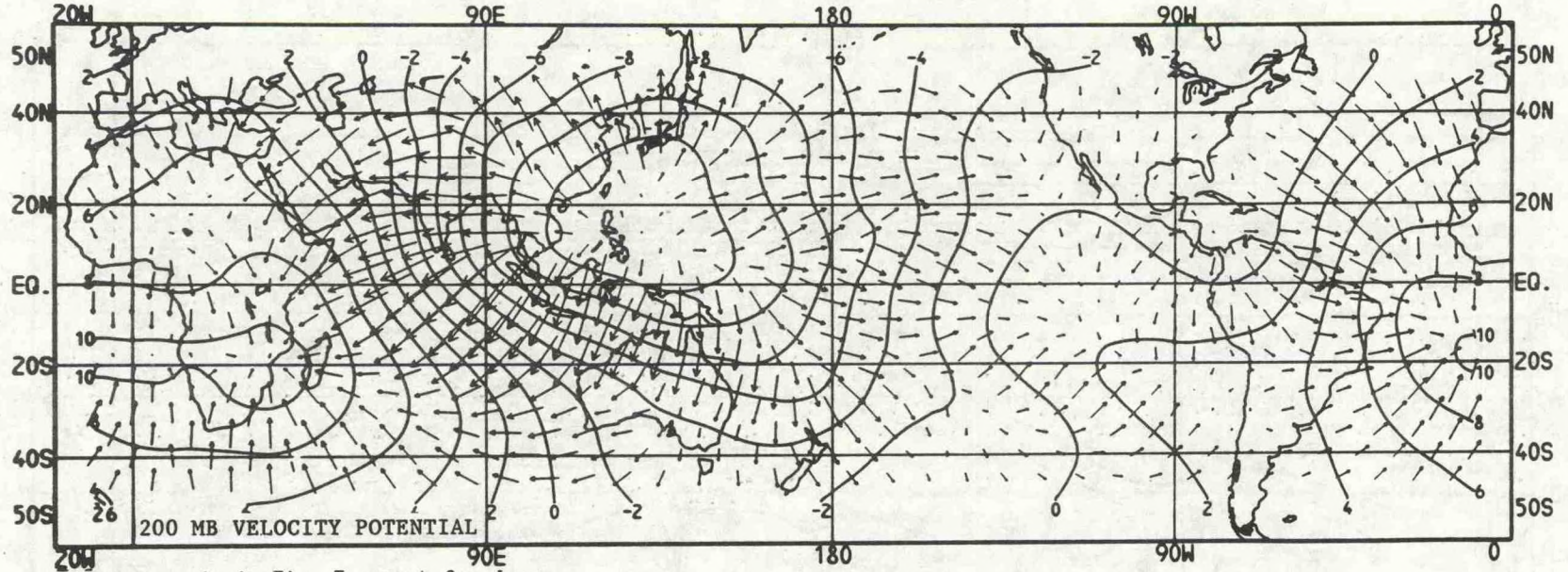

Figure 27. As in Fig. 7 except for June.

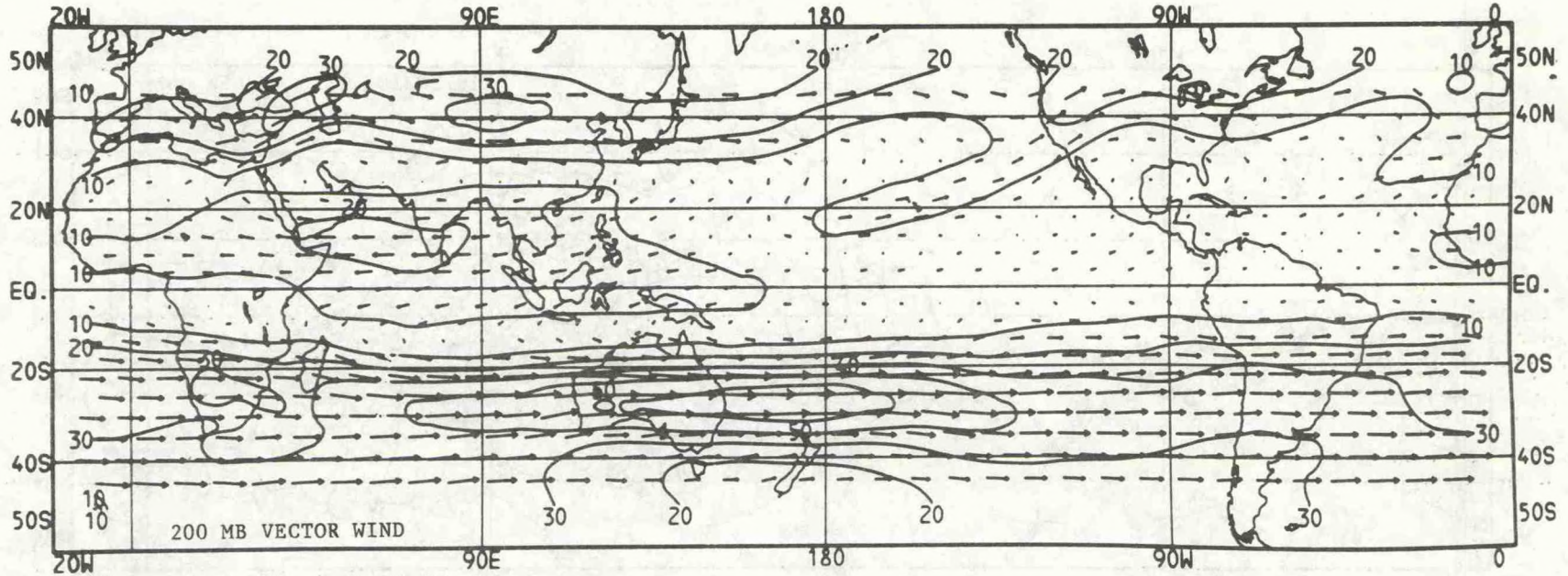

Figure 28. As in Fig. 4 except for July.

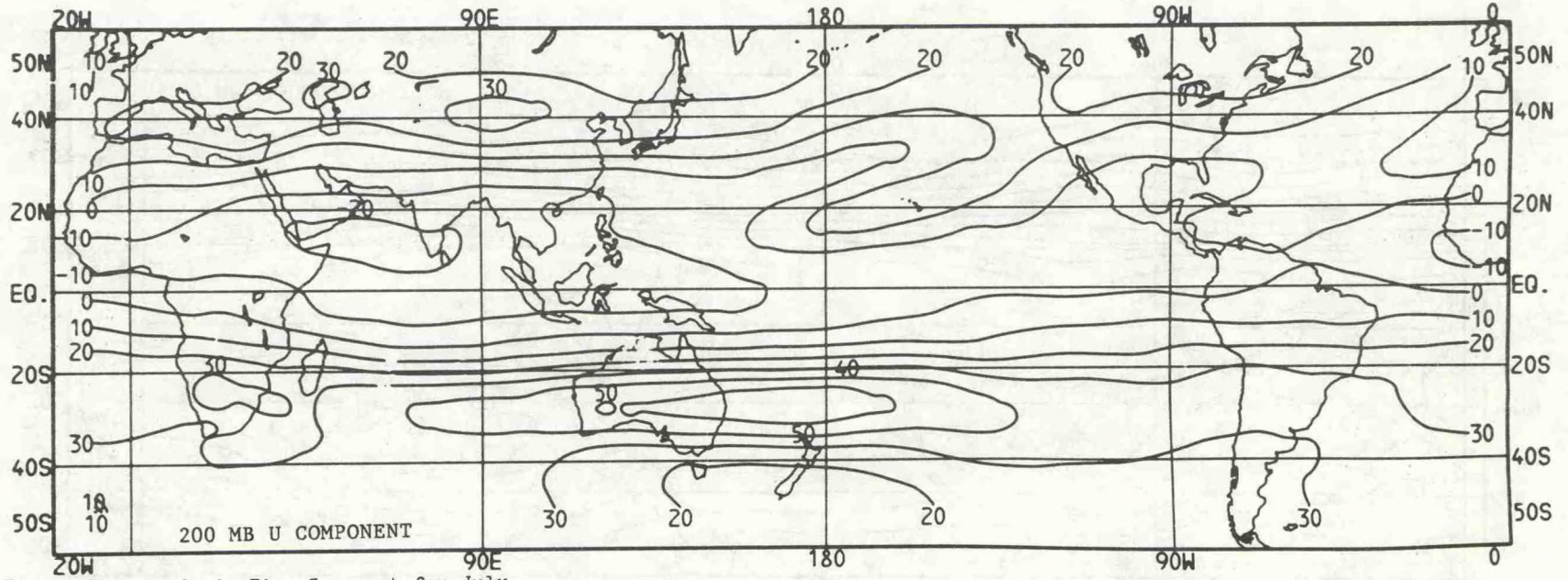

Figure 29. As in Fig. 5 except for July.

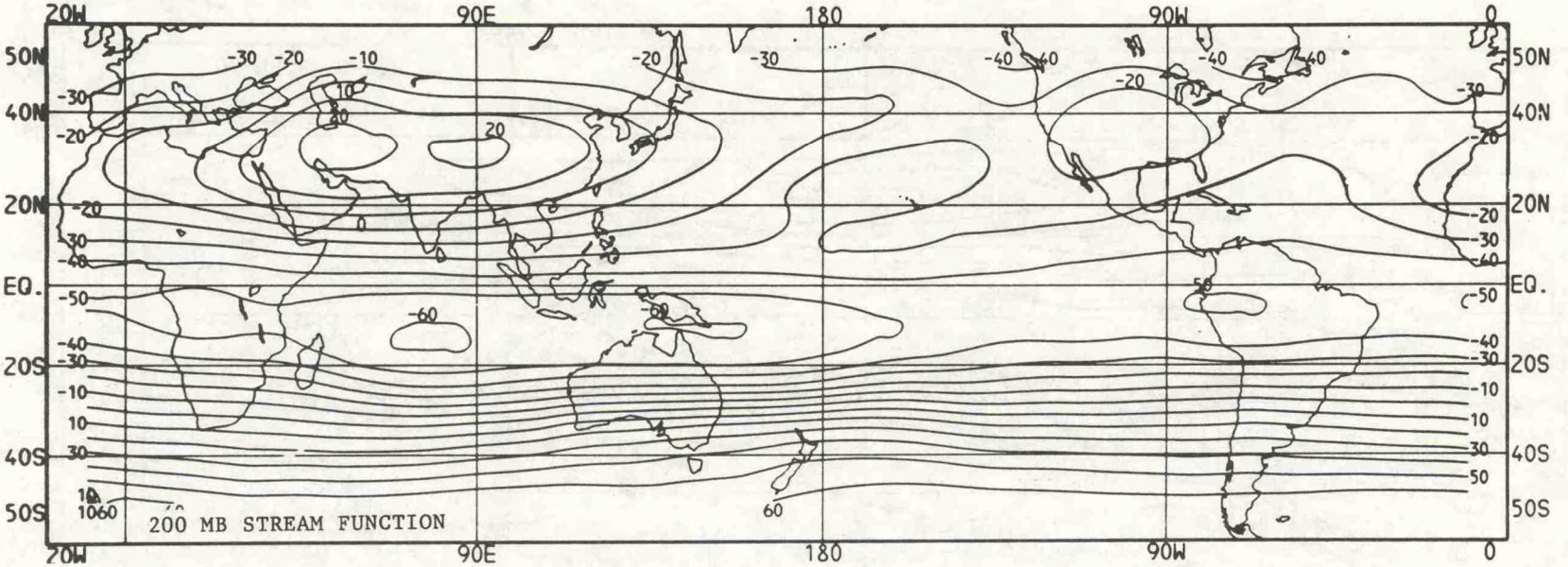

Figure 30. As in Fig. 6 except for July.

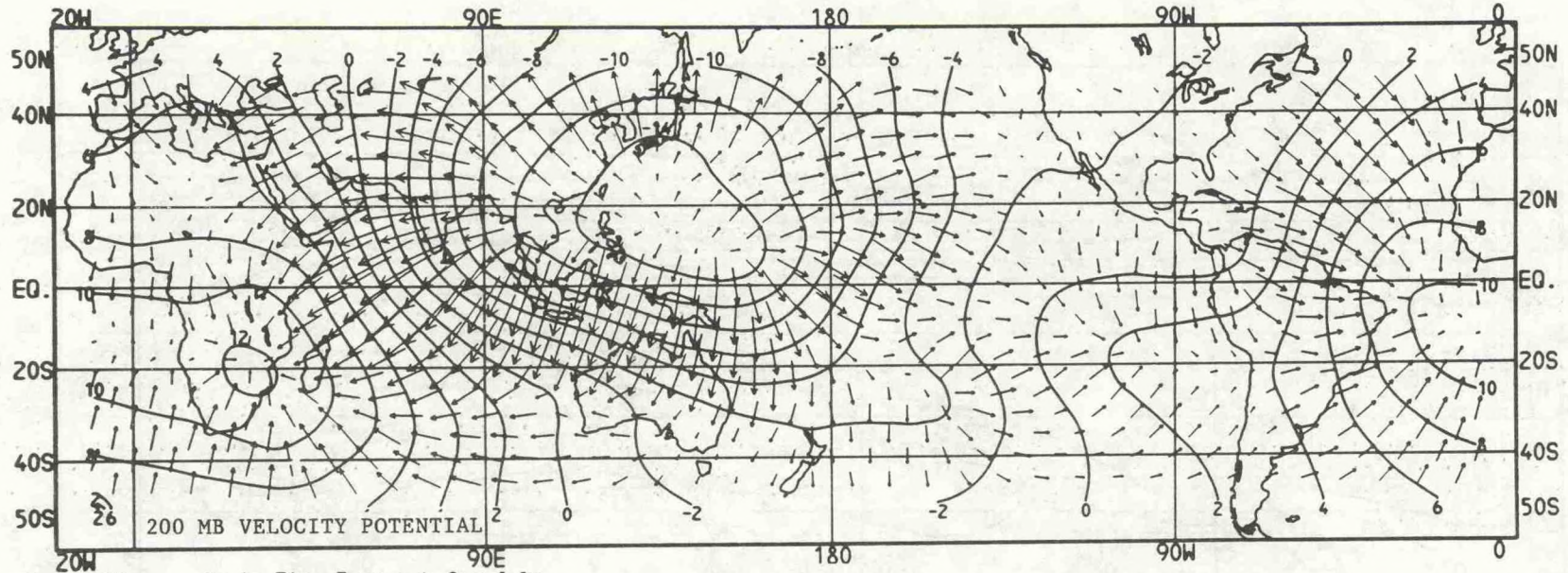

Figure 31. As in Fig. 7 except for July.

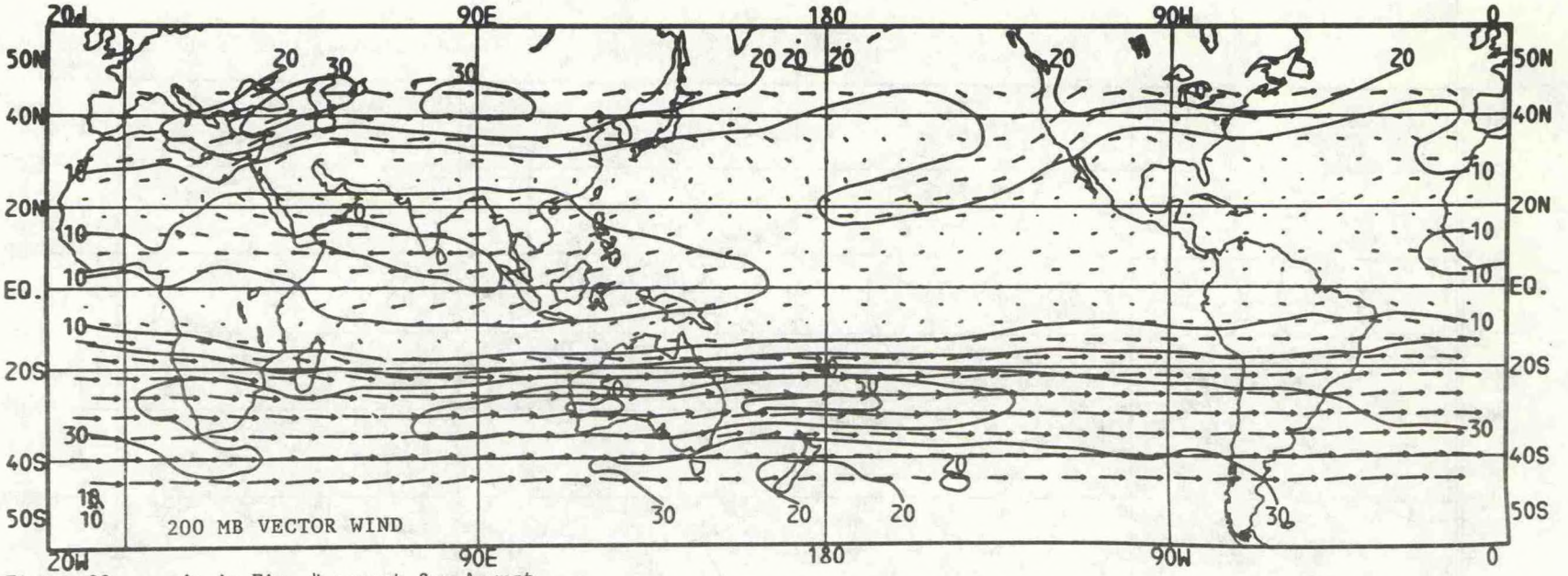

Figure 32. As in Fig. 4 except for August.

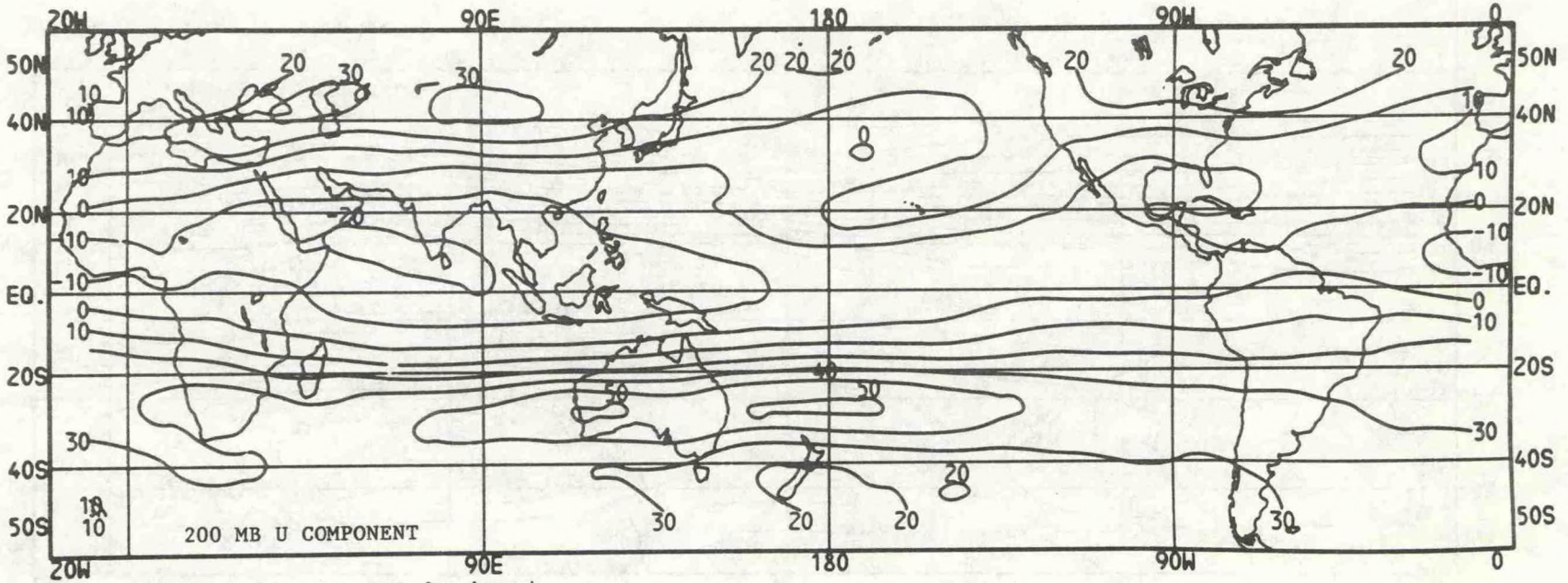

Figure 33. As in Fig. 5 except for August.

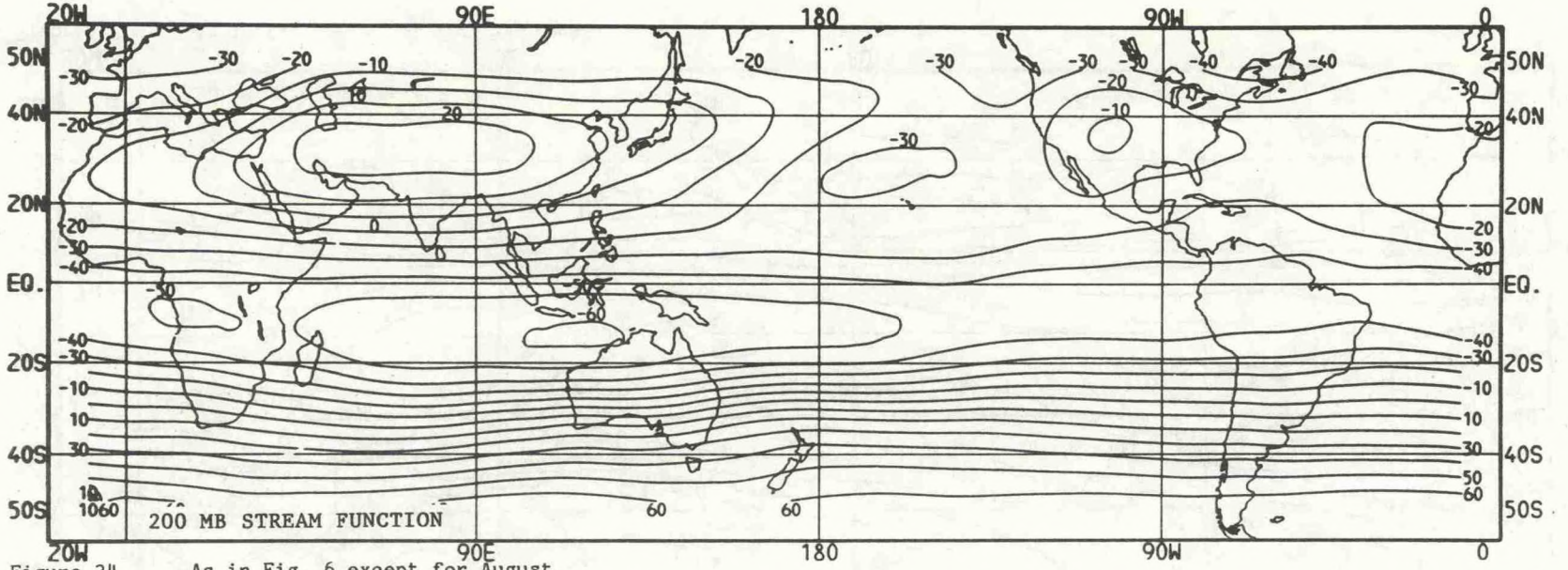

Figure 34. As in Fig. 6 except for August.

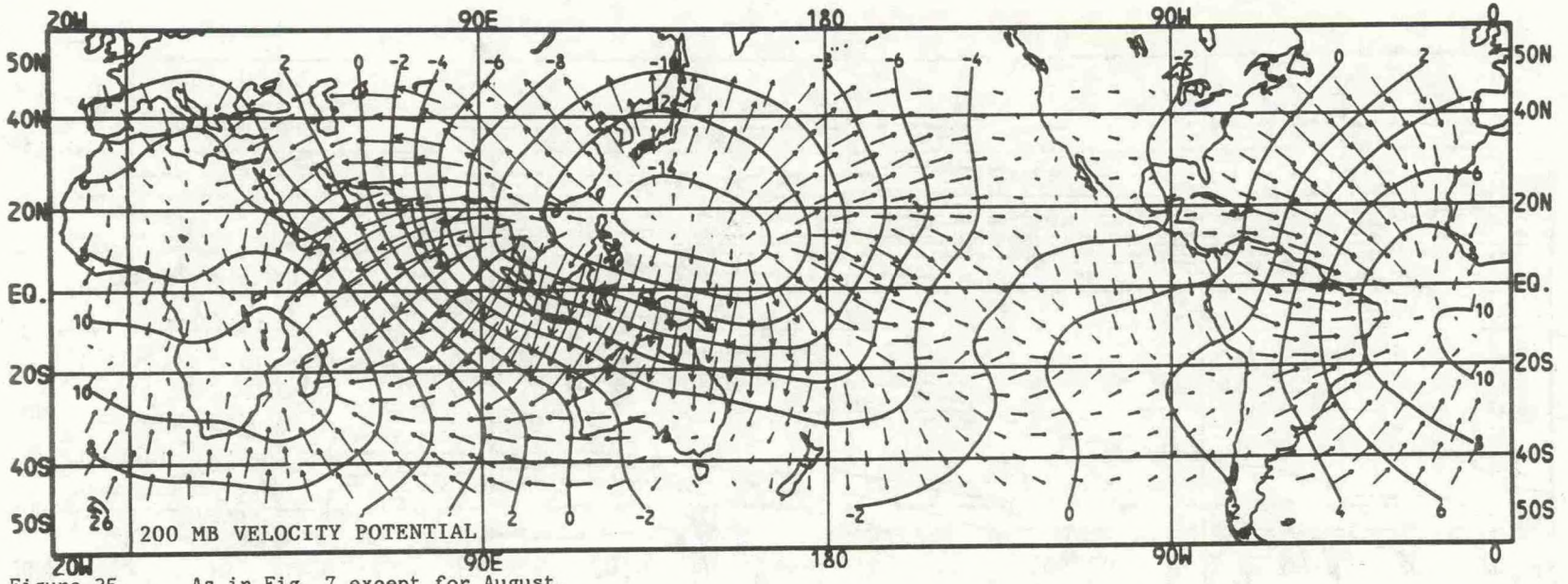

Figure 35. As in Fig. 7 except for August.

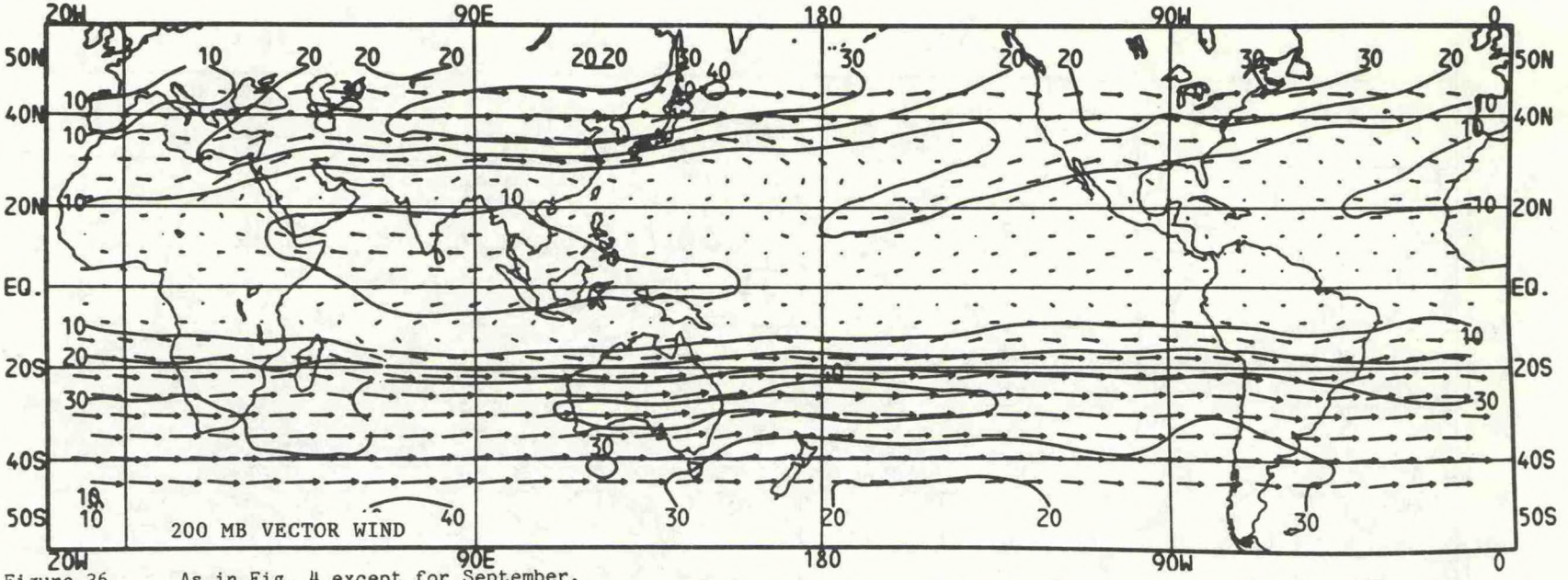

Figure 36. As in Fig. 4 except for September.

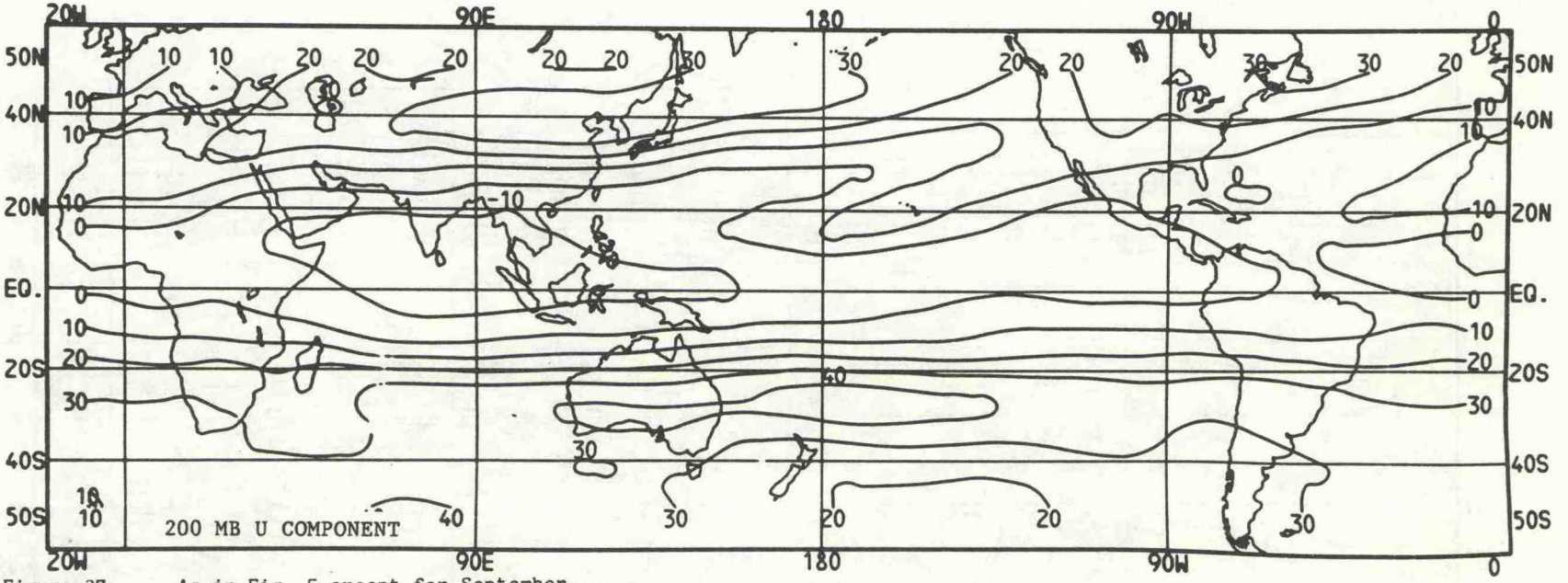

Figure 37. As in Fig. 5 except for September.

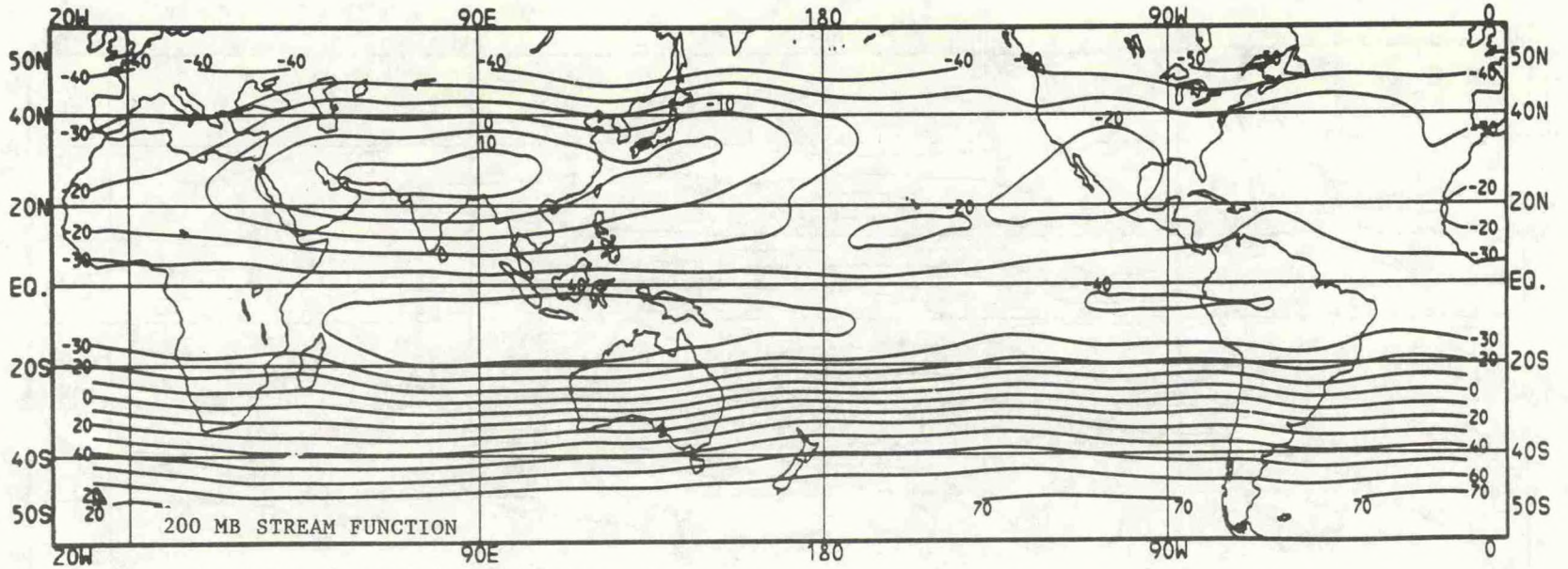

Figure 38. As in Fig. 6 except for September.

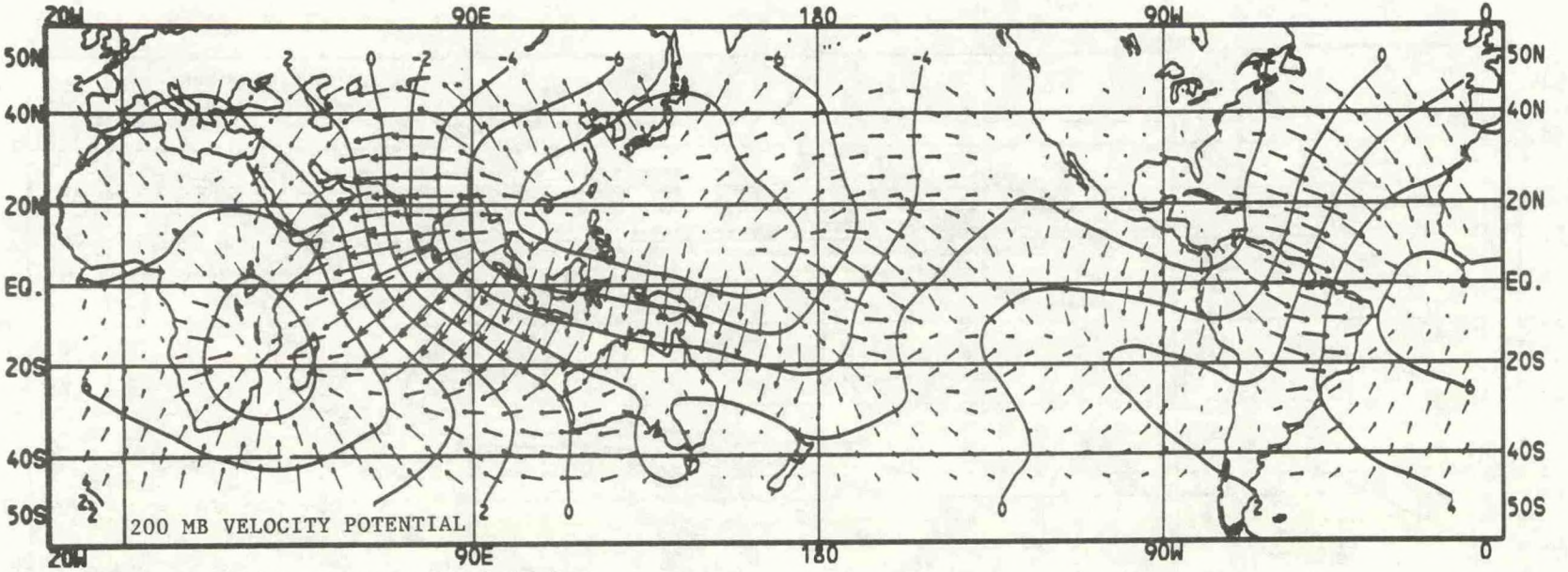

Figure 39. As in Fig. 7 except for September.

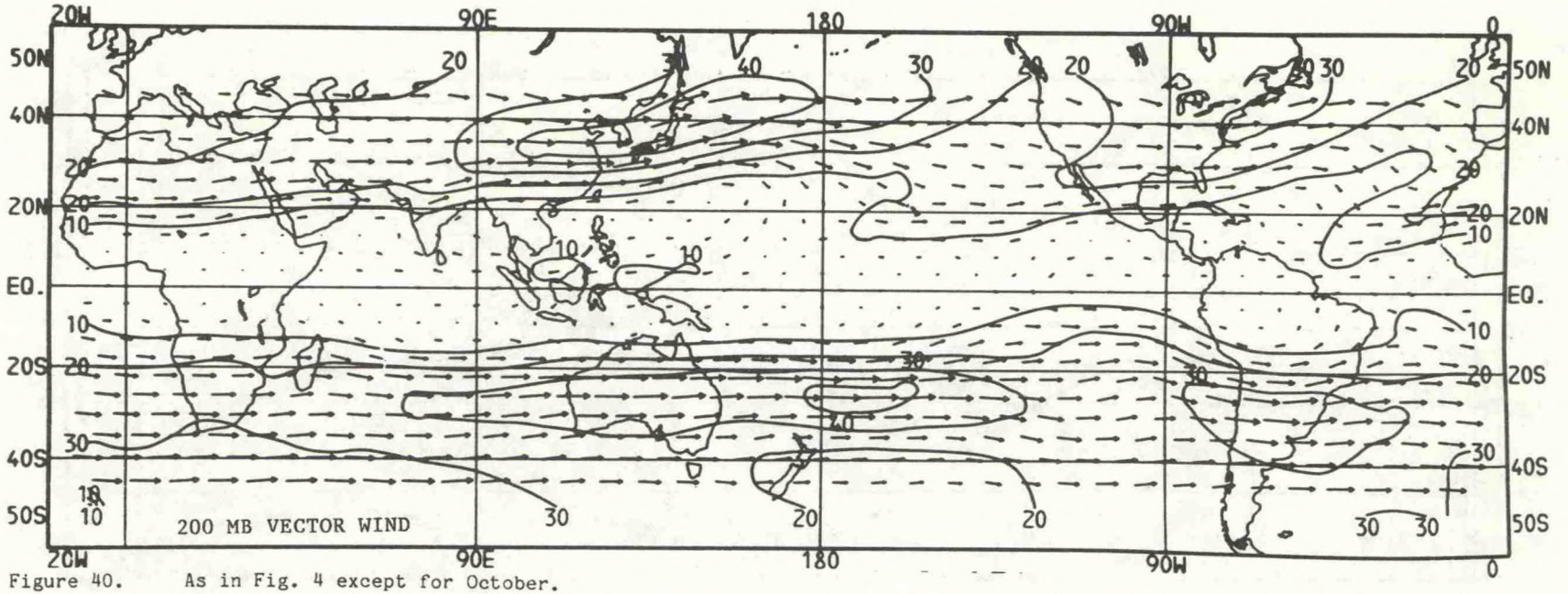

Figure 40. As in Fig. 4 except for October.

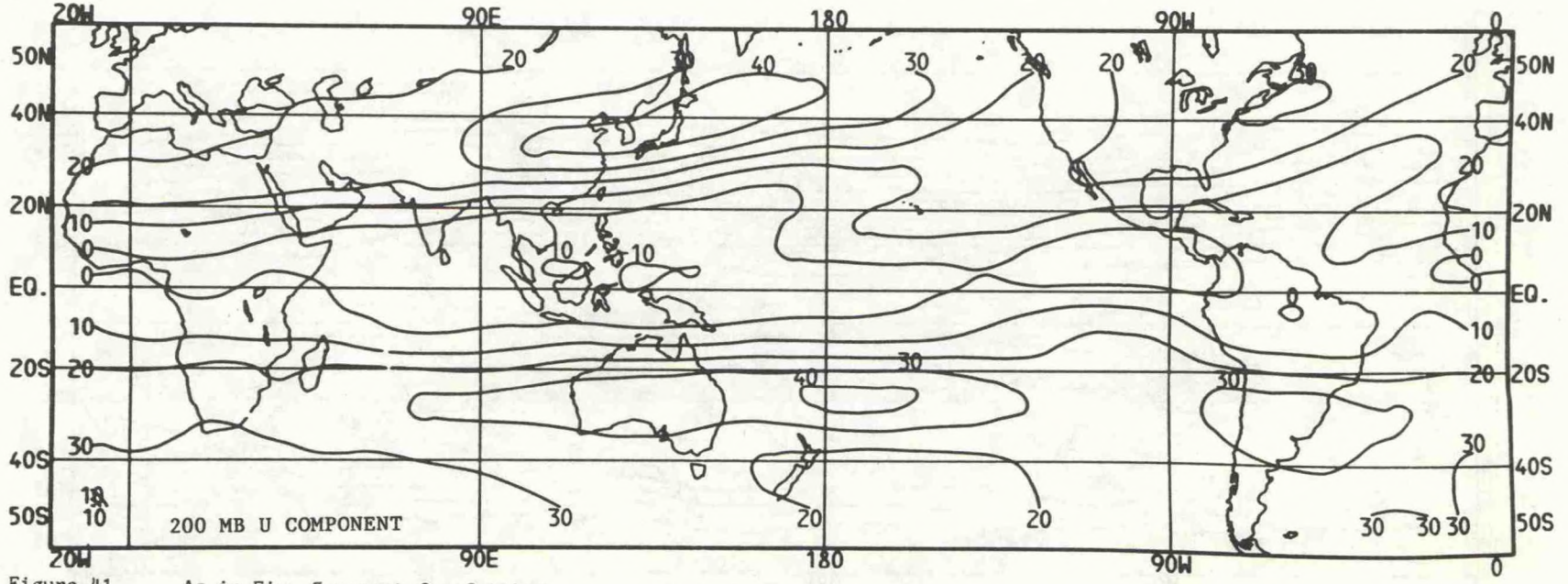

Figure 41. As in Fig. 5 except for October.

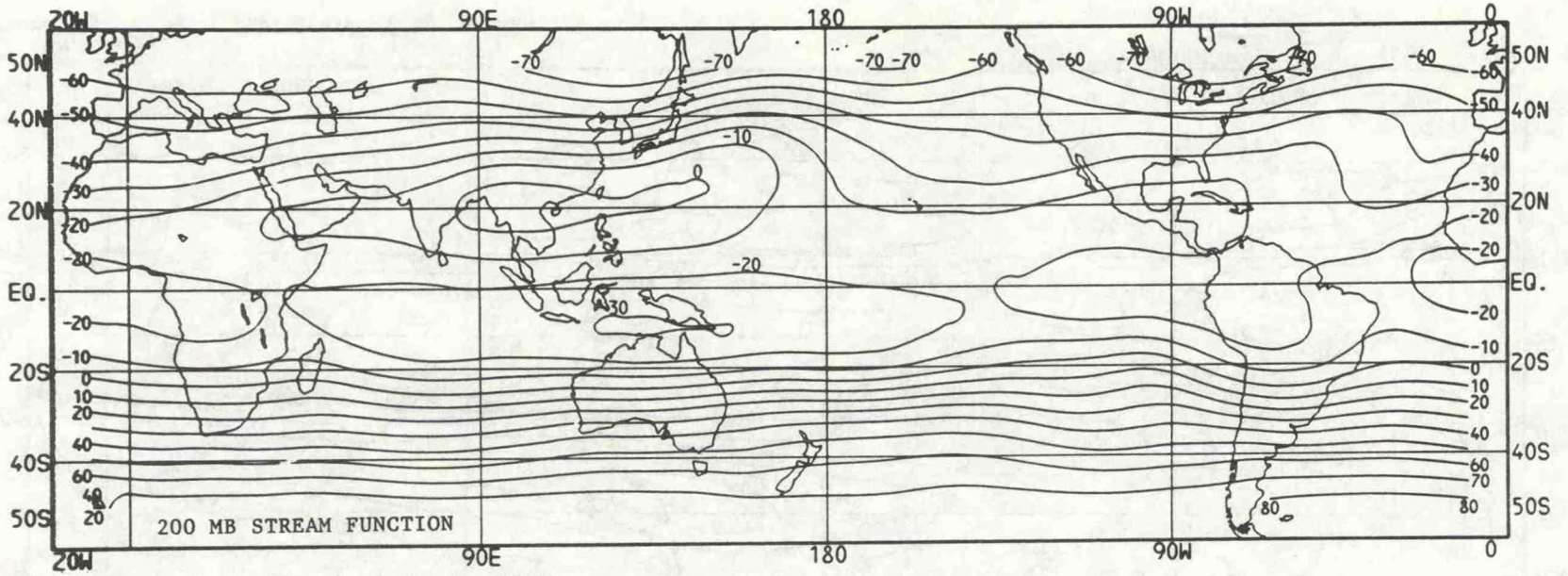

Figure 42. As in Fig. 6 except for October.

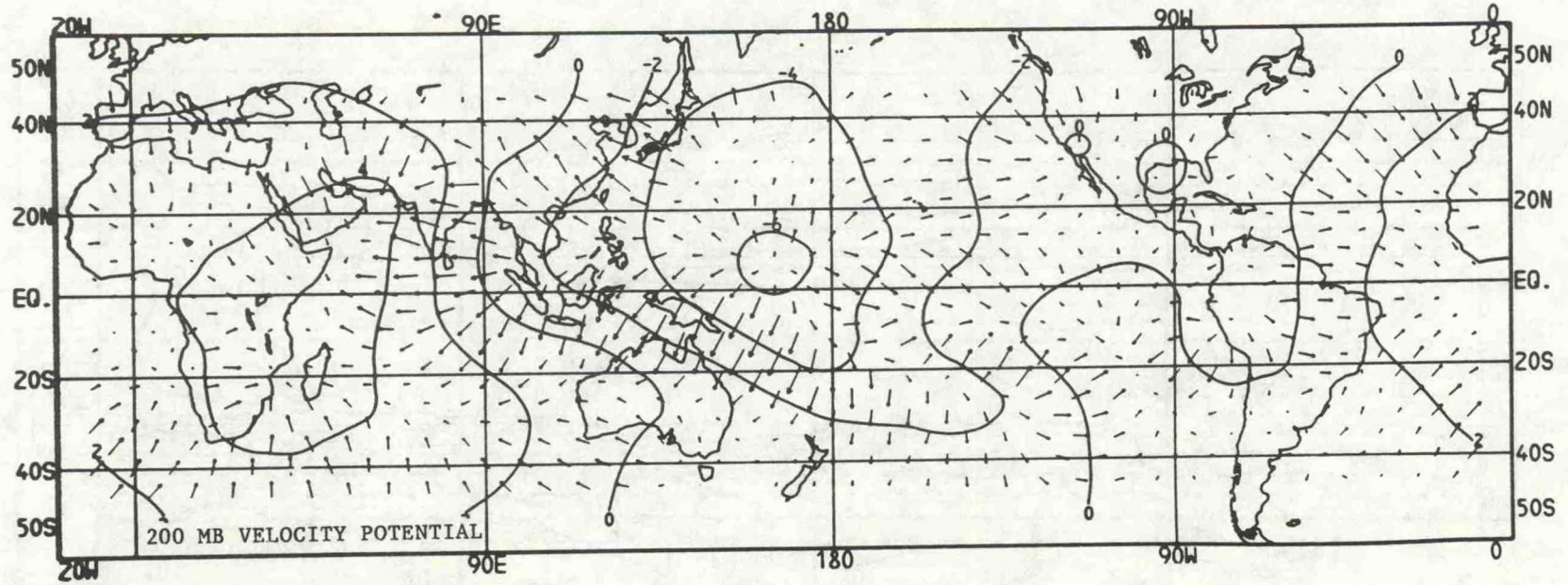

Figure 43. As in Fig. 7 except for October.

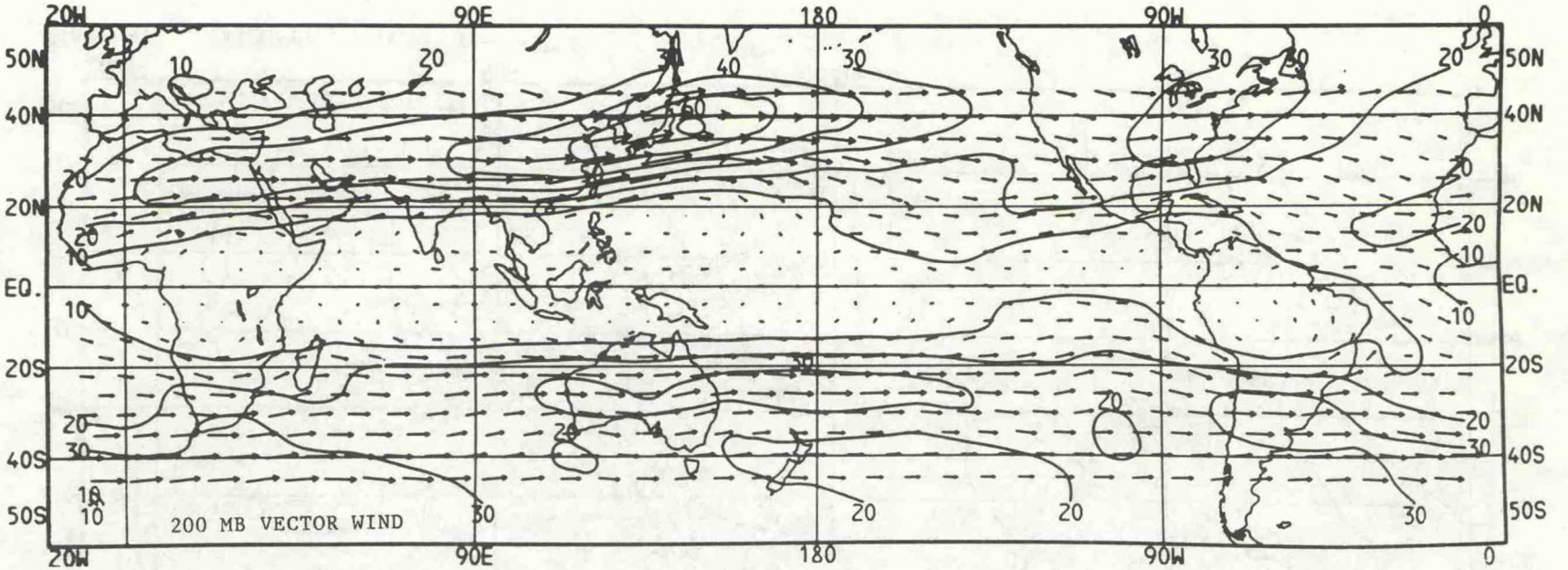

Figure 44. As in Fig. 4 except for November.

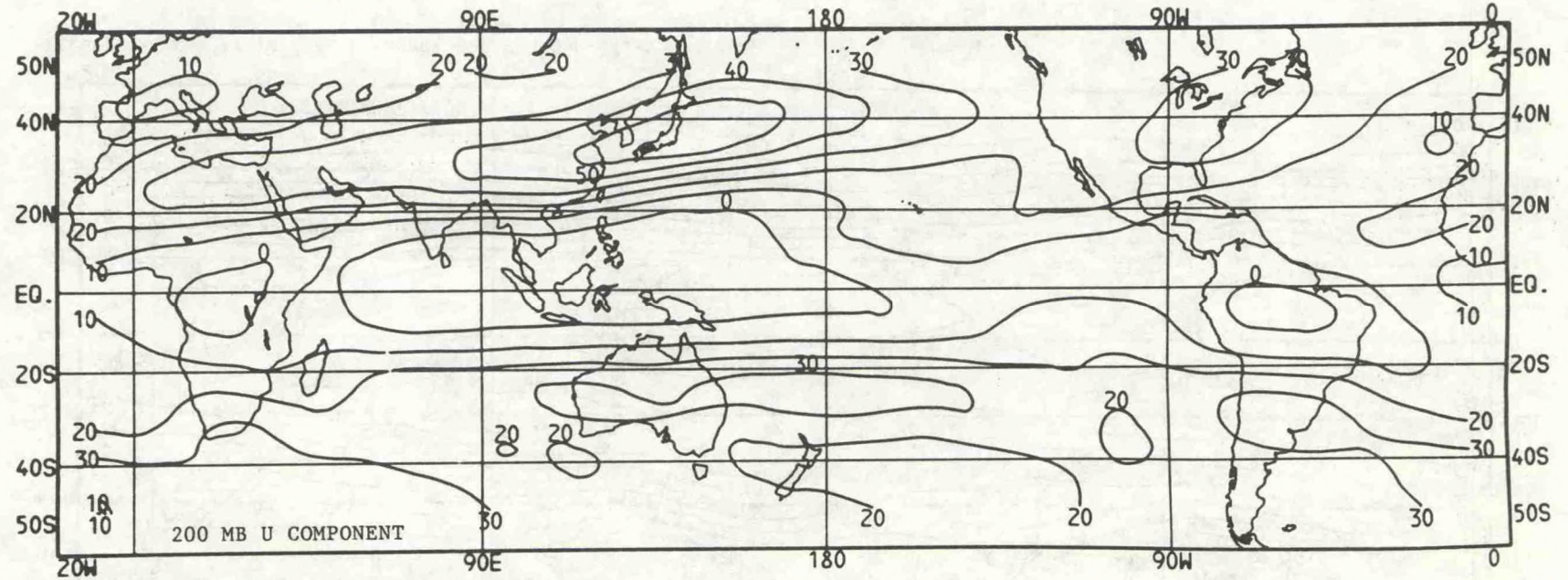

Figure 45. As in Fig. 5 except for November.

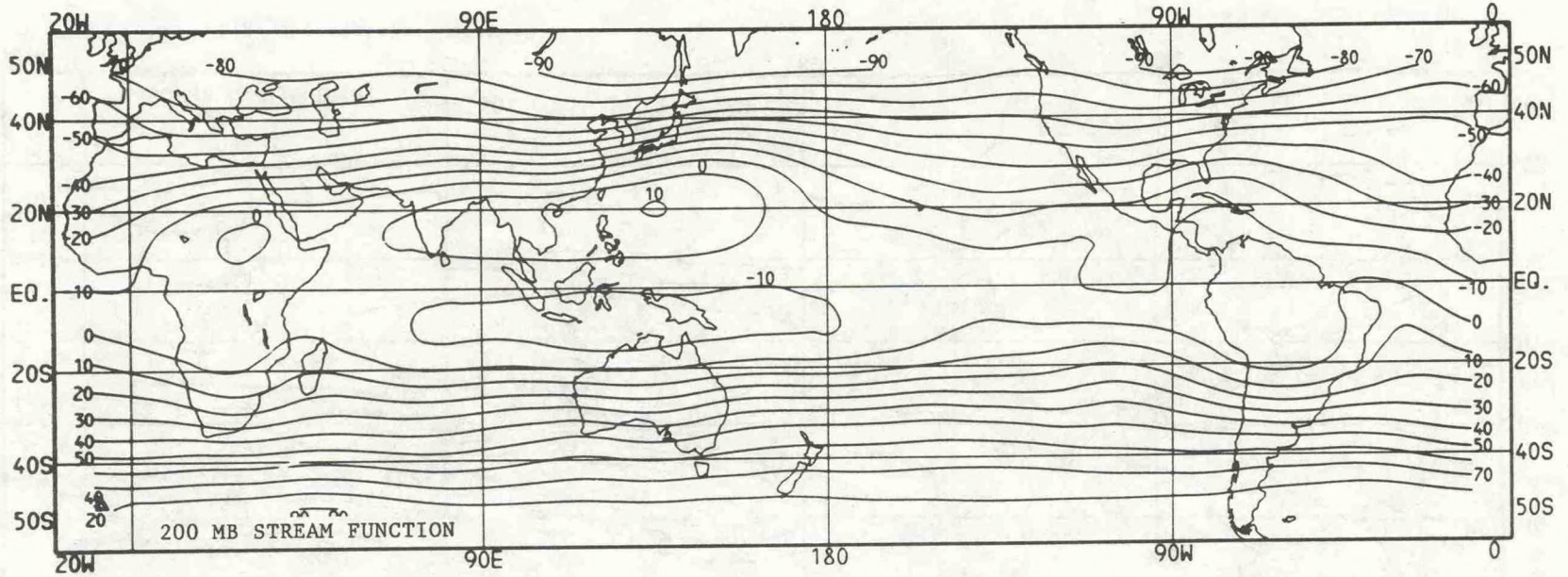

Figure 46. As in Fig. 6 except for November.

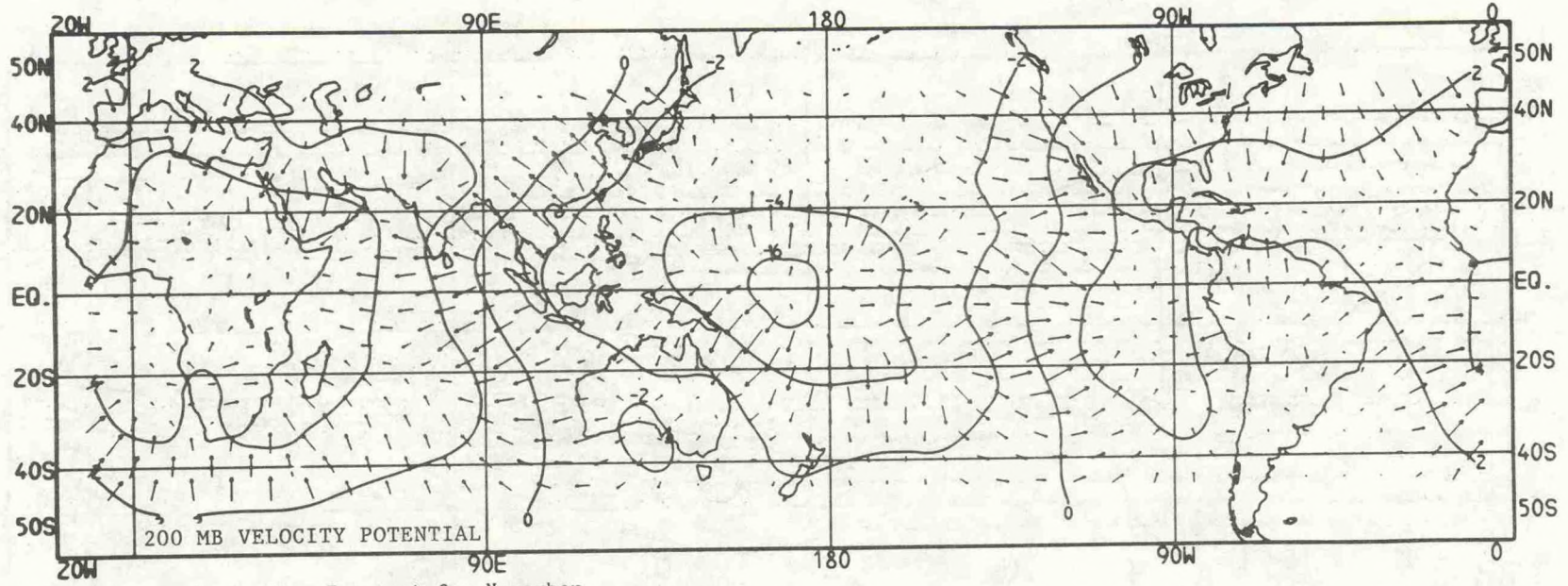

Figure 47. As in Fig. 7 except for November.

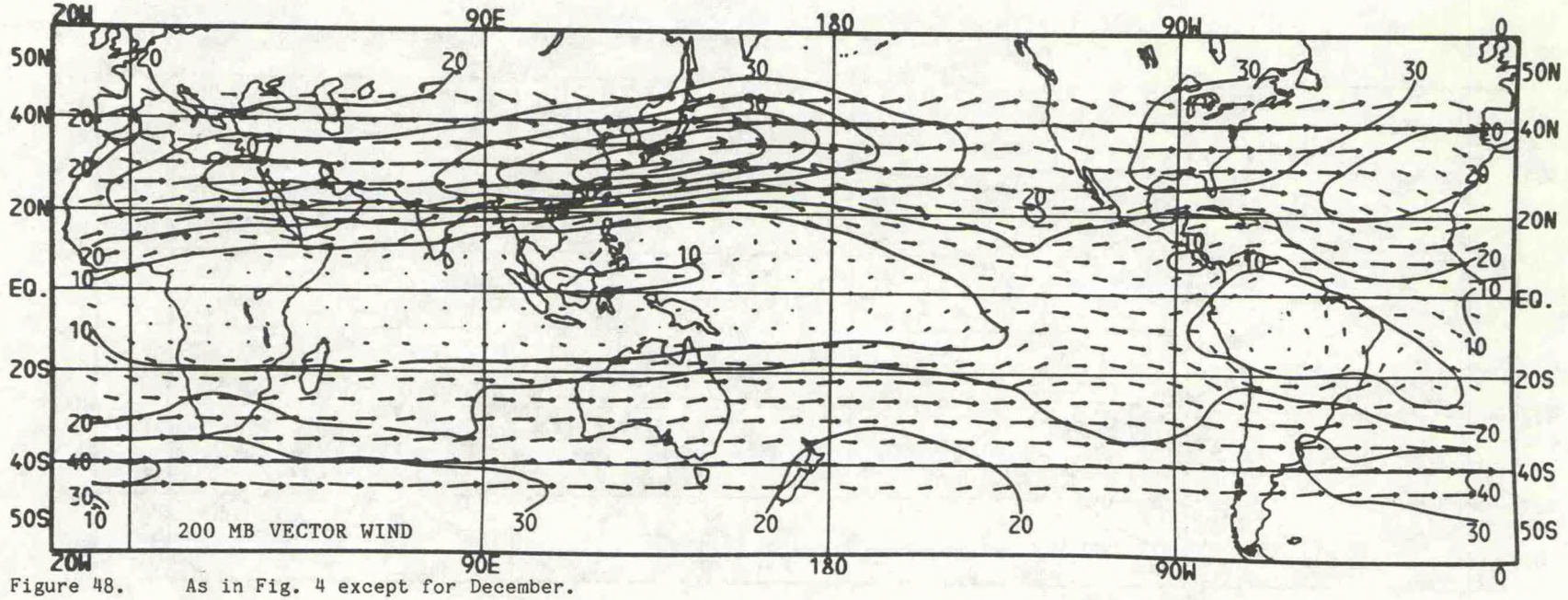

Figure 48. As in Fig. 4 except for December.

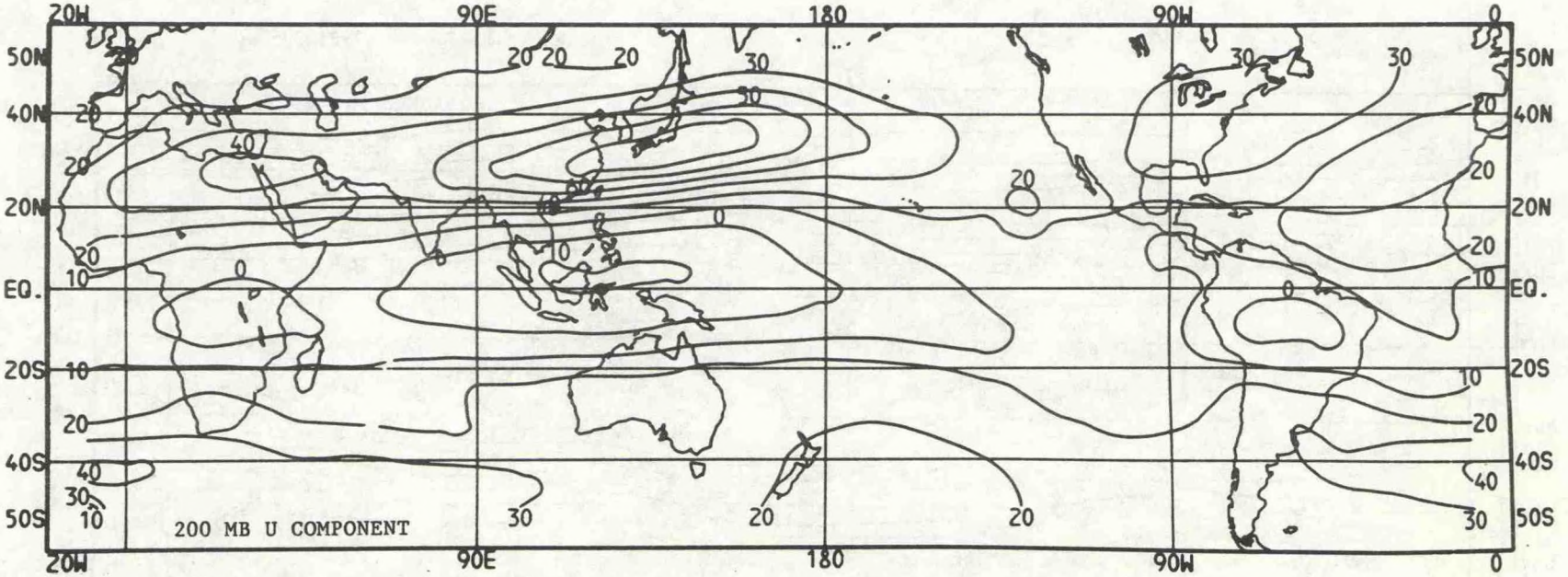

Figure 49. As in Fig. 5 except for December.

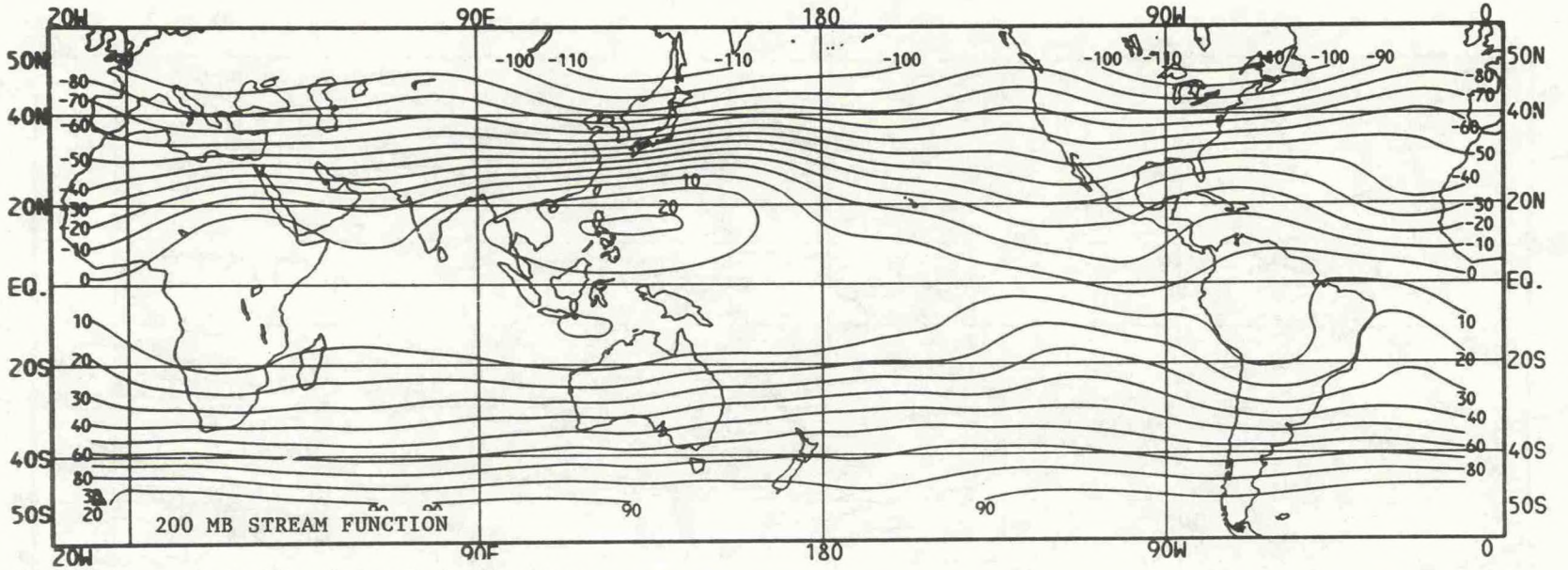

Figure 50. As in Fig. 6 except for December.

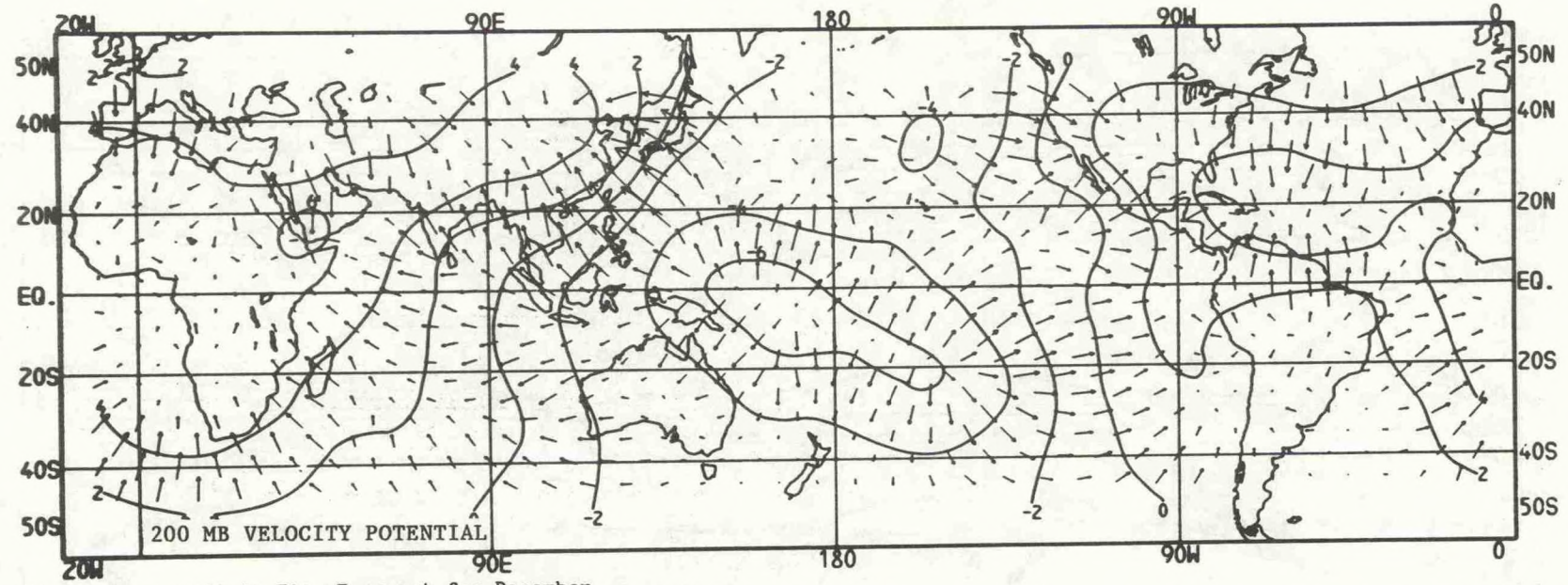

Figure 51. As in Fig. 7 except for December.

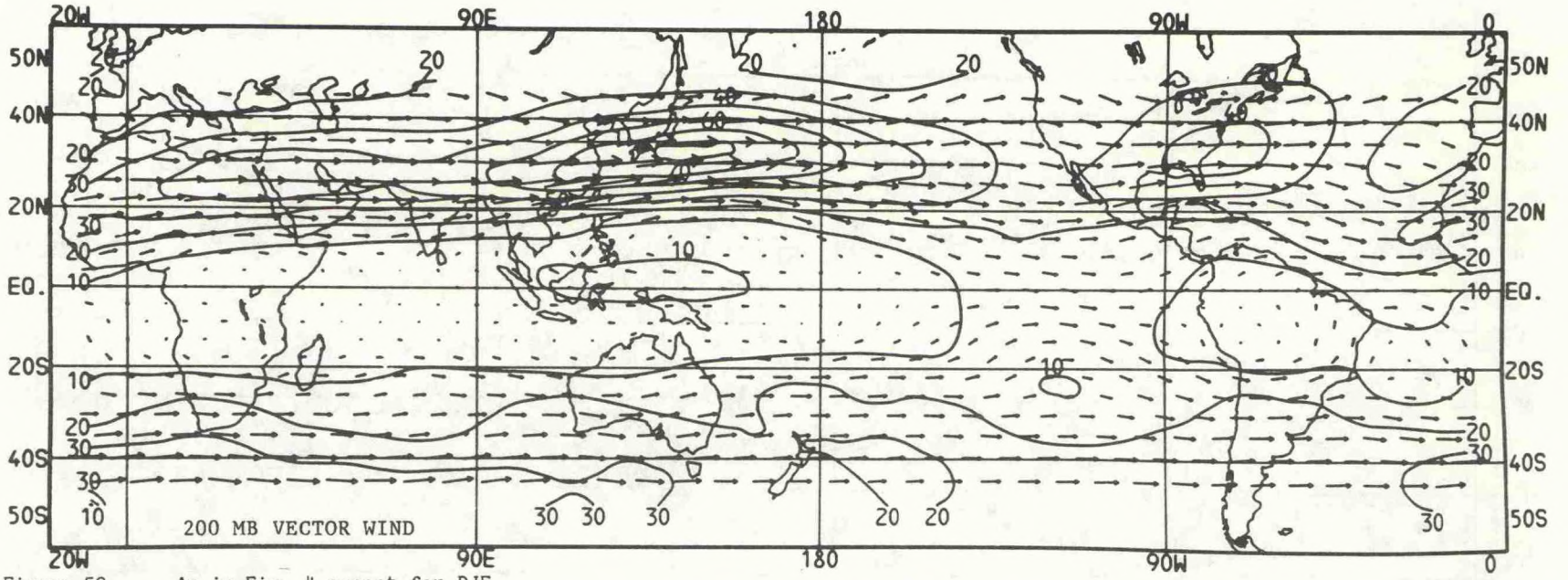

Figure 52. As in Fig. 4 except for DJF.

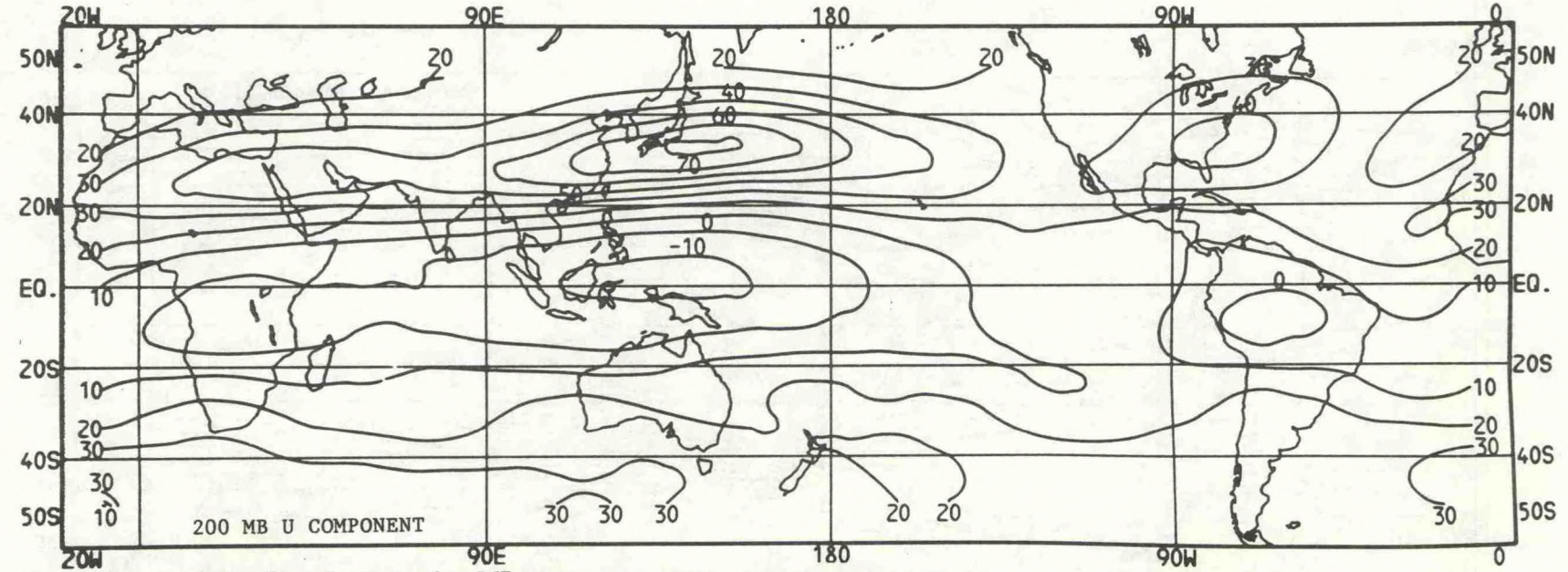

Figure 53. As in Fig. 5 except for DJF.

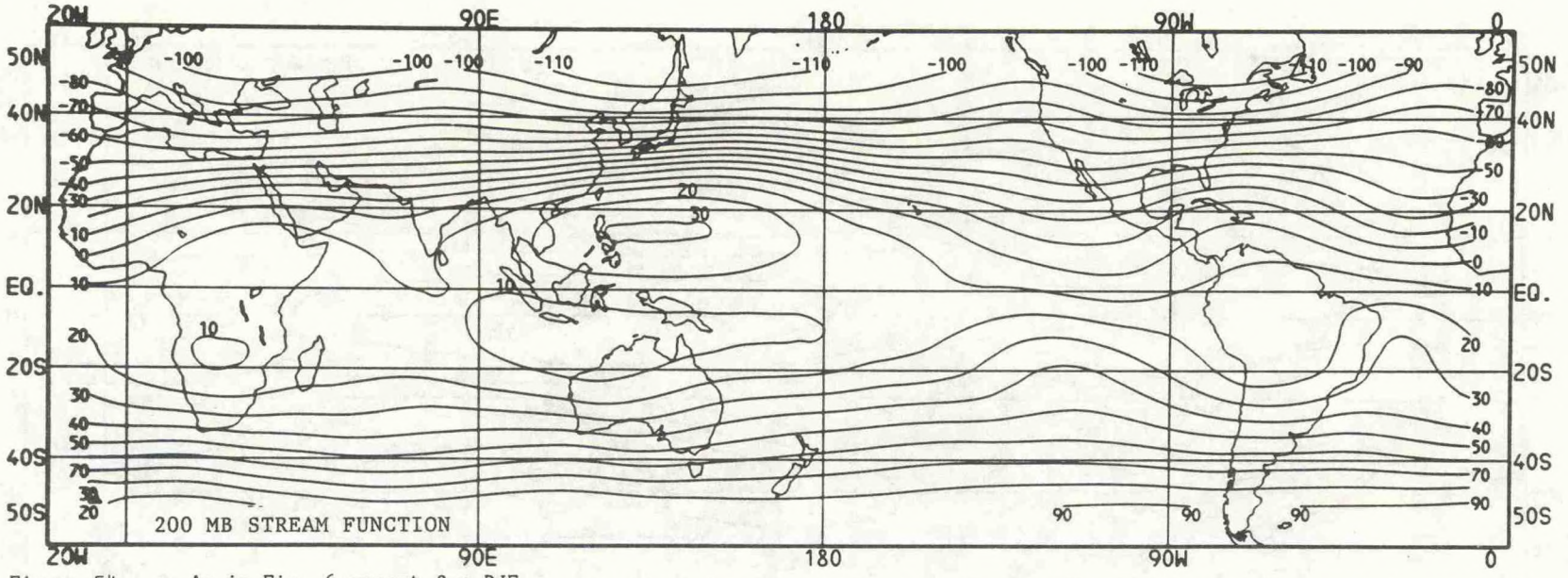

Figure 54. As in Fig. 6 except for DJF.

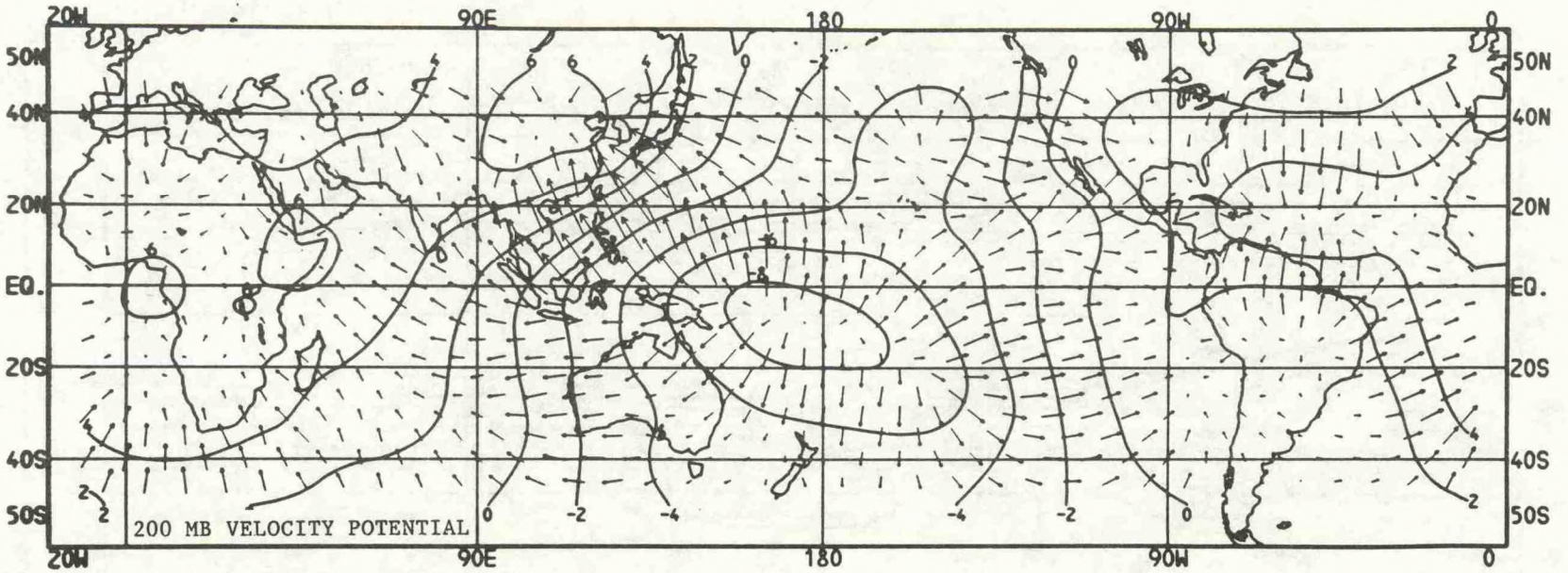

Figure 55. As in Fig. 7 except for DJF.

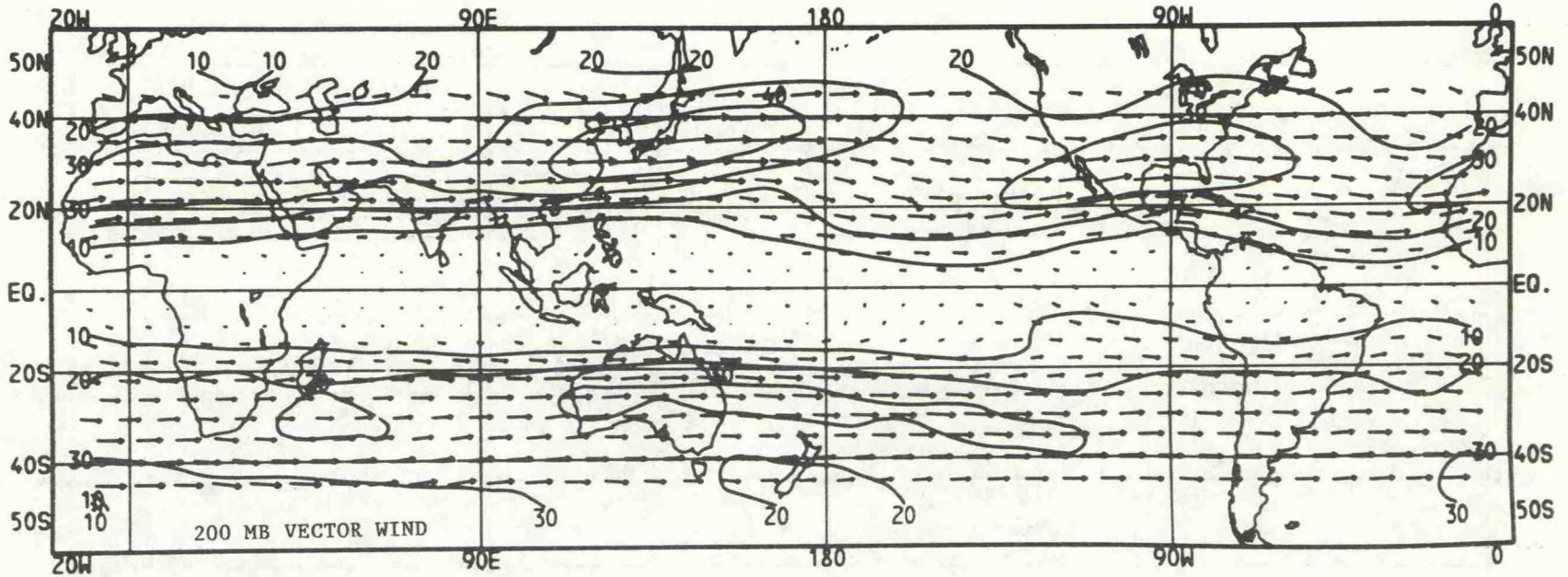

Figure 56. As in Fig. 4 except for MAM.

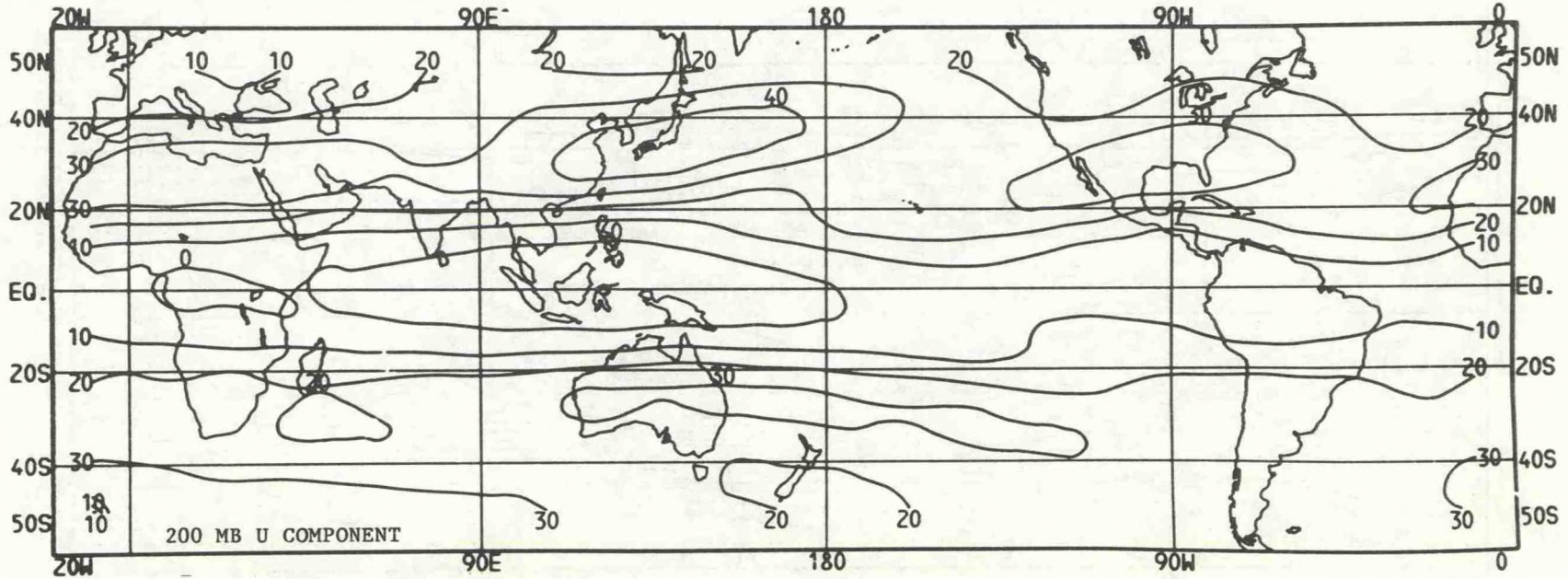

Figure 57. As in Fig. 5 except for MAM.

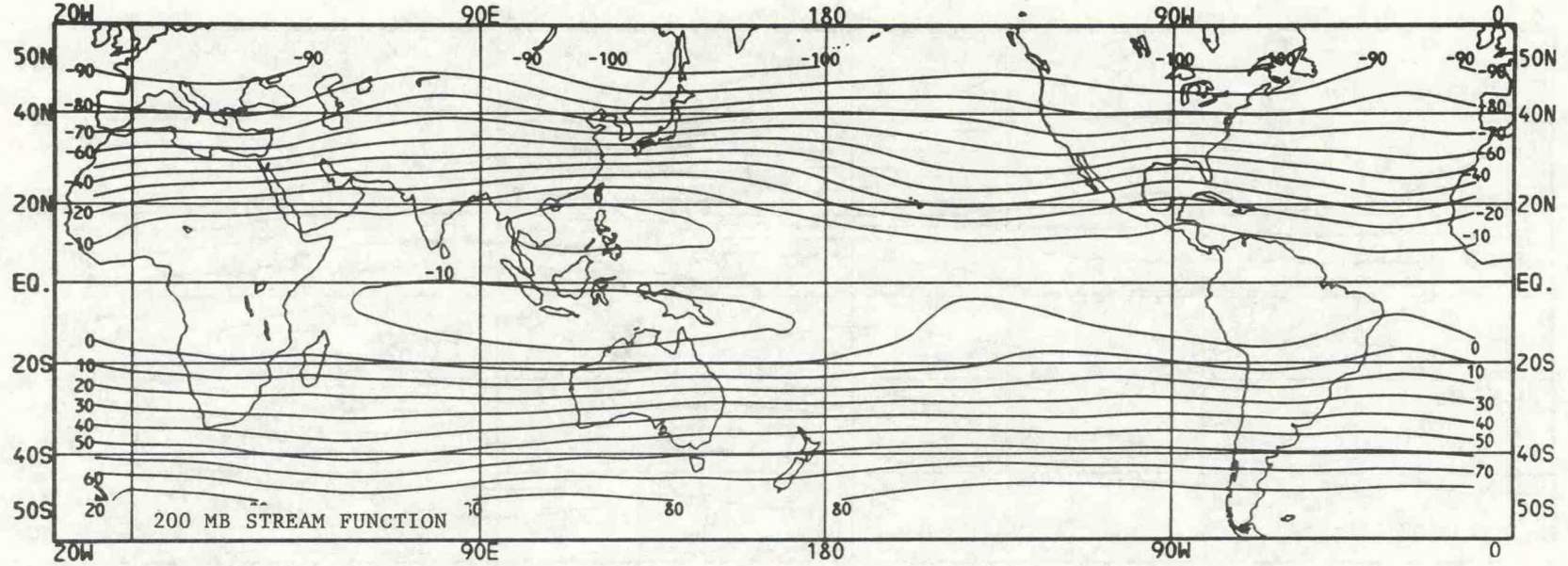

Figure 58. As in Fig. 6 except for MAM.

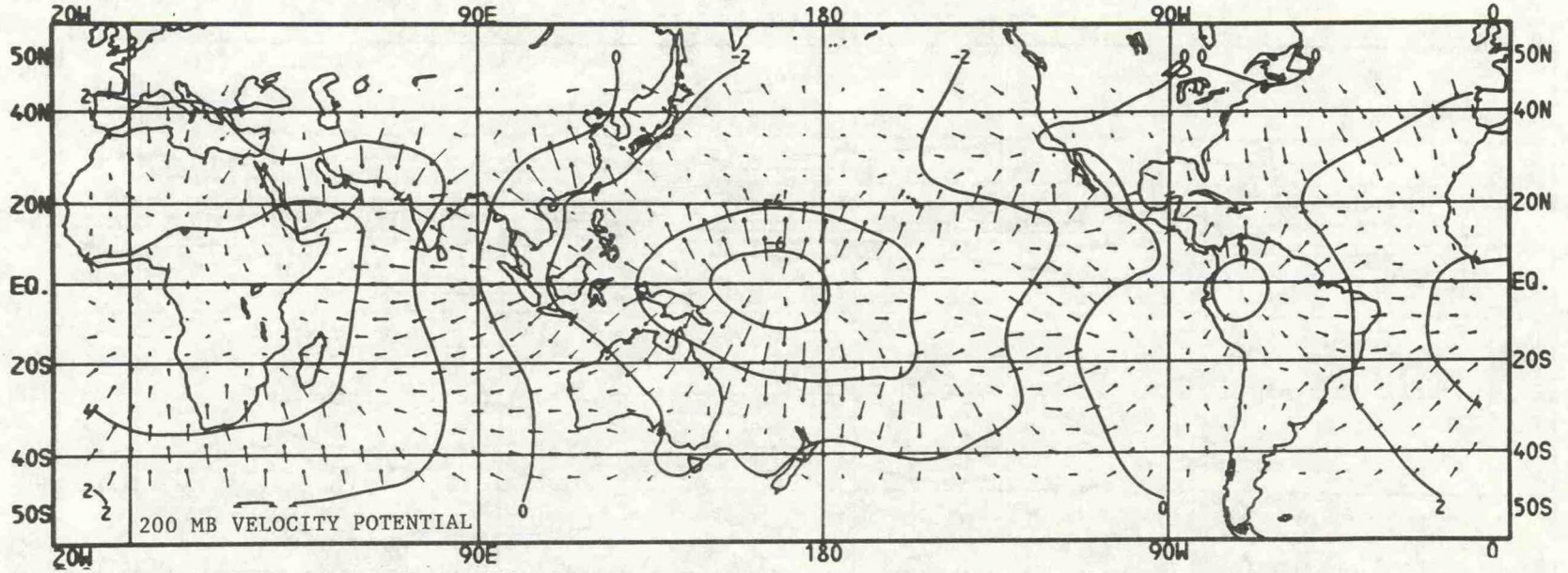

Figure 59. As in Fig. 7 except for MAM.

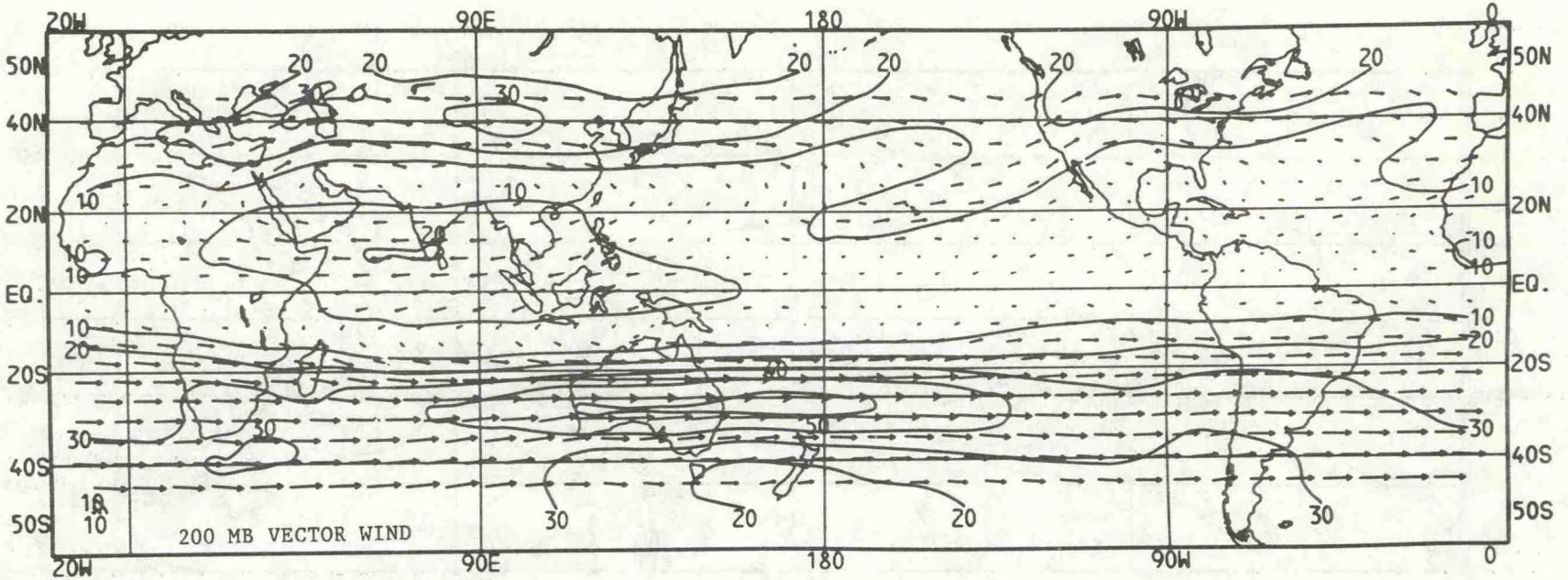

Figure 60. As in Fig. 4 except for JJA.

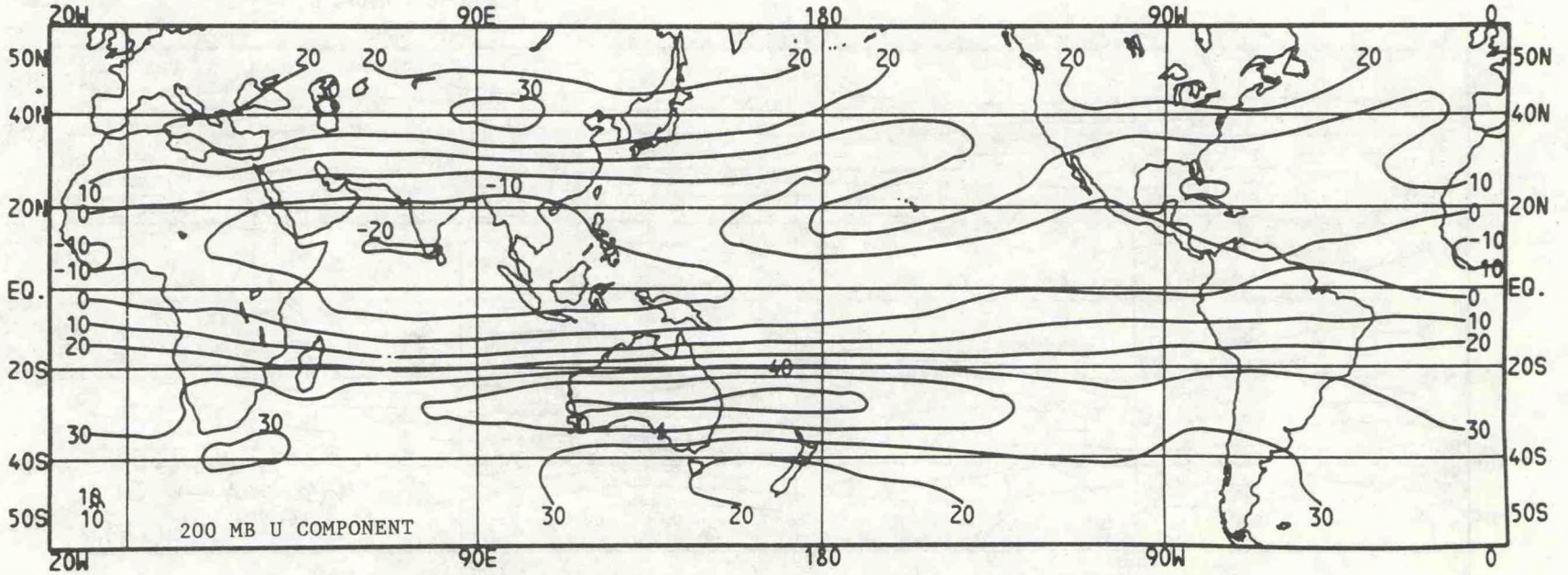

Figure 61. As in Fig. 5 except for JJA.

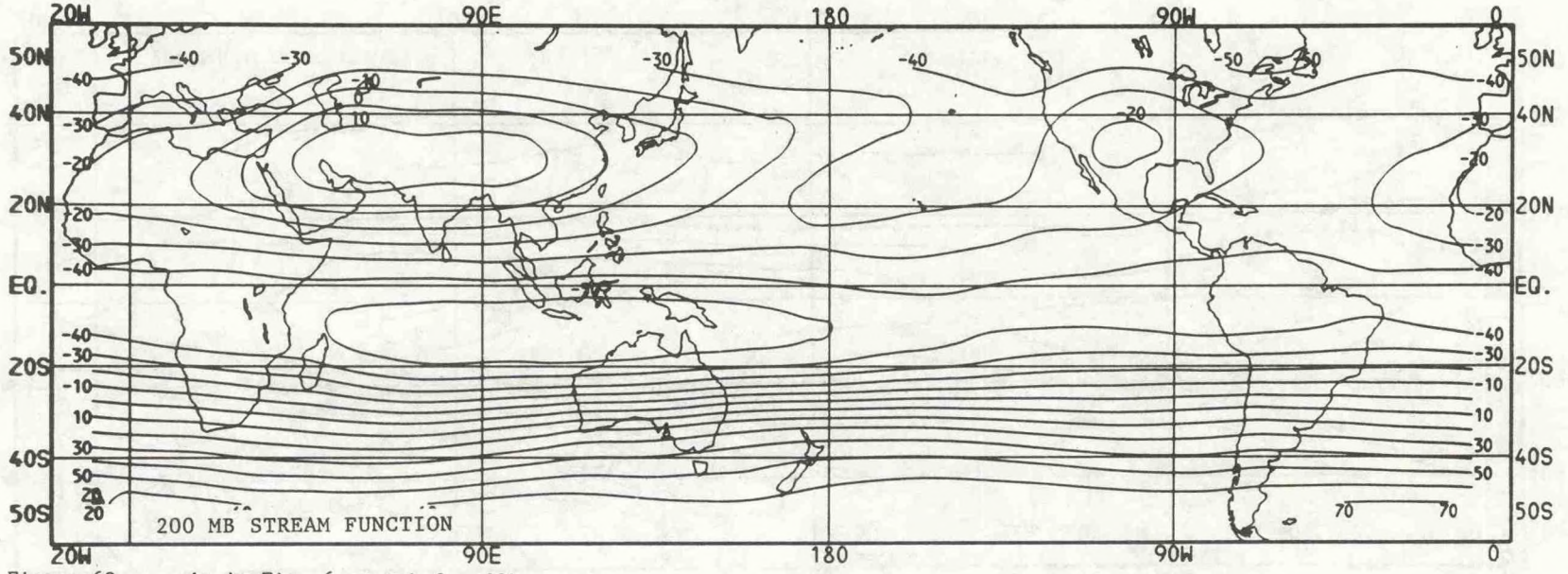

Figure 62. As in Fig. 6 except for JJA.

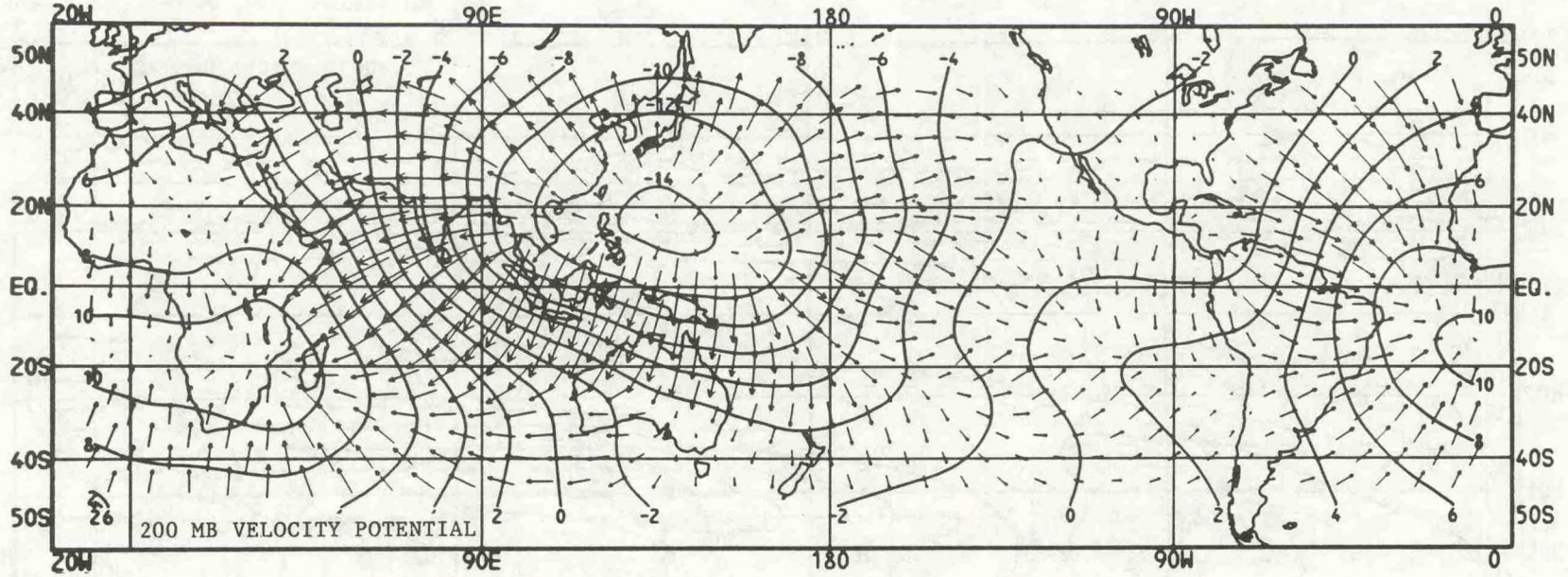

Figure 63. As in Fig. 7 except for JJA.

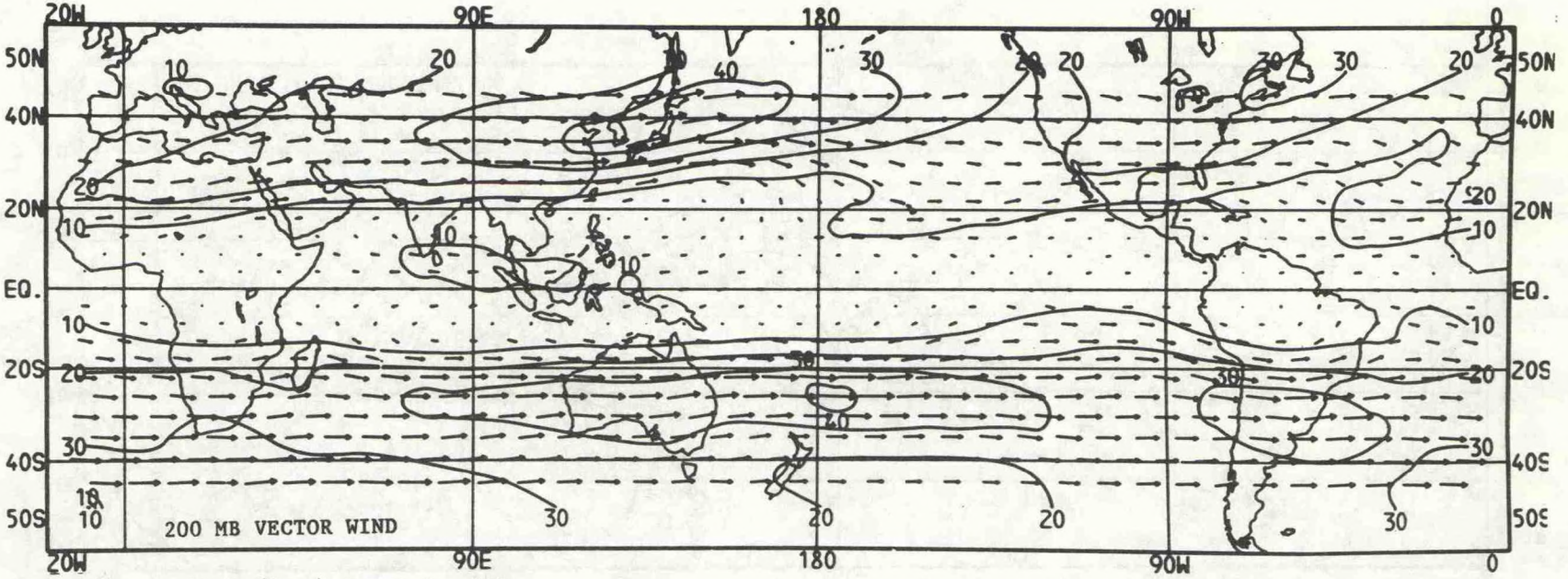

Figure 64. As in Fig. 4 except for SON.

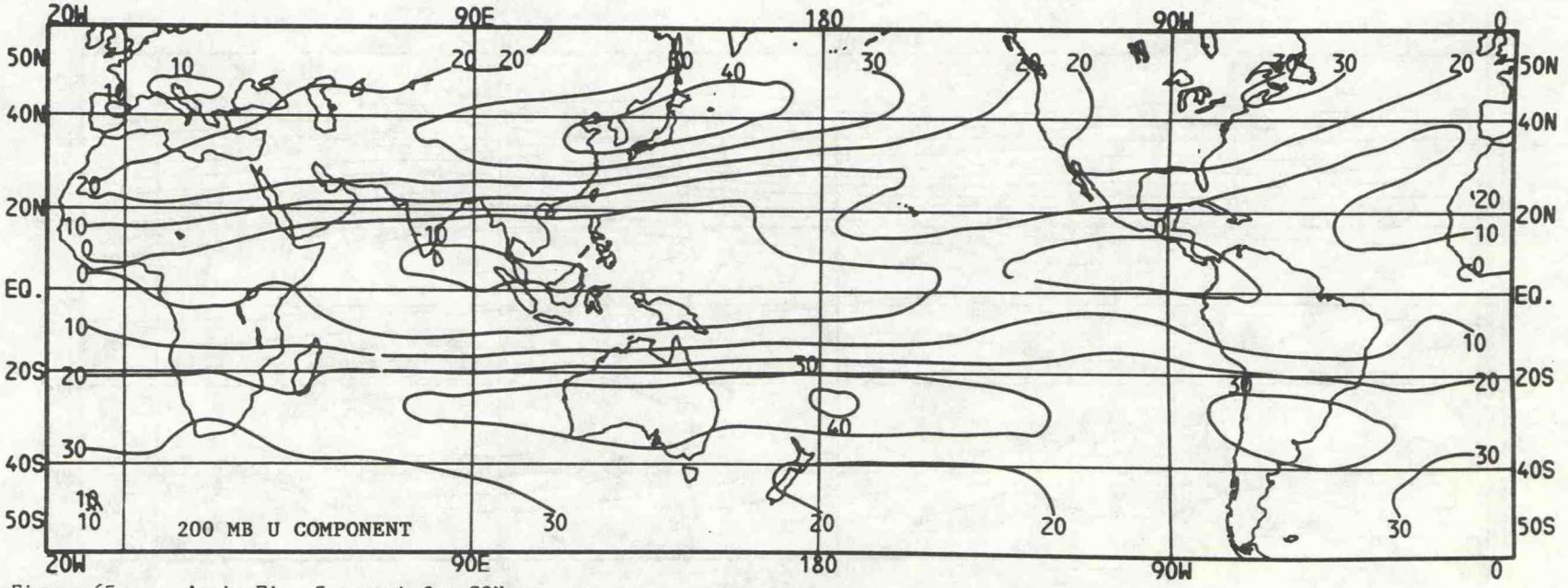

Figure 65. As in Fig. 5 except for SON.

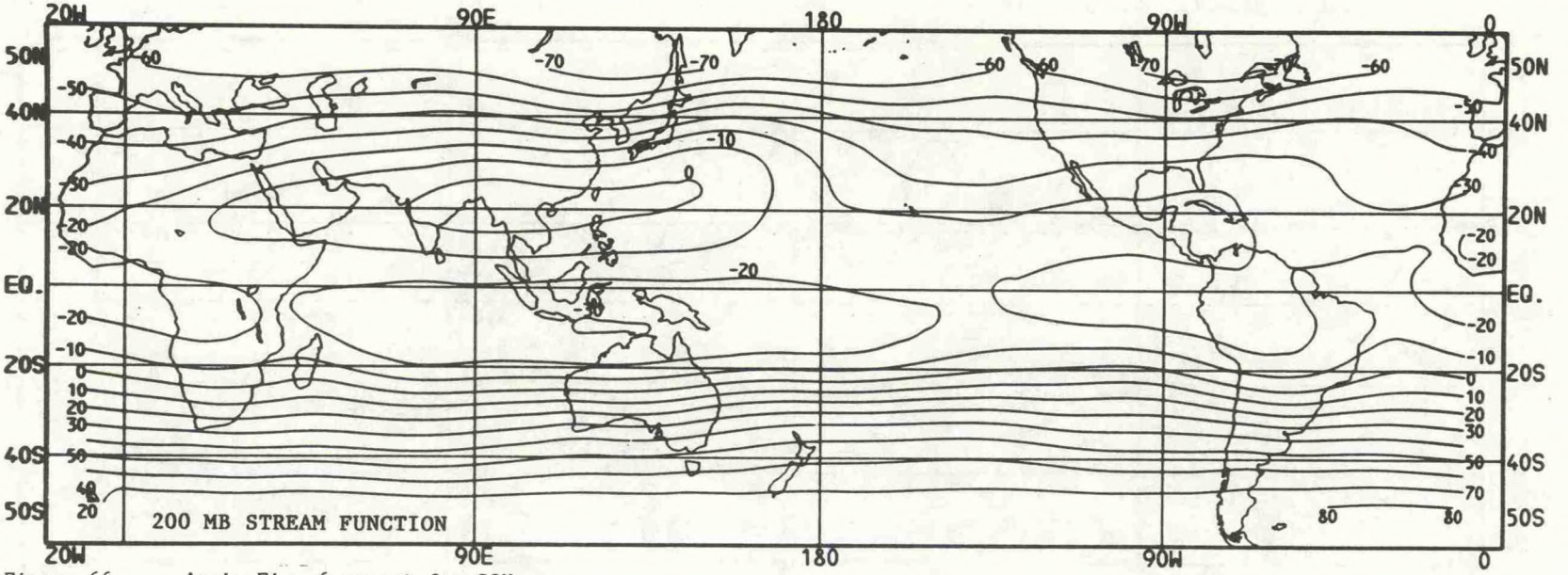

Figure 66. As in Fig. 6 except for SON.

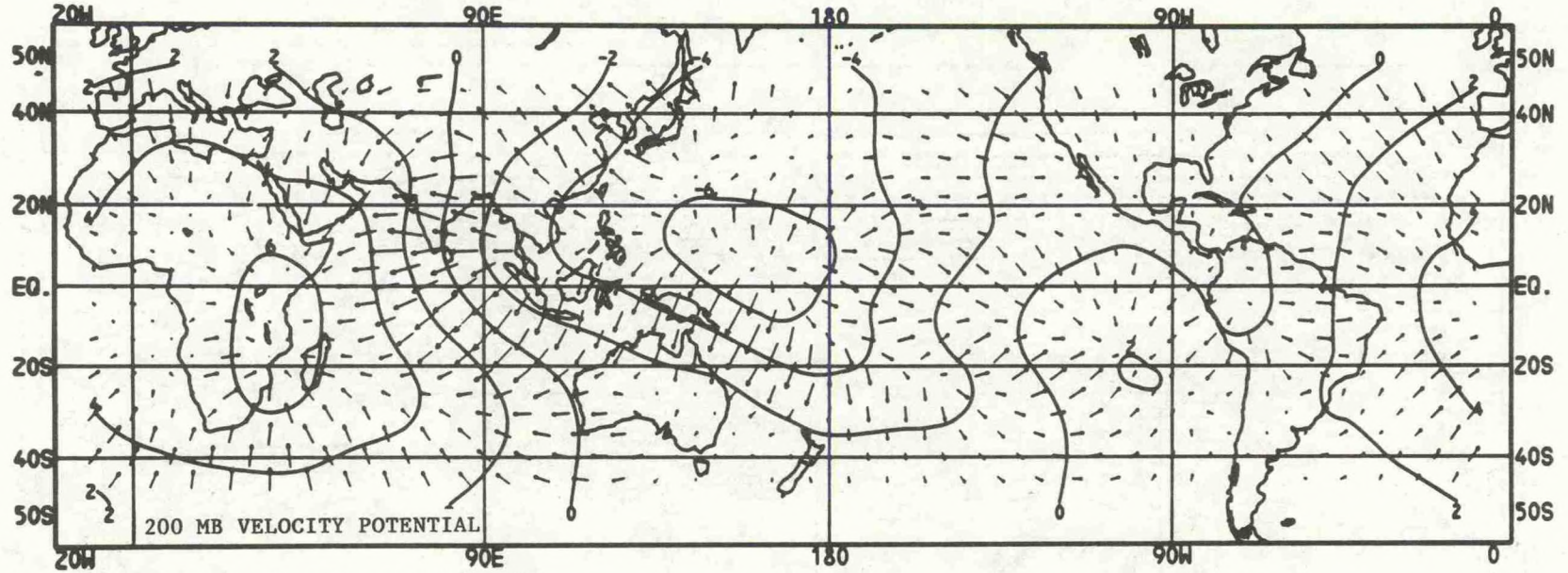

Figure 67. As in Fig. 7 except for SON.

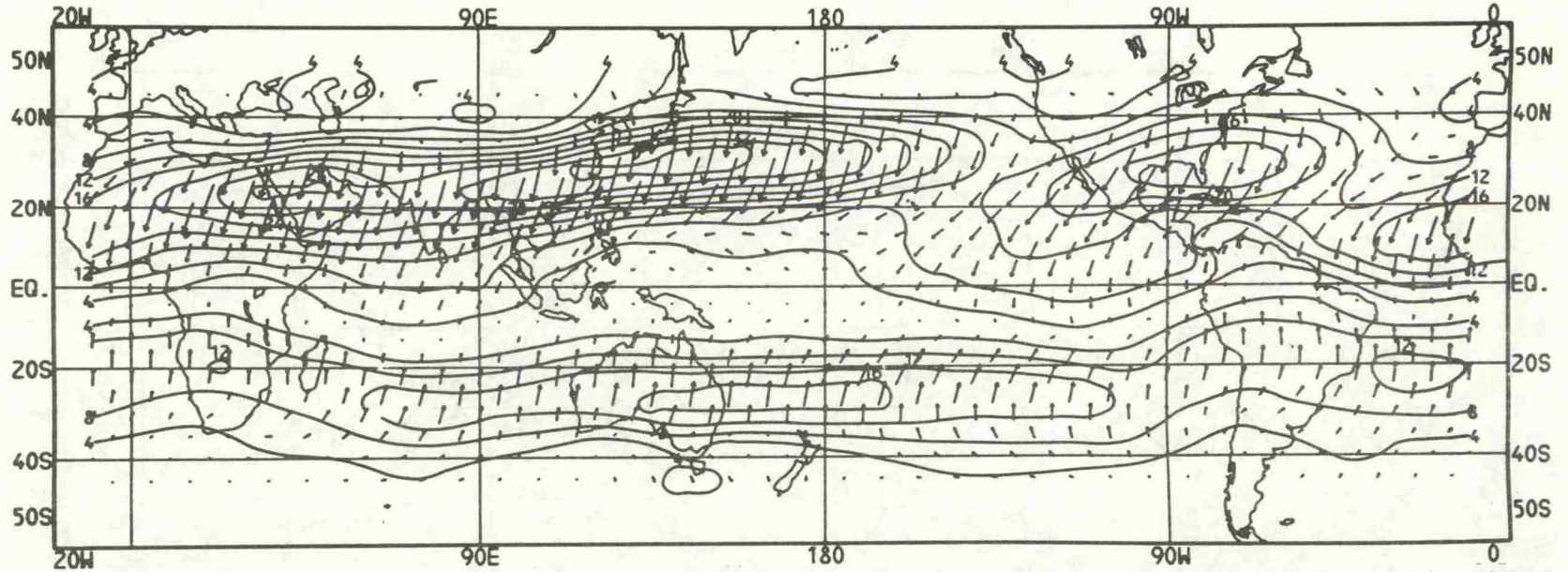

Figure 68. 12-month harmonic of the 5-year mean zonal component of the total 200 mb wind field. Contours (interval 4 m/s) indicate the amplitude and vectors indicate the phase, with a northward pointing vector indicating a maximum during mid-July, eastward indicating mid-October and so on.

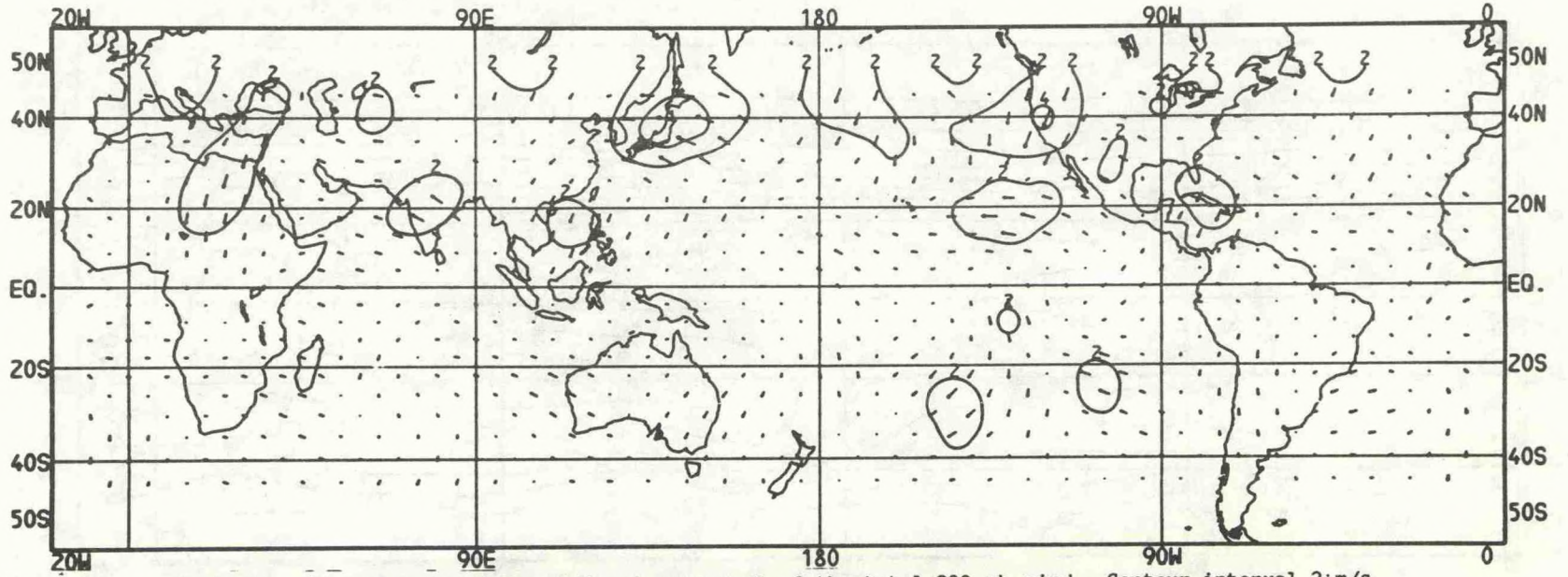

Figure 69. As in Fig. 68 except for the meridional component of the total 200 mb wind. Contour interval 2 m/s.

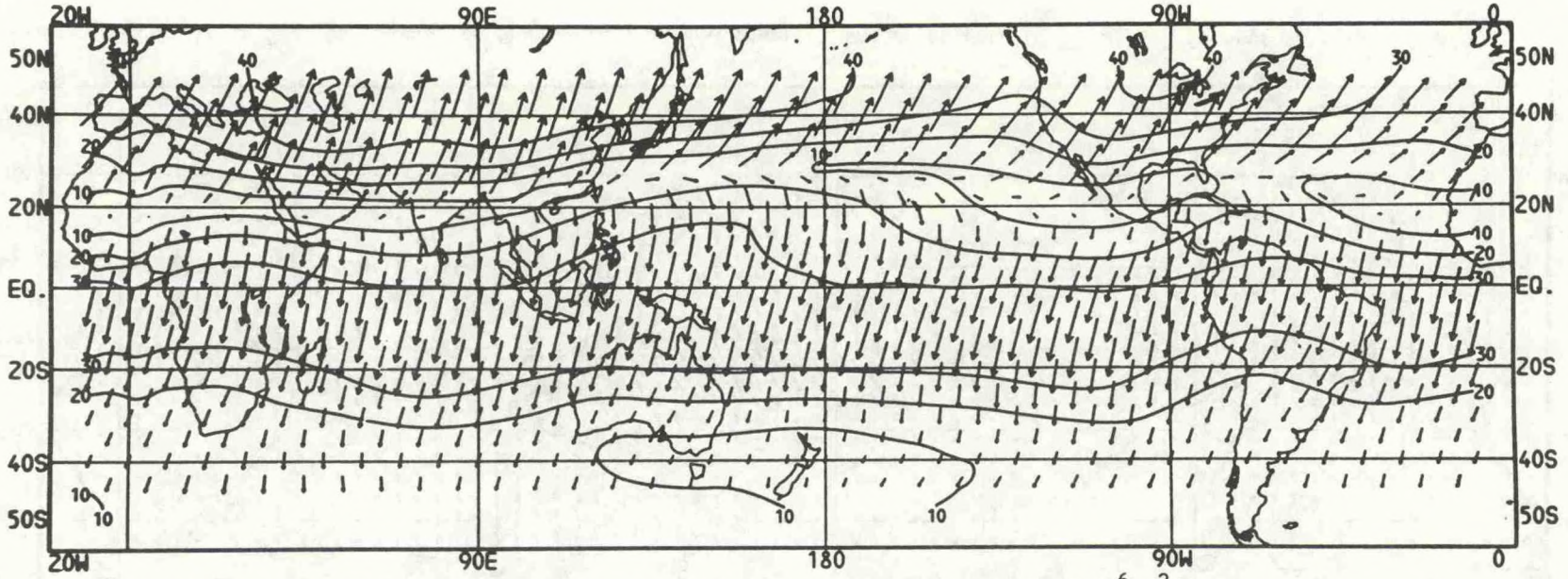

Figure 70. As in Fig. 68 except for the 200 mb stream function. Contour interval 10×10^6 m^2/s.

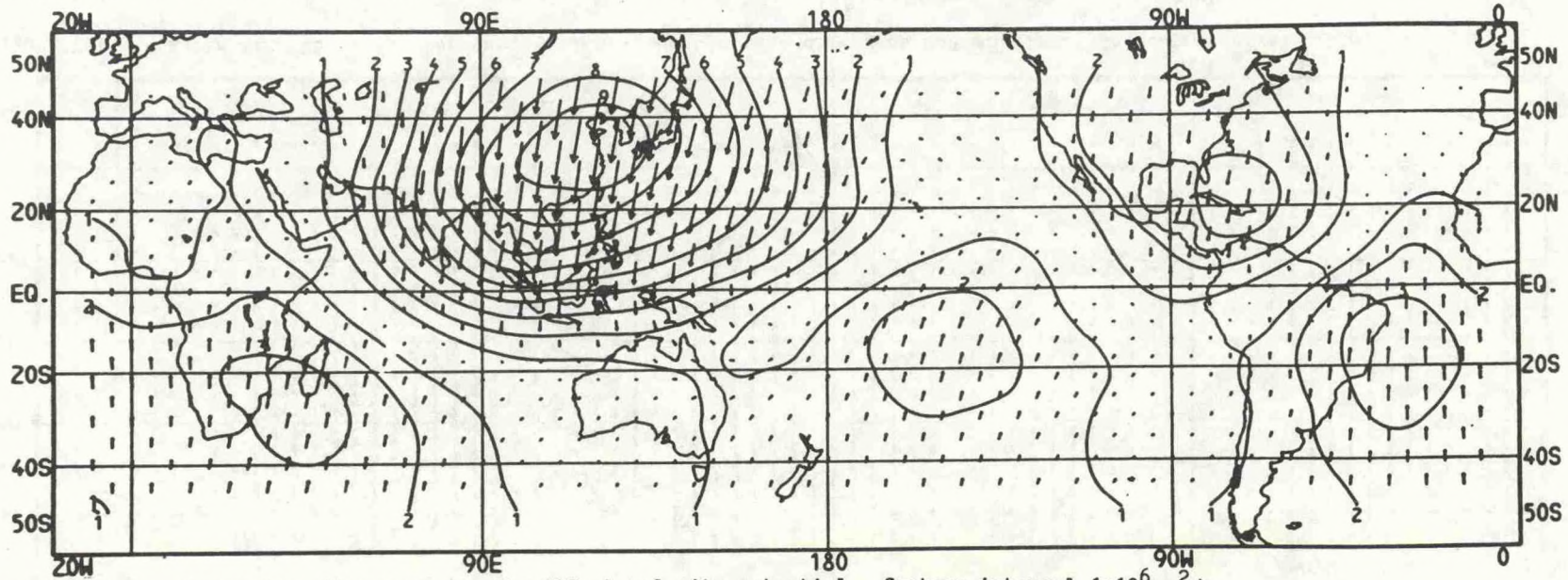

Figure 71. As in Fig. 68 except for the 200 mb velocity potential. Contour interval 1×10^6 m^2/s.

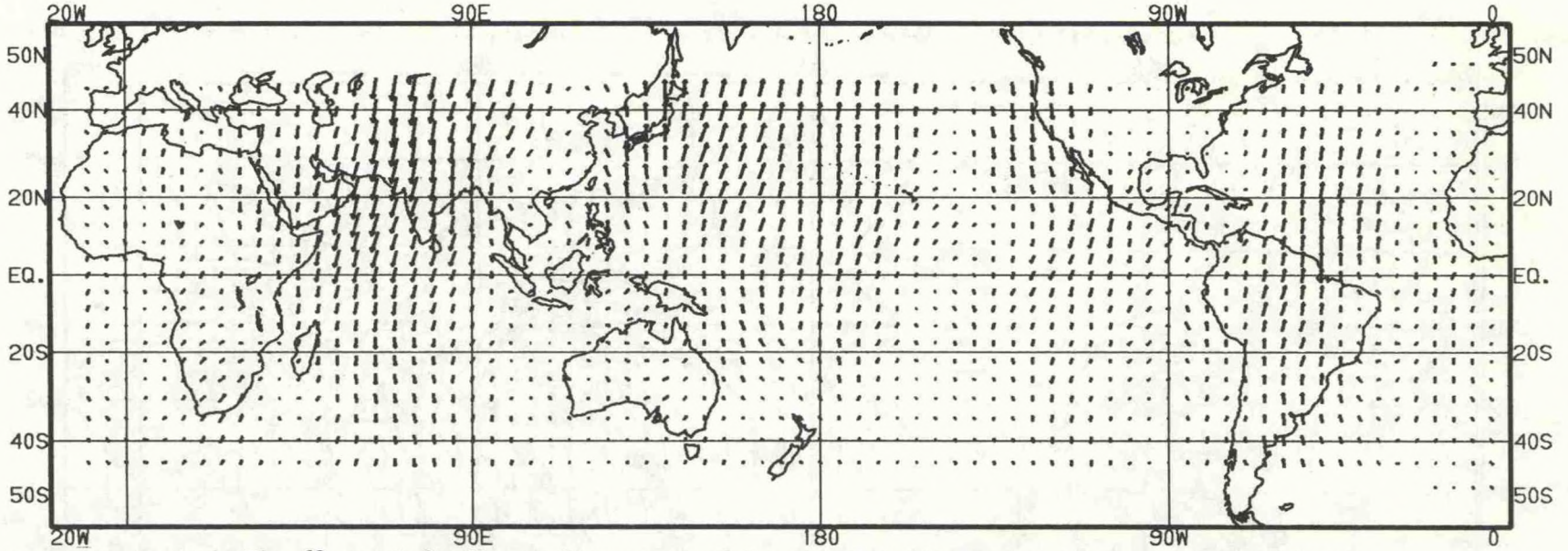

Figure 72. As in Fig. 68 except for the zonal component of the divergent 200 mb wind. Contour interval 0.5 m/s.

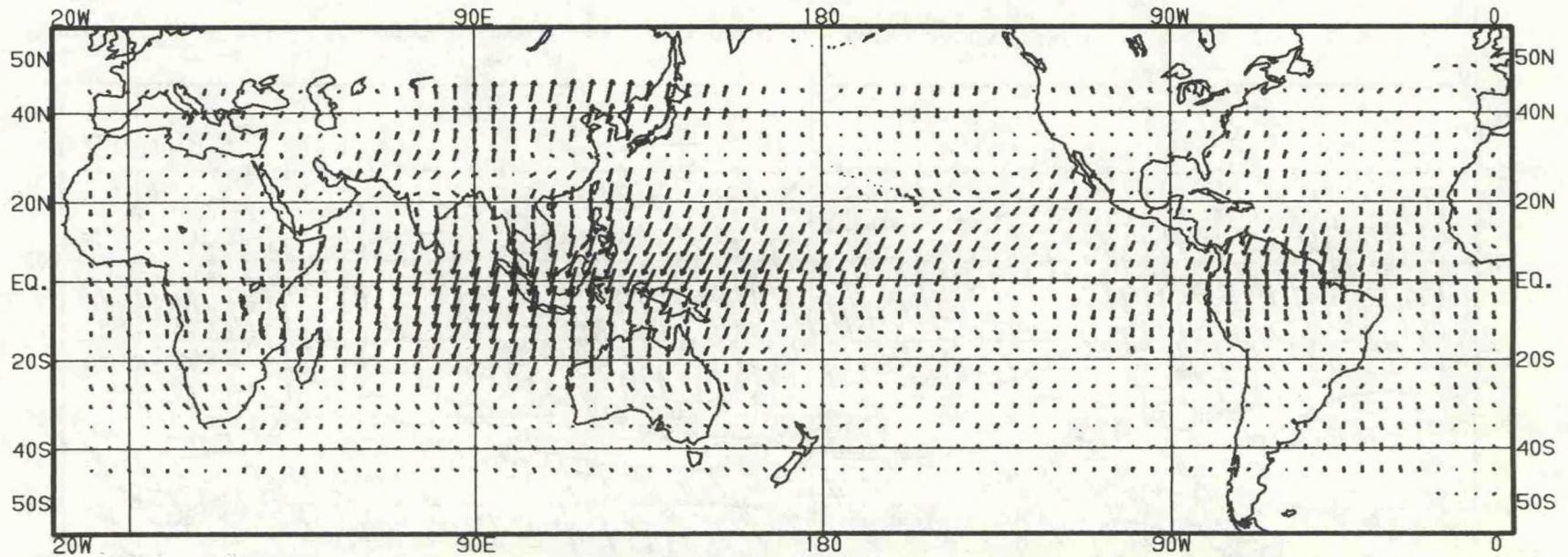

Figure 73. As in Fig. 68 except for the meridional component of the divergent 200 mb wind. Contour interval 0.2 m/s.

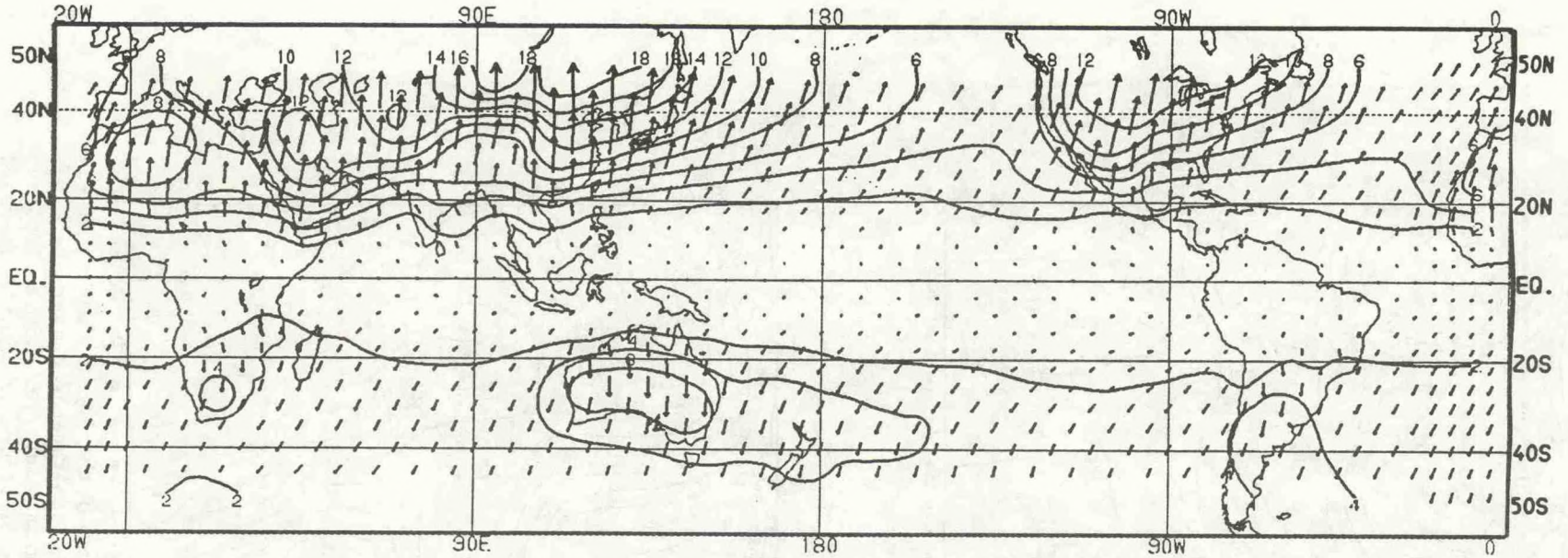

Figure 74. As in Fig. 68 except for the 850 mb temperature. Contour interval 2°C.

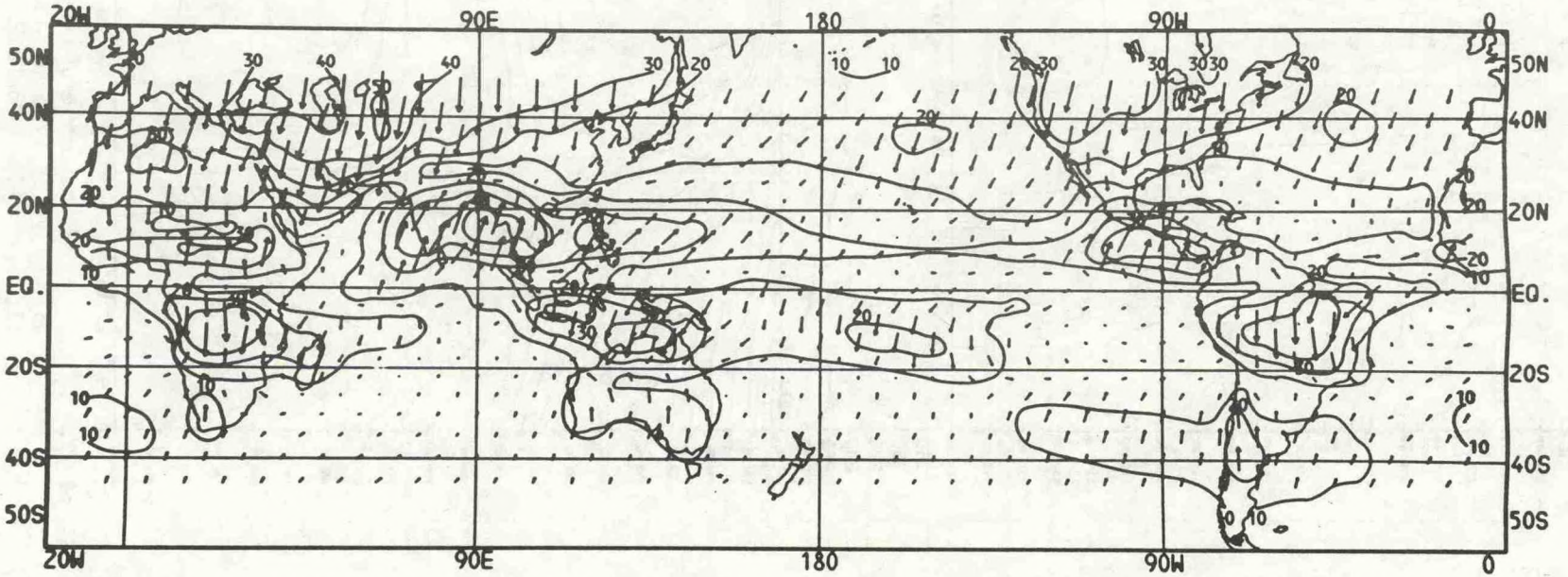

Figure 75. As in Fig. 68 except for the long-term mean OLR. Contour interval 10 W/m^2. Vector points to time of <u>minimum</u> OLR (which corresponds to maximum convective activity in the tropics).

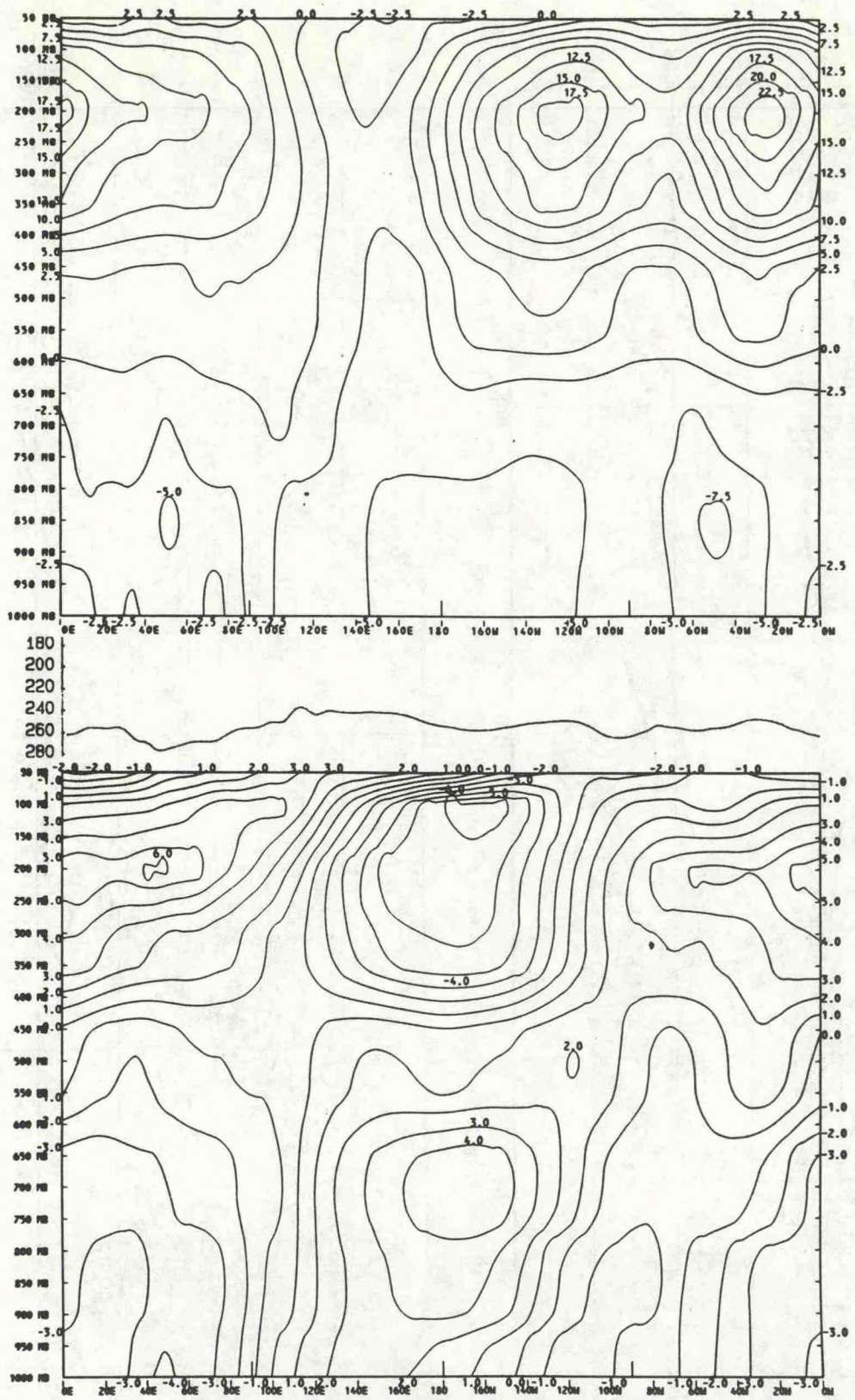

Figure 76. Longitude/pressure cross section of the 5-year mean zonal wind (top) and velocity potential (bottom) averaged over the latitudes 0^{o}-20^{o}N for DJF. Contour interval 2.5m/s (top) and $1x10^{6}$ m^{2}/s (bottom). In center of figure is the OLR averaged over the same latitudes with scale reversed so that peaks indicate maxima in convective activity.

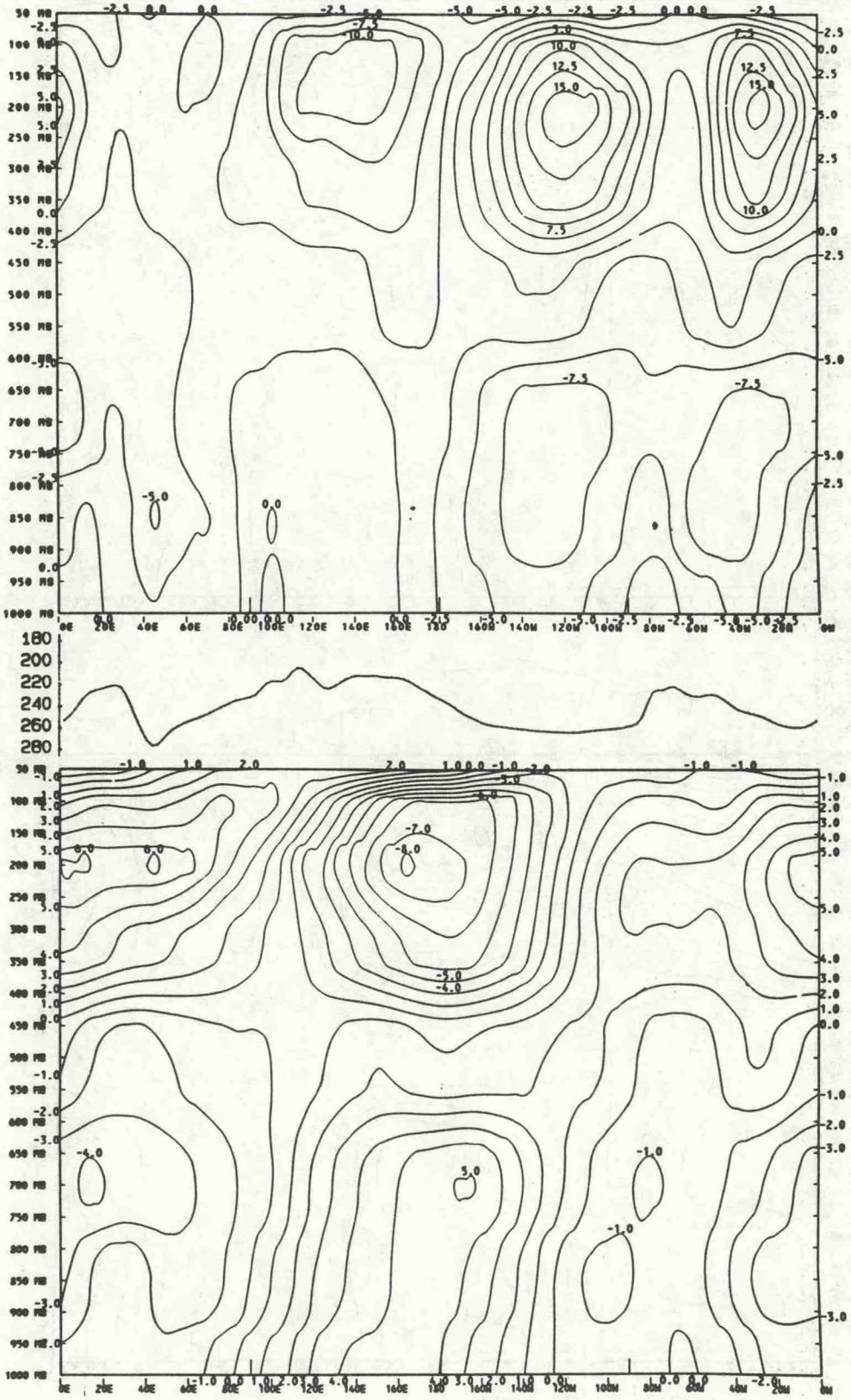

Figure 77. As in Fig. 76 except for latitudes 5°N-5°S.

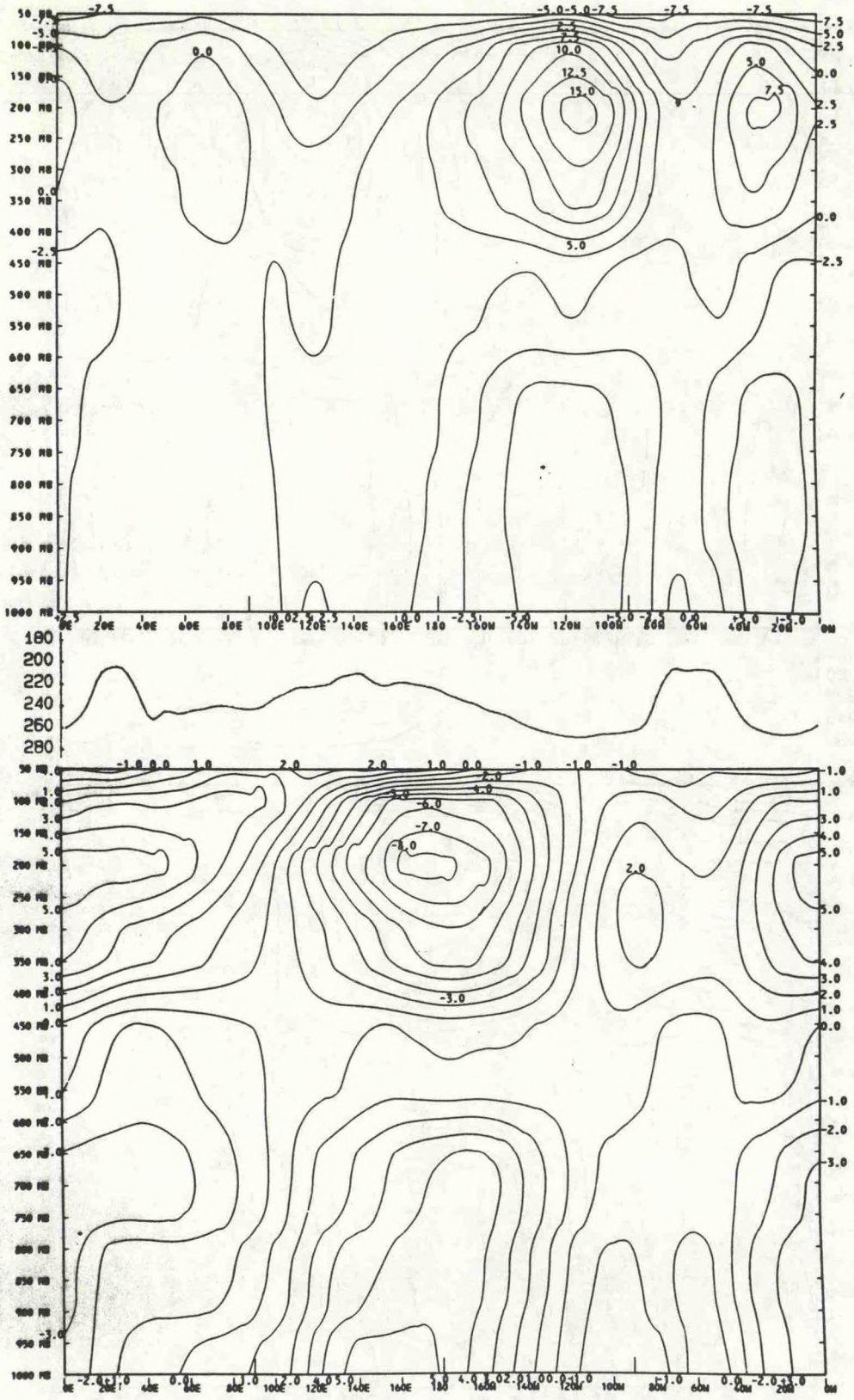

Figure 78. As in Fig. 76 except for latitudes 0°-20°S.

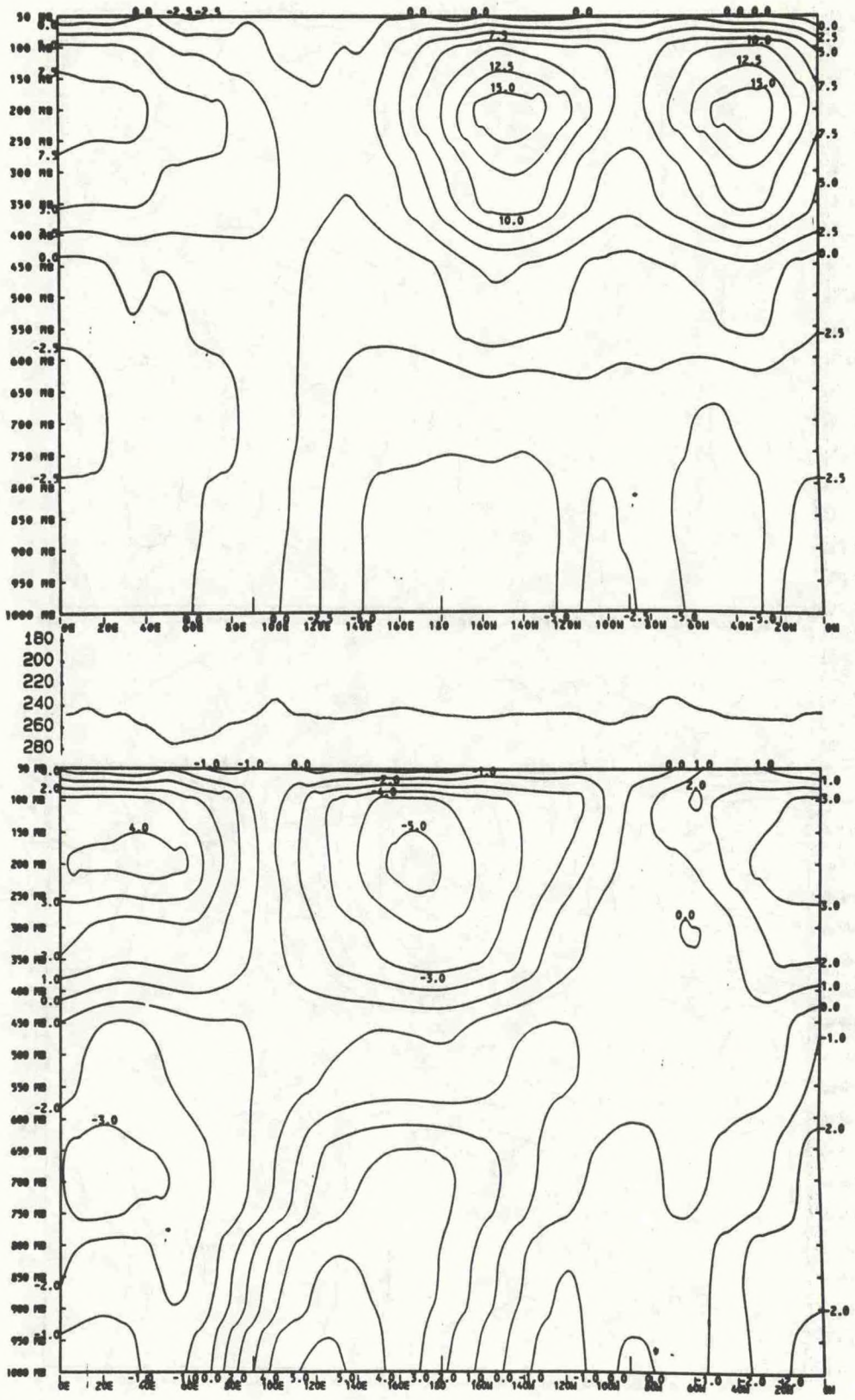

Figure 79. As in Fig. 76 except for MAM.

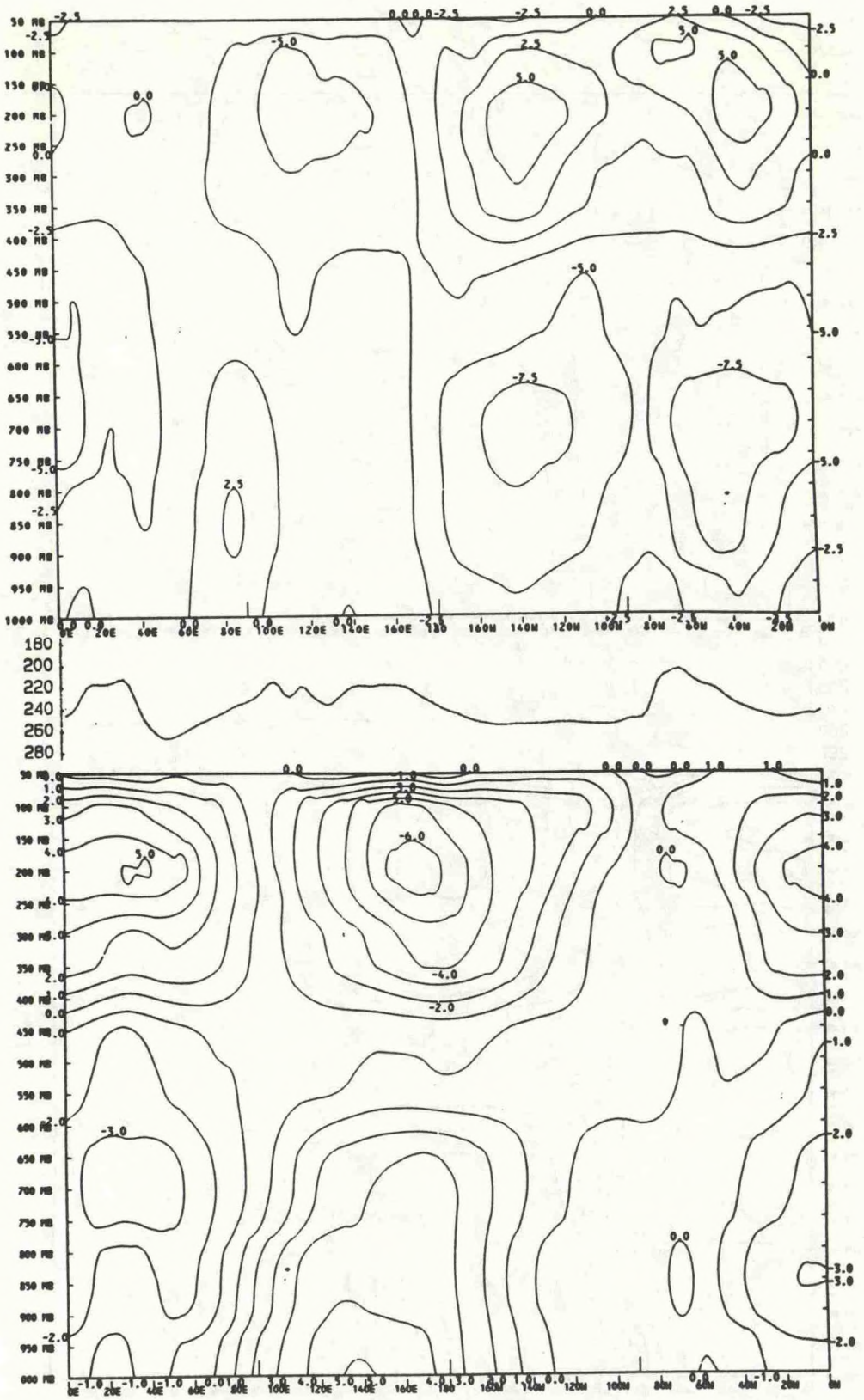

Figure 80. As in Fig. 77 except for MAM.

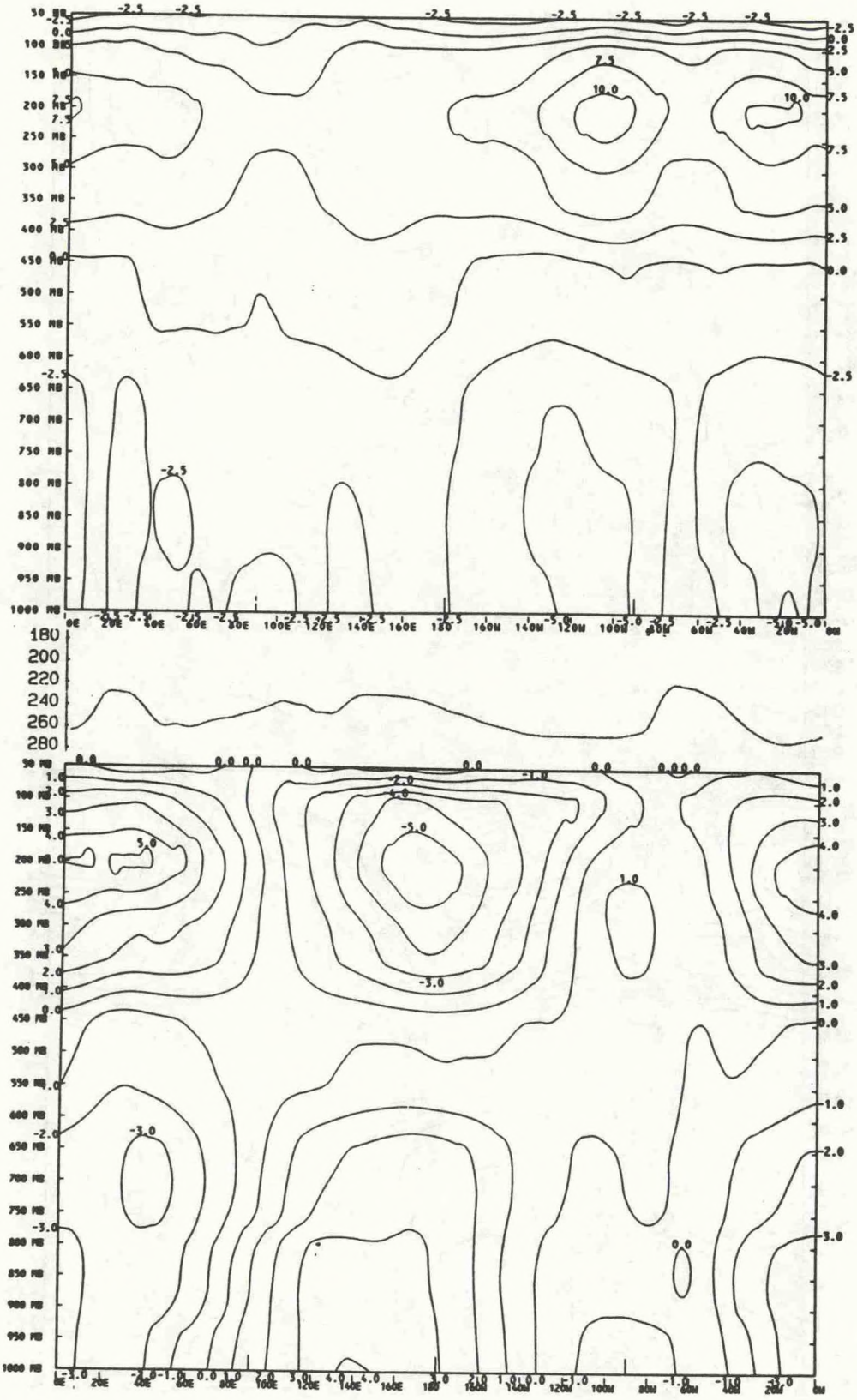

Figure 81. As in Fig. 78 except for MAM.

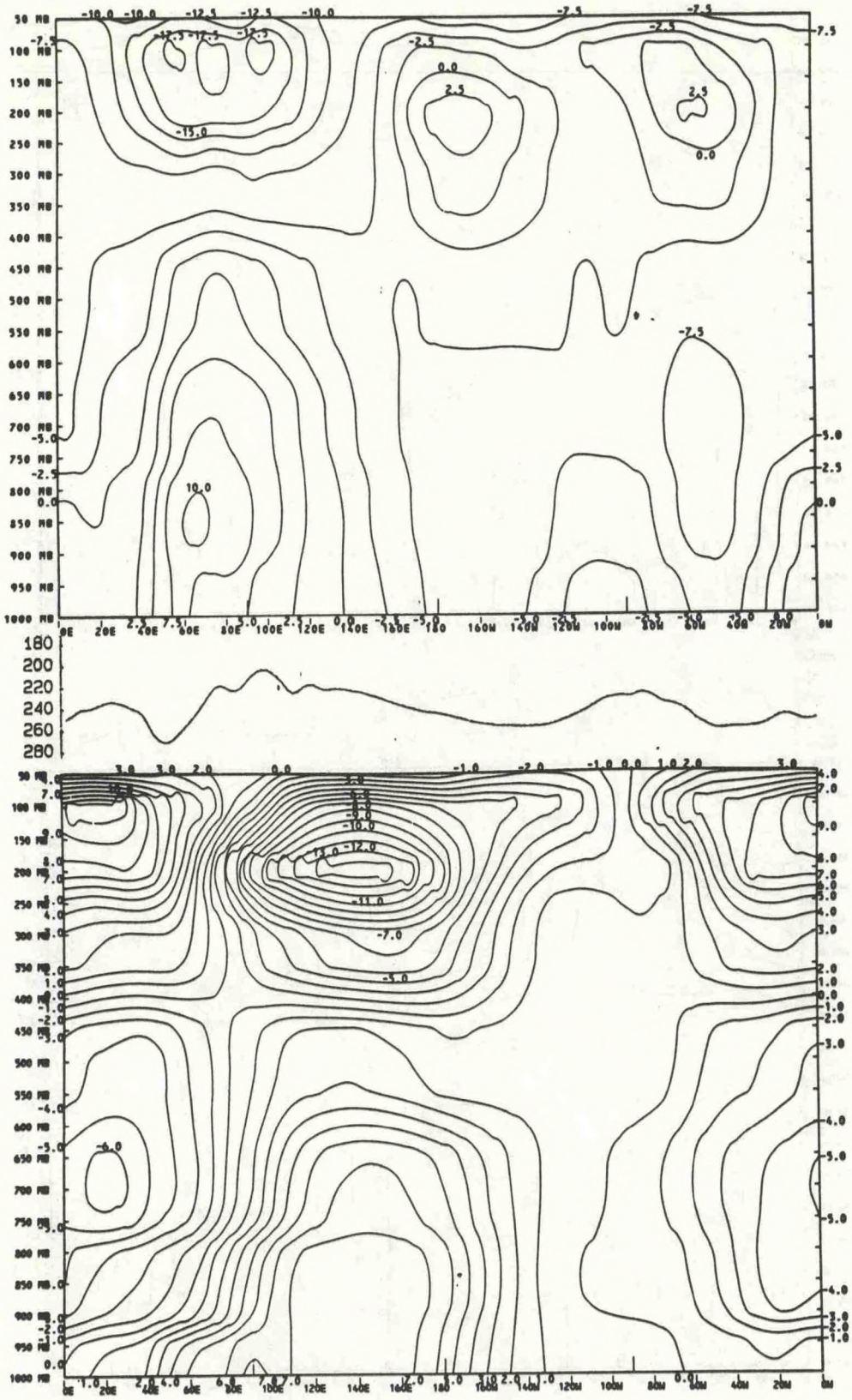

Figure 82. As in Fig. 76 except for JJA.

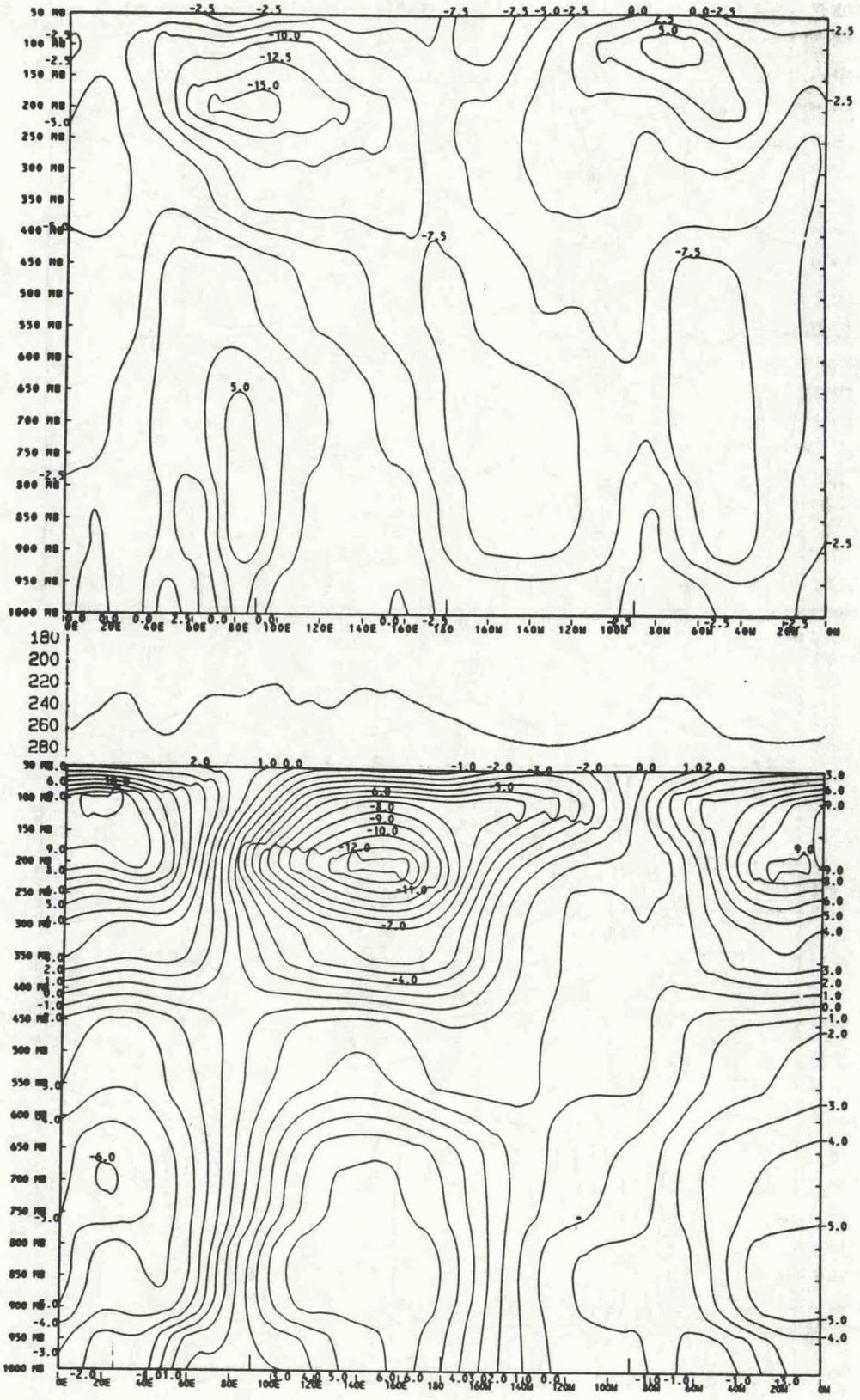

Figure 83. As in Fig. 77 except for JJA.

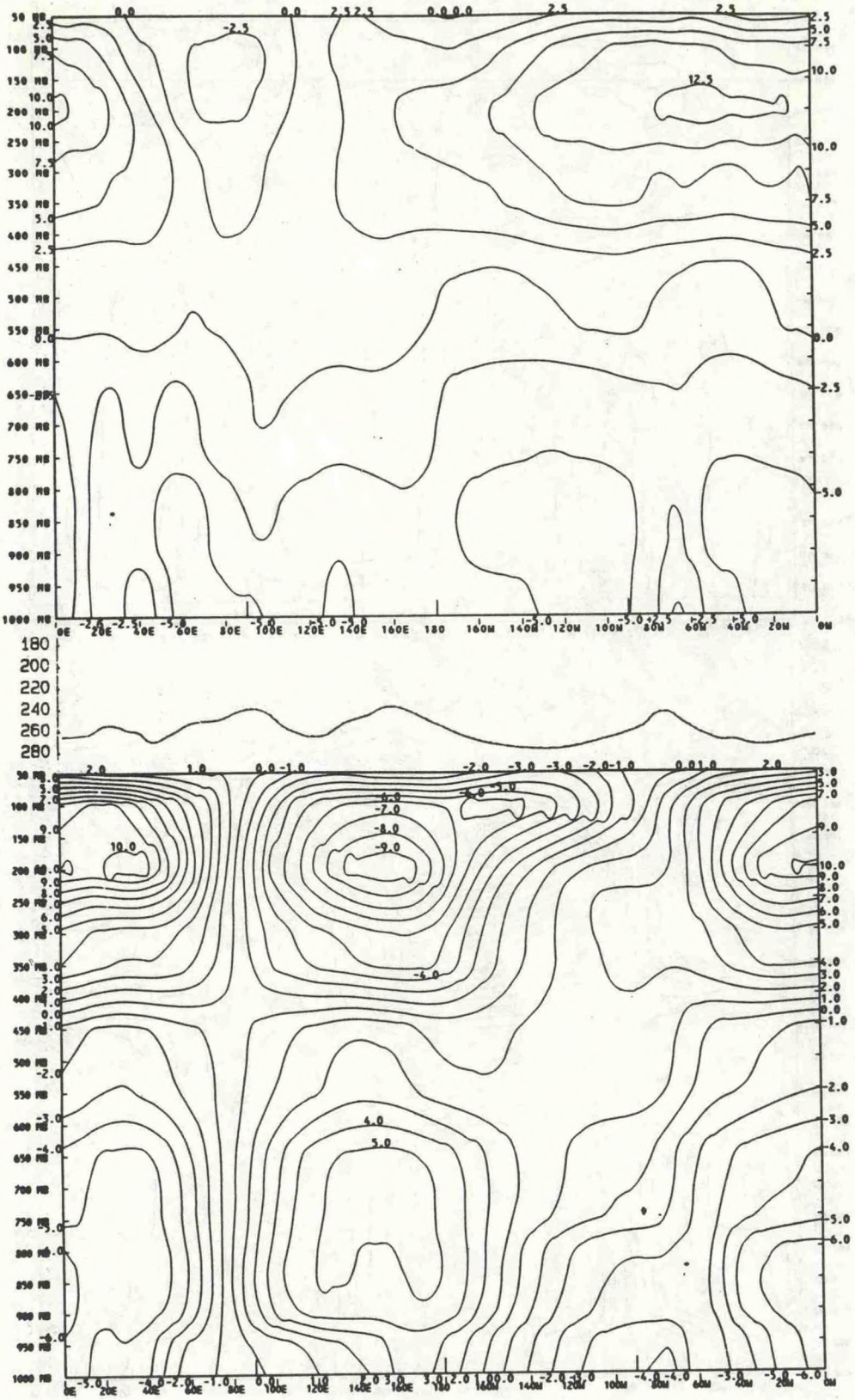

Figure 84. As in Fig. 78 except for JJA.

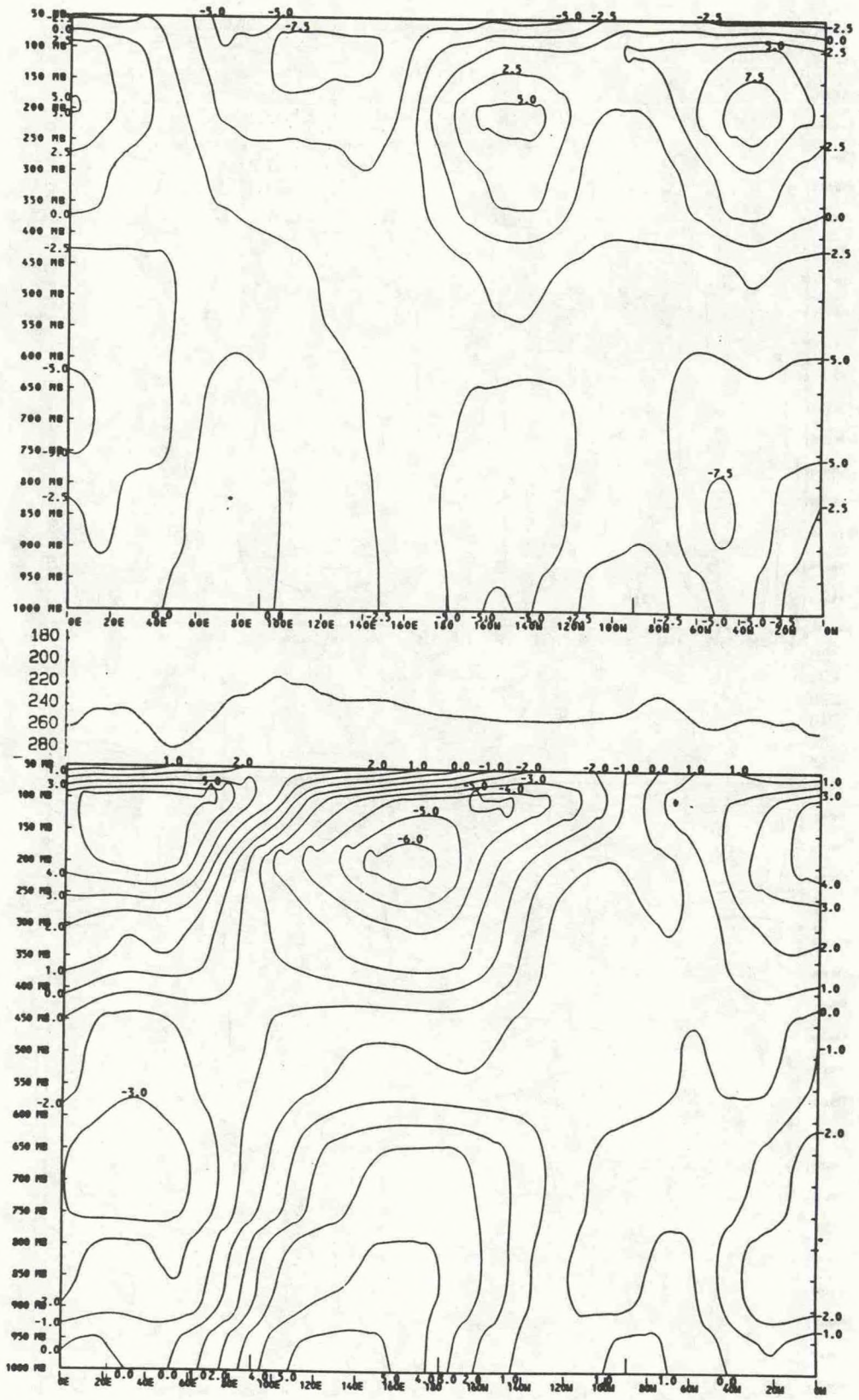

Figure 85. As in Fig. 76 except for SON.

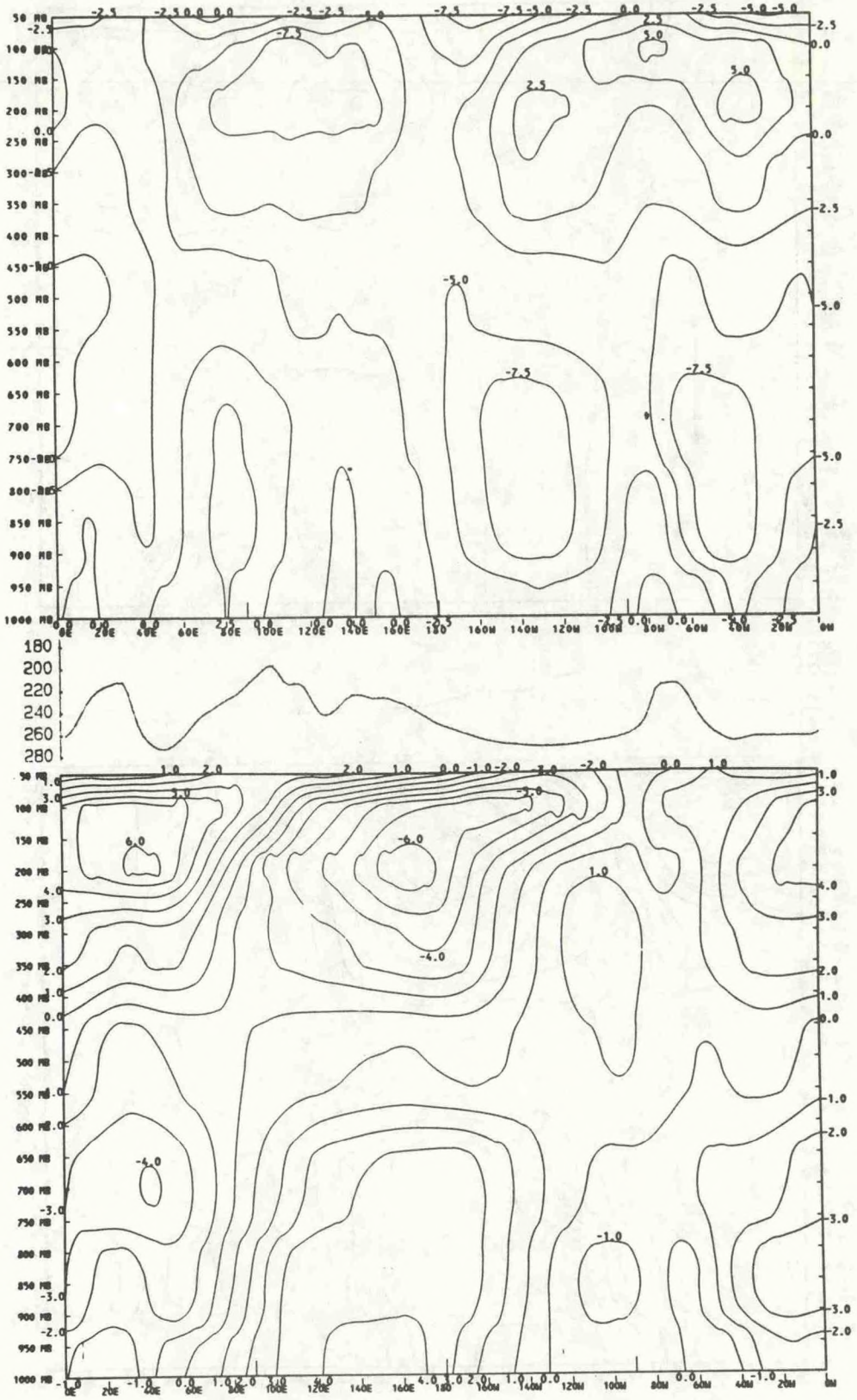

Figure 86. As in Fig. 77 except for SON.

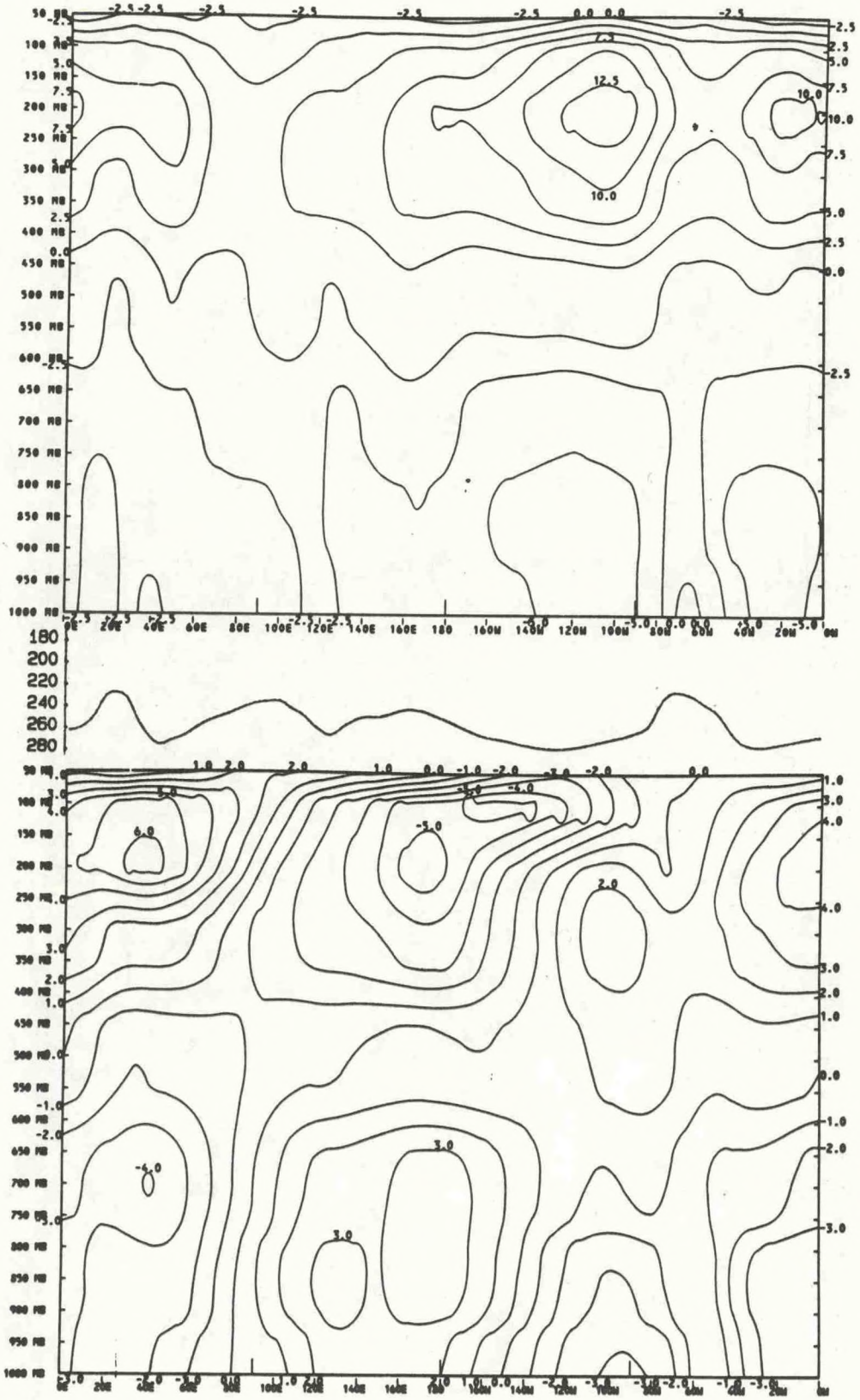

Figure 87. As in Fig. 78 except for SON.

☆U.S. GOVERNMENT PRINTING OFFICE: 1986 491 097 46861